

Synthesis of Enantioenriched Heterocycles by Tandem Sakurai Allylation/Intramolecular Cyclization Processes

Thesis by
Ciara M. Ordner

In Partial Fulfillment of the Requirements for
the degree of
Bachelor of Science



CALIFORNIA INSTITUTE OF TECHNOLOGY
Pasadena, California

2018

© 2018

Ciara M. Ordner

ACKNOWLEDGEMENTS

First, I would like to express my immense gratitude to Sarah Reisman for taking a chance on me and letting a freshman with no organic chemistry background enter into her lab. Research in her group has certainly been one of my most valued experiences at Caltech. Her door was always open for me to ask questions about issues with my research or just general questions about my academic studies. Sarah's passion for research has inspired me to continue my study of organic chemistry. I will be pursuing my doctoral degree at Stanford University.

It has been my absolute pleasure to work with Julie Hofstra. She has not only been an excellent, diligent mentor but also a great friend (and even water polo coach). Her constant support and invaluable advice, on topics ranging from chemistry to graduate school to just life in general, is something I am so grateful for, and I do not feel that words can properly express. Working with Julie has been a great experience, and she has helped me grow into the chemist I am today. She gave me the freedom to grow as an independent researcher while simultaneously providing the encouragement and assistance needed for a successful project. I truly have enjoyed the last three years working with her.

Being a part of the Reisman group for the past four years has been wonderful experience. I would like to thank the various members of the group for all of their help, especially Dana Gephart for her contributions to Team Tetrahydrofuran. Dana's efforts in constructing the *cis* diastereomers and assisting with characterization have been an invaluable part of this thesis work.

Finally, I would like to thank my family, as well as J.D. Feist (who really wanted a shout out), for their love, support, and encouragement over the past four years. I would not have survived Caltech without them.

This work has been supported in part by the Richard H. Cox and John Stauffer Fellowships of the Caltech SURF program. Financial support from the National Institutes of Health is gratefully acknowledged.

ABSTRACT

Organosilanes are advantageous in organic synthesis due to their ability to act as both stable products and reactive intermediates. A stereospecific one-pot cascade reaction that converts chiral allylic silanes into chiral heterocycles was developed using Lewis acid catalysis. We report on the development of this cascade reaction, optimization to benchtop-scale chemistry, and preliminary investigation into the synthetic scope. In our studies, we were successful in varying the cyclization ring size, investigating cyclization preference in the presence of multiple electrophilic leaving groups, and altering the functional groups present on the aldehyde starting material. Ultimately, we envision this method will be useful in the synthesis of a variety of enantioenriched heterocycles found in bioactive natural products, many of which have may find use as potential drug targets.

PUBLISHED CONTENT AND CONTRIBUTIONS

Portions of the work described herein were disclosed in the following communication:

Hofstra, J. L.; Cherney, A. H.; Ordner, C. M.; Reisman, S. E. *J. Am. Chem. Soc.* **2018**,
140(1), 139-142.

DOI: 10.1021/jacs.7b11707

This article is available online at: <http://pubs.acs.org/doi/abs/10.1021/jacs.7b11707>

Copyright © 2018 American Chemical Society

C.M.O. participated in the derivatization of the allylic silanes prepared via this method and participated in the writing of the supporting information.

TABLE OF CONTENTS

Acknowledgments	iii
Abstract.....	v
Published Content and Contributions	vi
Table of Contents	vii
Chapter I: Background on Allylic Silanes	1
1.1 Organosilanes as Tools in Organic Synthesis	1
1.2 Reactivity of Allylic Silanes with Electrophiles	2
1.3 Leveraging Reactivity to Make Stereospecific Transformations	3
1.4 Alternate and Optimal Reaction Conditions	6
1.5 The Sakurai Allylation in Total Syntheses	9
1.6 Other Reactions Between Allylic Silanes and Aldehydes	11
1.7 Selected Methods to Synthesize Chiral Allylic Silanes	13
1.7.1 Stereospecific Approaches	13
1.7.2 Stereoselective Approaches	15
1.8 Cross-Coupling as a Modular Approach to Chiral Allylic Silanes	18
Chapter II: Reaction Design and Results	23
2.1 Conception and Basis for Reactivity	23
2.2 Initial Screening of Lewis Acids	26
2.3 Screening of Additives to Promote Cyclization	29
2.4 Applying the Method to Tetrahydrofurans	31
2.5 A More Efficient Route Toward Allylic Silane Reagents	32

2.6 Modifications to a Generalized Bench Top Procedure.....	34
2.7 Substrate Scope.....	37
2.8 Conclusions and Future Directions	41
Supporting Information	42
Methods	43
Chiral SFC Traces	60
¹ H and ¹³ C Spectra	62
Bibliography	98

Chapter 1

Background on Allylic Silanes

1.1 ORGANOSILANES AS TOOLS IN ORGANIC SYNTHESIS

Organosilanes are valuable compounds due to their applications in medicinal chemistry and as reagents for chemical synthesis. In pharmaceutical pursuits, the replacement of carbon with silicon has a twofold effect. In some cases, exchanging a carbon atom for a silicon atom has been shown to improve therapeutic effects of known drugs **1-3** (Figure 1).¹ While the two atoms have similar electronic properties, there are subtle differences between the two such as the increased C–Si versus C–C bond length. This can result in drastic in vitro effects, such as modified selectivity or metabolic rate.² Furthermore, sila-substitution can lead to better definitions of intellectual property in the pharmaceutical industry, making these molecules more enticing for companies to invest time and money into their development.

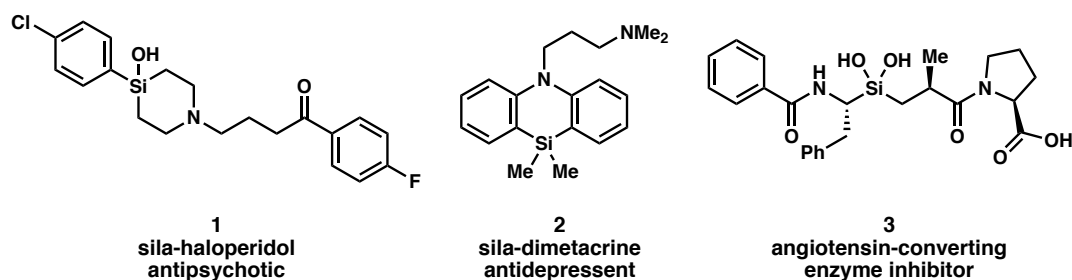


Figure 1. Sila-substituted analogues of known drugs.

In order to synthesize complex organic compounds such as the bioactive molecules (**1-3**) in Figure 1, the synthetic organic chemist must construct these molecules in a stepwise fashion, drawing on reactions available to them from their synthetic toolkit. The use of organosilicon compounds as reagents has garnered increasing interest in the organic chemistry community.³⁻⁶ The advantages these reagents are numerous – stability under a variety of reaction parameters, reactivity under mild conditions, and functional group compatibility for use on a wide variety of compounds. These benefits open up new avenues for reaction design, thus adding new reaction methods to the synthetic organic chemist's toolkit. In comparison to other organometallic reagents, silicon is significantly less ionic than other metal atoms, only forming a weakly polar bond with carbon. However, this property makes silicon-based groups generally unreactive toward electrophilic species. Nevertheless, given certain conditions, reactions with electrophiles can occur.

1.2 REACTIVITY OF ALLYLIC SILANES WITH ELECTROPHILES

In terms of reaction development, the allyl silyl motif has become an increasingly popular candidate for starting materials as their electronics lend themselves to regioselective

reactions with electrophilic compounds. Silyl groups are electron-donating and therefore are capable of stabilizing carbocations that are β to the silicon atom. More specifically, in the case of allylic silanes, the carbon-silicon σ bond exhibits conjugation with the π bond of the olefin.⁷ This electronic structure increases the energy of the highest occupied molecular orbital and therefore allylic silane motifs (**4**) can be highly reactive with electrophiles, forming carbocation intermediate **5** en route to **6** (Figure 2). Additionally, allylic silanes do not readily isomerize like their allyl metal counterparts; this isomerization only occurs at temperatures of 500 °C, thus making reactions of allylic silanes with electrophiles regioselective, unlike with other allyl metal compounds.⁸

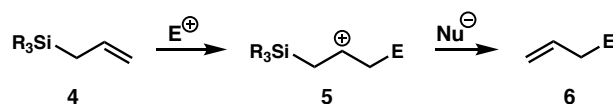


Figure 2. General reaction scheme of allylic silanes with electrophiles.

1.3 LEVERAGING REACTIVITY TO MAKE STEREOSPECIFIC TRANSFORMATIONS

One of the first reactions between allylic silanes and carbonyl compounds was performed in 1974 in order to do synthesize homoallylic alcohols. Calas and coworkers reported the synthesis of homoallylic alcohols using activated organosilanes, such as allylic silanes, in the presence of catalytic, chlorinated Lewis acids (e.g. aluminum trichloride, gallium trichloride, and indium trichloride).^{9,10} Although the work was groundbreaking for its unique use of organosilanes as reagents, the scope remained limited to only two chlorinated carbonyl substrates (**8**): chloral and chloracetone (Figure 3). Another

shortcoming of the reaction was the additional desilylation step required to get to the alcohol product, as the addition of the allylic silane (**7**) to the chlorinated carbonyl compounds (**8**) results in a silyl ether intermediate (**9**). In terms of reaction development, this linear sequence left room for further studies to optimize a one-step procedure. Furthermore, a more expansive substrate scope beyond the two chlorinated carbonyl substrates became necessary for this reaction to have broad-reaching synthetic utility.

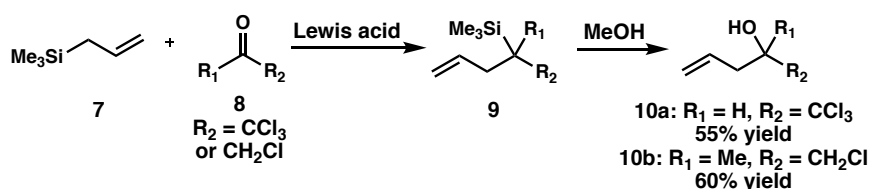


Figure 3. Selected reactions of allylic silanes reacting with chlorinated aldehydes and ketones, catalyzed by chlorinated catalytic Lewis acid.

At roughly the same time as Calas' work, a major breakthrough happened in the field. Sakurai et al. reported the reaction between allylic silanes and Lewis acid-activated carbonyl compounds, expanding the scope to a wide variety of carbon electrophiles (**11**) with varying degrees of success. Addition of the allyl fragment and loss of the silyl group provides γ,δ -unsaturated alcohols (Figure 4). This stereospecific reaction built upon previous work done by Calas and coworkers through use of stoichiometric titanium tetrachloride as the activating Lewis acid. Through use of this reagent, the scope of carbon electrophiles that could react with allylic silanes expanded to include aliphatic, aromatic, and alicyclic carbonyl compounds (**11**).⁷

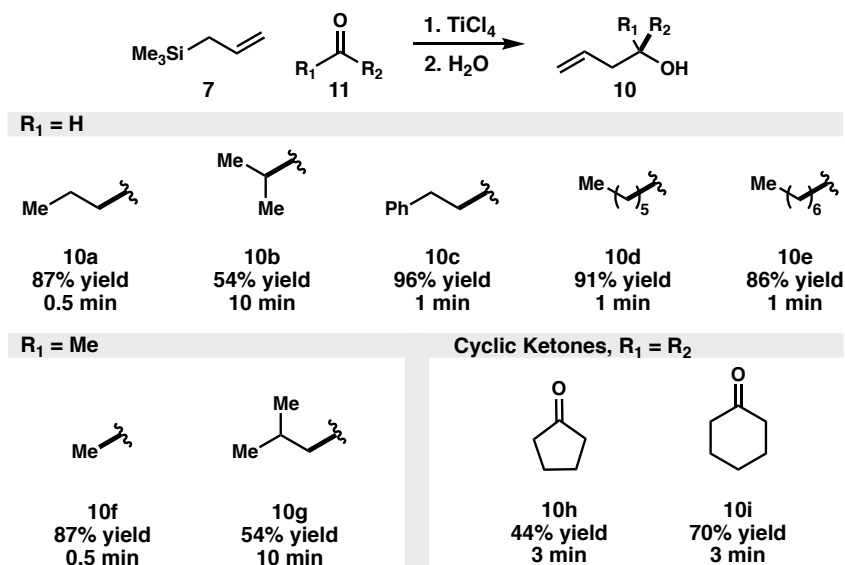


Figure 4. General reaction scheme for the Hosomi-Sakurai allylation between trimethylallylsilane and selected substrates.

When analyzing the results in Figure 4, certain patterns begin to emerge regarding steric demand and yield. Linear carbonyl compounds (**11a,11c-f**) tend to react quickly with high yields. The addition of steric bulk at the β or γ carbons both decreases yield and requires an increase in reaction time, as with isobutyraldehyde (**11b**) and 4-methylpentan-2-one (**11g**). As the sterically encumbering groups increase in distance from the site of the reaction, the yield increases and less reaction time is needed, as with 3-phenylpropanal (**11c**). These trends also explain the decrease in yield of cyclic ketones (**11h,i**) with the decrease in ring size. Smaller rings are more rigid and are more susceptible to steric issues.

The Sakurai allylation is relatively simple to carry out in a synthetic chemistry laboratory. Typically the reaction is run under a nitrogen atmosphere with dichloromethane as the solvent, and an aqueous workup is performed in order to protonate the alkoxide to the homoallylic alcohol product. This carbon-carbon bond formation is conducted on

relatively short timescales, such as 0.5 to 10 minutes (Figure 4). When exposed to the Lewis acid for extended periods of time, the yield of the desired product diminishes due to side reactions such as polymerization.

While the Sakurai allylation provides a robust method to produce alcohols from the acid-catalyzed reaction between allylic silanes and carbonyl compounds, the value of the alcohol product is often overlooked. The alcohol functional group can be viewed as a stopping point in a synthetic scheme rather than a useful tool for chemists in their pursuit of constructing complex molecules. Building upon this notion, the reaction conditions reported by Sakurai became the starting point for our own work. Instead of isolating the homoallylic alcohol (**14**), we envisioned avoiding the aqueous workup and hypothesized whether or not the alcohol intermediate could be used to synthesize a heterocyclic product (**15**) in situ (Figure 5). Progressing this established methodology onward to more complex and synthetically challenging heterocycle motifs is the core focus of this thesis work.

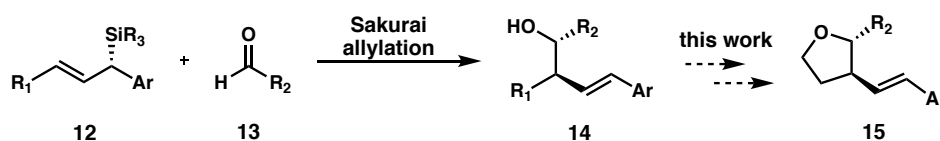


Figure 5. Conceptual basis for thesis work stemming from the Sakurai allylation.

1.4 ALTERNATE AND OPTIMAL REACTION CONDITIONS

In these allylation reactions, a Lewis acid is required to activate the carbonyl moiety. Sakurai first reported the use of titanium tetrachloride which provides relatively good yields of the desired allylation products when using a wide variety of carbonyl

compounds. However, this Lewis acid is not always optimal. In fact, Sakurai reports on using other Lewis acids on a case-by-case basis, such as boron trifluoride diethyl etherate, ethylaluminum dichloride, and tin tetrachloride.^{7,11} Even still, titanium tetrachloride tends to be the more universally accepted activating agent for these allylation reactions.

A shortcoming of the Sakurai allylation reaction is that it requires stoichiometric amounts of Lewis acid in order to activate the carbonyl species present in the reaction mixture. However, stoichiometric quantities of Lewis acid are not ideal when it comes to method development. It is economically inefficient and, depending on the reagent, can be somewhat dangerous. Therefore, it is desirable to develop methods which use catalytic amounts of the Lewis acid.

Catalytic Lewis acids were discovered to work in the Sakurai allylation with aldehydes nearly two decades later using a chiral (axyloxy)borane catalyst. Ishihara and coworkers report their synthesis of the chiral (axyloxy)borane catalyst (**8**) and showcase its utility in terms of great yields, good diastereoselectivity, and excellent enantiomeric excess, especially when using substituted allylic silane reagents (**17**).¹² They found that 20 mol% loading of the catalyst to be the most successful, as lower catalyst loading resulted in severe decreases in yield. The catalyst produces silylated homoallylic alcohols (**19**) and upon further treatment with tetrabutylammonium fluoride, the desilyated alcohol product was observed. Yields were improved by substituting the allylic portion of the silyl starting material, due to improved asymmetric induction (Figure 6). Although they developed a catalytic allylation reaction, the types of carbonyl compounds that could participate in this reaction limited to simple aldehydes and ketones.

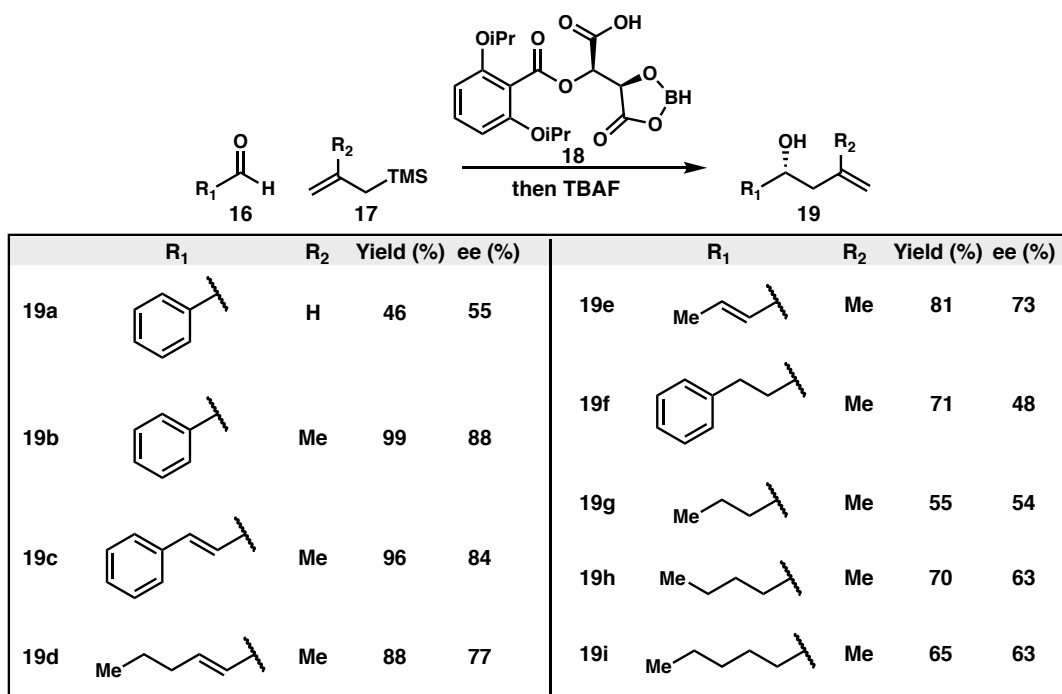


Figure 6. Asymmetric allylation with a chiral (acyloxy)borane catalyst.

Due to the need for a catalytic Sakurai allylation that could react with more complex aldehydes and ketones, efforts continued in order to develop methods with more expansive substrate scopes, particularly those that included cyclic ketones (**20**). In 2005, Wadamoto and Yamamoto reported a method which used a silver catalyst to form chiral homoallylic alcohols from allyltrialkoxysilanes (**21**) and ketones.¹³ Using (*R*)-DIFLUOROPHOS (**22**) as a ligand that complexes with silver fluoride (1:1 molar ratio), Wadamoto was able to access a wide variety of homoallylic alcohol products (**10**) with excellent enantioselectivity and good yields using only 5 mol% catalyst loading (Figure 7).

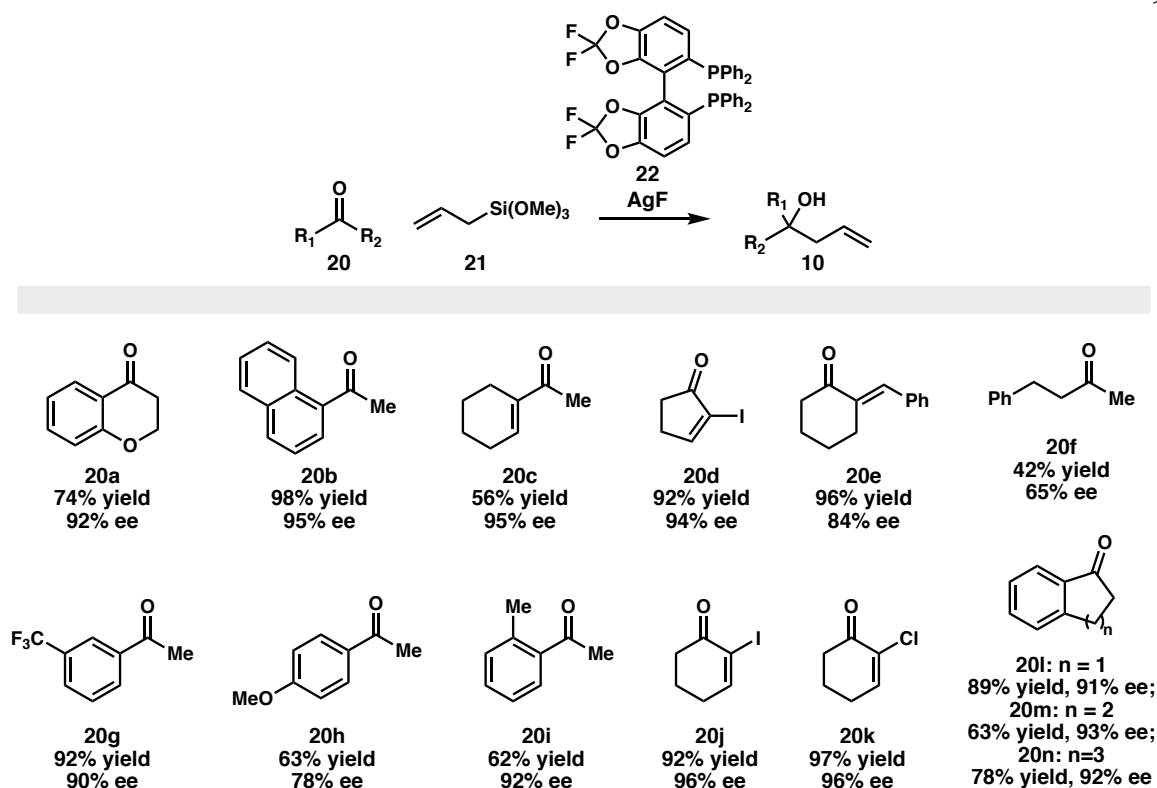


Figure 7. Catalytic, asymmetric Sakurai allylation with various ketone substrates.

It is evident from these selected reactions that the Sakurai allylation has been elaborated upon extensively since its initial report. Each of these reactions has showcased a way in which one could access enantioenriched homoallylic alcohol products in good yields, demonstrating the synthetic value of this transformation.

1.5 THE SAKURAI ALLYLATION IN TOTAL SYNTHESSES

Reactions between aldehydes and allylic silanes, particularly the Sakurai allylation reaction, have been used in several total syntheses in the past few decades. One synthesis that showcases the Sakurai allylation is Williams' asymmetric construction of (+)-amphidinolide P (**25**). This macrolactone is a molecule in the amphidinolide family, known

for its cytotoxic and potential antitumor activity. Using boron trifluoride diethyl etherate as the Lewis acid for the Sakurai allylation, Williams was able to construct the hydroxyl stereocenter with moderate selectivity and good yield (60%).¹⁴ The alcohol (**24**) is used to later form the heterocyclic ring of the macrolide (Figure 8). Although the diastereomeric ratio of 2:1 leaves room for improvement, the minor diastereomer can be converted to the desired isomer through use of the Mitsunobu reaction which inverts the stereochemistry at the site of the carbon-oxygen bond. The allylation product is then advanced to complete the first total synthesis of (+)-amphidinolide P.

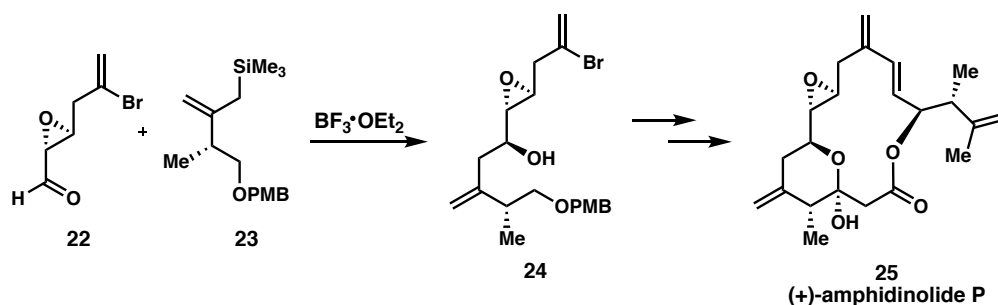


Figure 8. Williams' use of the Sakurai allylation has poor diastereocontrol, but the undesired isomer can be inverted with a Mitsunobu reaction.

In 2003, the Trost laboratory used the Sakurai allylation in synthesis of three furaquinocins (**28a** and **28b**), a class of molecules known primarily for their antibiotic activity but which also show cytotoxic and antihypertensive activity.¹⁵ The aldehyde moiety on the bicyclic core of the molecule (**26**) was used as a functional handle for the allylation step in the total synthesis (Figure 9). The diastereoselective Sakurai allylation of the core with allyltrimethylsilane (**7**) was able to introduce the alcohol stereocenter with moderate selectivity (dr 4:1). From this allylation product, the two isomeric forms of the

olefin could be elaborated upon using alkene metathesis to complete the total synthesis of furaquinocin A and furaquinocin B.

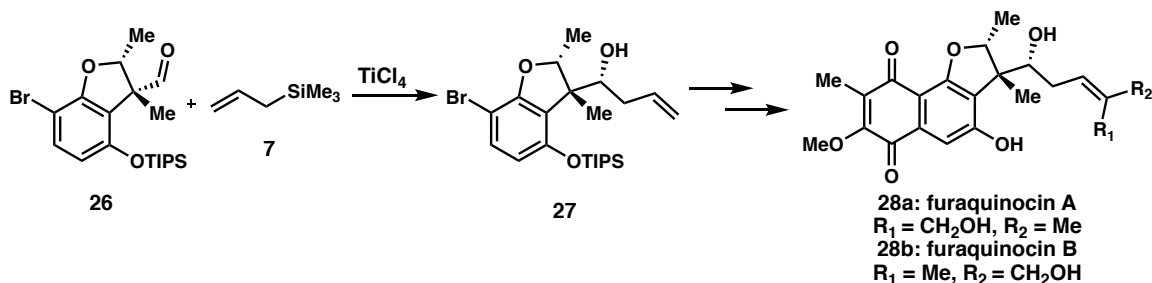


Figure 9. Late stage Sakurai allylation in Trost's synthesis of furaquinocins.

1.6 OTHER REACTIONS BETWEEN ALLYLIC SILANES AND ALDEHYDES

While all of the previous examples include the loss of the silyl group upon addition of the allyl fragment to the aldehyde, other transformations between allylic silanes and aldehydes have been reported. De Fays and coworkers were able to synthesize enantioenriched β -hydroxy allylsilanes (**32**) using allylic silanes (**28**).¹⁶ Through transmetallation with stoichiometric *n*-butyllithium and then a chiral allyltitanium compound (**29**), stereochemical information is transferred from the organometallic reagent to the final cyclic diene (**32**), creating two stereocenters on the molecule with good yield and in excellent enantioselectivity (Figure 10).

It has been established that the Sakurai allylation can be initiated through activation of the aldehyde with various Lewis acids such as titanium tetrachloride and boron

trifluoride etherate. Similarly, chiral organoborane compounds can be used in place of a chiral titanium complex in order to prepare chiral hydroxysilanes with excellent yields.

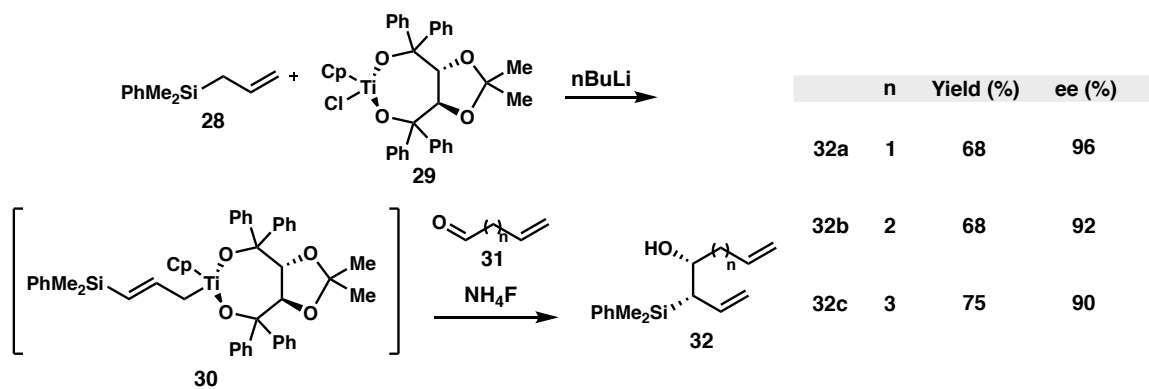


Figure 10. Asymmetric allylmethylation of aliphatic aldehydes with an allylic silane.

According to Chabaud et al., the use of organoboranes is of growing interest to the organic community, as it provides a means to both efficiently and reliably synthesize chiral allylic silanes.⁵ A γ -silylallylboronate intermediate (**34**) can be synthesized easily with one step from a simple allylic silane starting material (Figure 11). This intermediate is then exposed to an aldehyde with a terminal olefin, and upon a basic workup, β -hydroxyallylsilane **36** is formed in great yield (86%) and with excellent enantiomeric excess (94%).¹⁷ Roush and coworkers do not report on an extensive substrate scope using this method, but were able to run it on an additional aldehyde containing benzyl ether functional groups in some of their later studies.¹⁸ They can elaborate these β -hydroxyallylsilane intermediates using Grubbs' second-generation catalyst with ring closing metathesis in order to generate chiral cyclic allylic silanes (**37**).

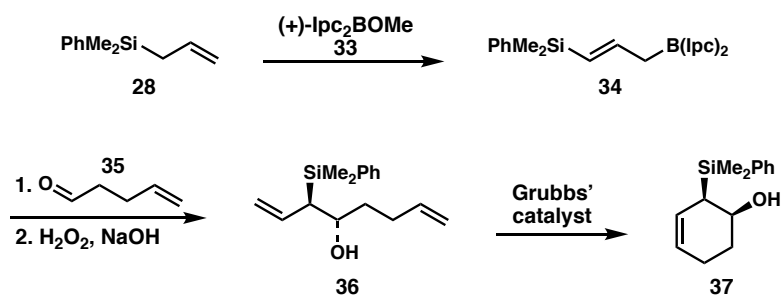


Figure 11. Synthesis of chiral β -hydroxyallylsilanes can undergo ring-closing metathesis to a cyclic form, starting from a γ -silylallylboronate intermediate.

1.7 SELECTED METHODS TO SYNTHESIZE CHIRAL ALLYLIC SILANES

1.7.1 STEREOSPECIFIC APPROACHES

Although recent work by Roush showcases a unique method with which to synthesize allylic silanes, the synthesis of these compounds have intrigued the community for decades. In 1991, Panek and coworkers reported a series of papers on the Claisen rearrangement of chiral vinyl silanes to optically pure α -chiral- β -silyl-(*E*)-hexanoic acids (**38**).^{19,20} The diastereoselectivity of the products could be altered by changing the reaction conditions, strongly favoring either the syn (**39**) or anti (**40**) products (Figure 12). Their methodology was able to tolerate silyl groups of various steric demands, as well as various functional groups at the second stereocenter on the molecule. Product yields using this method were quite good, ranging from 55-95%. However, the reaction was somewhat limited as all products contained either a terminal ester or acid group, and all products were synthesized from very specific chiral vinyl silane motifs.

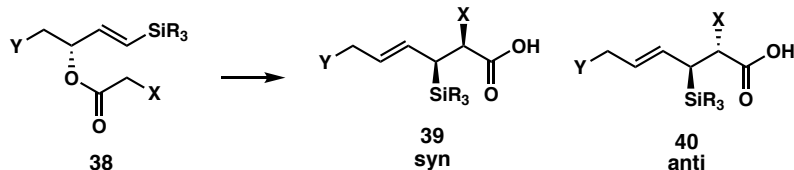


Figure 12. Synthesis of chiral silyl hexanoic acids via a Claisen rearrangement.

With the lack of a relatively generalized synthesis of these allylic silane reagents, the Ito group later reported on a method to diastereoselectively convert chiral allylic alcohols to allylic silanes via a disilanyl ether intermediate (Figure 13).²¹ By first reacting the allylic alcohol with 1-chloro-1,1-dimethyl-1,1,2-triphenyldisilane (**42**), they were able to access a silyl ether (**43**) that could undergo an intramolecular cyclization using catalytic amounts of 1,1,3,3-tetramethylbutyl isocyanide and palladium acetylacetonate. The silicon-oxygen bonds on the heterocyclic intermediate (**44**) were cleaved through use of an organolithium reagent, affording chiral allylic silane products (**45**) with good yields and excellent enantioselectivity. This bis-silylation methodology allowed for access to a wide variety of aliphatic allylic silane products. However, the use of strong organometallic reagents limits the functional group tolerance of this reaction.

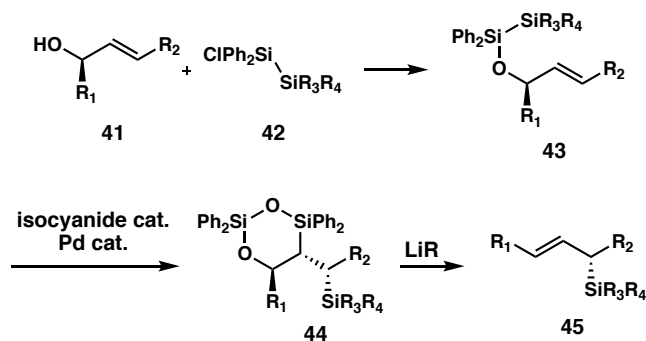


Figure 13. Bis-silylation of allylic alcohols to afford chiral allylic silane products.

Due to challenges in the synthesis of these compounds, such as poor functional group compatibility, work continued on developing new methods to construct these allylic silanes. Shortly after Ito's work, the Woerpel group reported on the use of various silver and copper catalysts for silylene insertions into carbon-oxygen bonds in order to produce chiral allylic silanes (Figure 14).²² Depending on the catalyst and substrate used, they were able to access dilanes in addition to allylic silanes. Starting from optically pure allylic alcohols (**46**), they are able to produce the desired allylic silanes (**48**) in moderate yields (63-74%) but with severe erosion of enantioselectivity (36% ee).

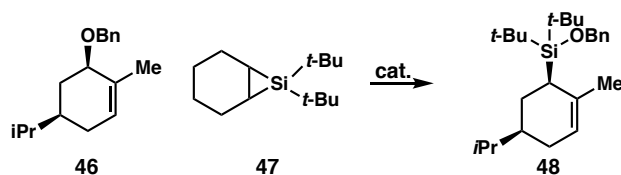


Figure 14. Silylene insertion of allylic ethers to chiral allylic silanes.

1.7.2 STEREOSELECTIVE APPROACHES

The previous methods all leverage the chirality of the starting material in order to produce enantioenriched allylic silanes through stereospecific transformations. Recently, efforts have focused on using chiral catalysts in order to set the stereocenters of the molecule using stereoselective approaches. In the past few decades, there have been numerous metal catalysts used to perform silicon-hydrogen insertion of vinylcarbenoids.²³ Davies and coworkers reported some of this asymmetric methodology in 1997. Through use of a rhodium (II) propionate catalyst (**51**), they were able to convert vinyl diazomethanes (**49**) to allylic silanes (**52**) with excellent enantiomeric purity (77-95%

ee) and high yields (63-77%).²⁴ The silyl group is introduced through use of dimethylphenylsilane (Figure 15). This reactivity pattern was later explored in greater detail.

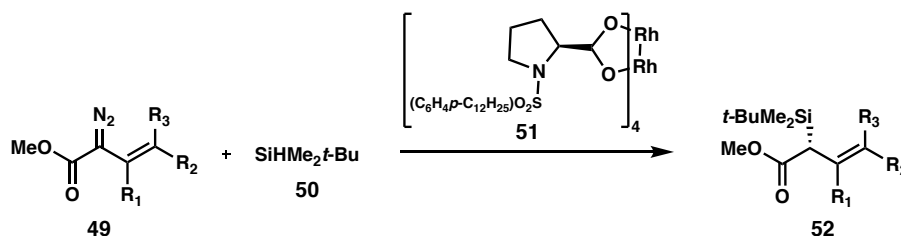


Figure 15. Use of rhodium (II) catalyst to form chiral allylic silanes.

In 2010, Wu, Chen, and Panek elaborate on the work of Davies by developing copper(I) catalysts to prepare chiral allylic silanes from similar vinyl diazomethane (**53**) and dimethylphenylsilane (**54**) starting materials.²⁵ These copper catalysts tend to provide the products in decreased yields (44-55%) and with lower levels of enantioselectivity (70-78%), but they can be run at higher temperatures (0 °C) in comparison to the same reactions with the rhodium catalyst (−78 °C). They are able to further elaborate these allylic silane products (**55**) via an allylation reaction to obtain products (**56**) in excellent yields (61-88%) but with moderate diastereoselectivity (Figure 16).

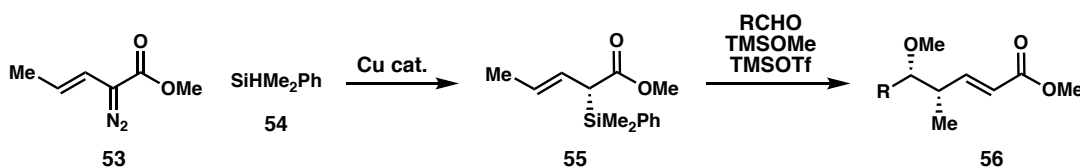


Figure 16. Use of copper(I) catalyst to synthesize chiral allylic silanes, which can be further reacted with aldehydes.

Copper catalysts continued to be investigated for their use in setting stereocenters on allylic silanes. Kacprzyński and coworkers reported a method which uses copper catalysts to perform asymmetric alkylation reactions using silyl-substituted unsaturated phosphates.²⁶ This reaction differs from the previously mentioned metal-catalyzed syntheses of allylic silanes, as its method does not hinge upon the formation of carbon-silicon bonds to form the stereogenic center. Instead, aryl or alkyl substitution to the silyl-substituted carbon (**57**) provides for a route with which tertiary and quaternary silyl-substituted carbons can be formed from secondary or tertiary silyl-substituted carbons, respectively (Figure 17). This methodology uses a chiral *N*-heterocyclic carbene ligand (converted to copper-based catalysts generated in situ with a copper salt) in conjugation with an organozinc reagent in order to form chiral allylic silanes (**58**) with excellent enantioselectivity. The shortcoming of this procedure is that it requires the starting material to already have a silyl group on the molecule. This lack of modularity prevents this reaction from being universally applicable in the synthesis of chiral allylic silanes from simple starting materials.

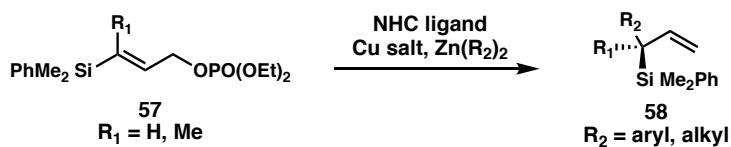
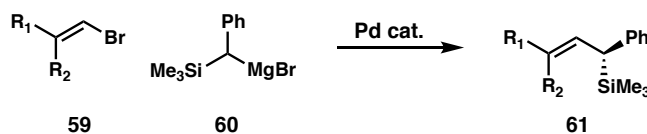


Figure 17. Allylic substitution reaction with a copper catalyst generated in situ to form chiral allylic silanes.

1.8 CROSS-COUPLING AS A MODULAR APPROACH TO CHIRAL ALLYLIC SILANES

Cross-coupling methodology can also be used to synthesize the chiral allylic silane compounds prepared by Kacprzynski and coworkers. However, this approach which sets the sp^3 stereogenic center in a direct carbon-carbon bond formation has the benefit of allowing for more modularity when synthesizing allylic silanes. The cheap, simple starting materials can be easily modified prior to the cross-coupling in order to produce a wide variety of substituted allylic silanes. The first synthesis of enantioenriched chiral allylic silanes was reported in 1982 through a cross-coupling reaction developed by Kumada et al. (Figure 18).²⁷ Kumada employed the use of a ferrocenyl-palladium complex to promote catalysis and the fidelity of the olefin substitution is retained. This reaction is not only important due to its ability to form the allylic silane products (**61**) with high levels of enantioselectivity, but it is also important due to its lack of E-Z isomerization of the olefin.



R ₁	R ₂	Olefin	% Yield	% ee
H	H	-	42	95
Me	H	E	77	85
H	Me	Z	38	24
Ph	H	E	93	95
H	Ph	Z	95	13

Figure 18. Kumada's cross-coupling methodology to synthesize chiral allylic silanes.

Kumada further elaborated his work by demonstrating the first stereoselective Sakurai allylation using these enantioenriched allylic silanes. His work helped elucidate the acyclic linear diastereomeric transition states of the allylation reaction, where disfavored steric interactions lead to the formation of products with high levels of diastereoselectivity. The anti-selectivity of this reaction can be explained through an acyclic linear transition state (**62** and **63**), which minimizes steric interactions between the bulky alkyl groups (Figure 19). In this study, allylic silanes with E olefin configuration (**61**) were observed to consistently have good yields and excellent enantioselectivity when forming the homoallylic alcohol products (Figure 20).²⁸ Despite the novelty of Kumada's approach to synthesizing chiral allylic silanes, the utility of his method utilized a Grignard reagent in the cross-coupling reaction, which limits the functional group tolerance of the transformation.

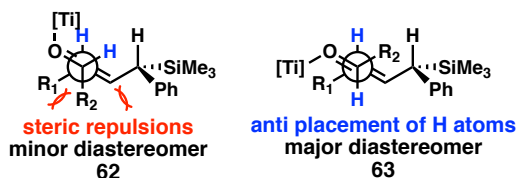


Figure 19. Newman projections show the minimizing of gauche interactions in Kumada's allylation.

Organomagnesium halides, such as the magnesium bromide group in Kumada's reaction, are highly reactive and exhibit limitations in functional group compatibility. Additionally, Grignard reagents are both air and water sensitive and often are not amenable for long-term storage. Since the initial report by Kumada, no syntheses of chiral allylic

silanes have used this cross-coupling approach to set the Csp³ stereocenter, possibly due to the use of sensitive Grignard reagents.

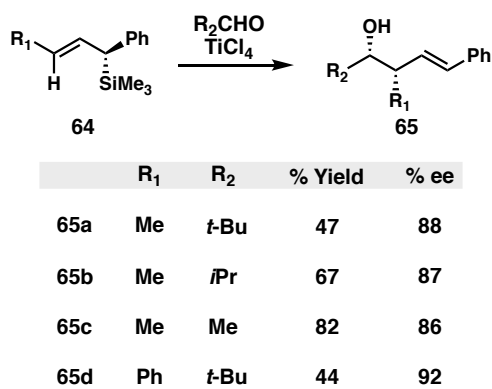


Figure 20. Kumada's Sakurai allylation.

In order to overcome this shortcoming, the Reisman group was able to develop a nickel-catalyzed asymmetric reductive alkenylation reaction to afford chiral allylic silanes (**68** and **70**).²⁹ This method allows for the use of stable electrophiles as both coupling partners and alleviates the need for sensitive organometallic reagents (Figure 21). This particular method was realized following the development of related nickel-catalyzed alkenylations, first between vinyl and benzyl electrophiles (**66** and **67**) and later between *N*-hydroxyphthalimide esters (**69**) with vinyl bromides (**67**).^{30,31} Through use of a manganese as a reducing agent which can turn over the nickel catalytic cycle, allows two electrophilic components to be cross-coupled, minimizing any typical issues found with nucleophilic reagents, such as cost, stability, and somewhat uncontrolled reactivity. Nickel, as a group 10 metal, does exhibit much of the same reactivity as palladium, however it can access more oxidation states which leads to a wider variety of potential mechanistic pathways. Nickel can access up to five different oxidation states (0, +1, +2, +3, +4), whereas the

palladium catalytic cycle typically only undergoes redox reactions between the 0 and +2 states. Given its ability to access odd oxidation states, nickel can also participate in a variety of radical mechanisms, unlike palladium.³² Overall, nickel is a much more reactive and economical catalyst choice, however tuning this reactivity to afford desired reaction products in place of undesired side products becomes the main challenge in optimizing nickel-catalyzed cross-coupling reactions.

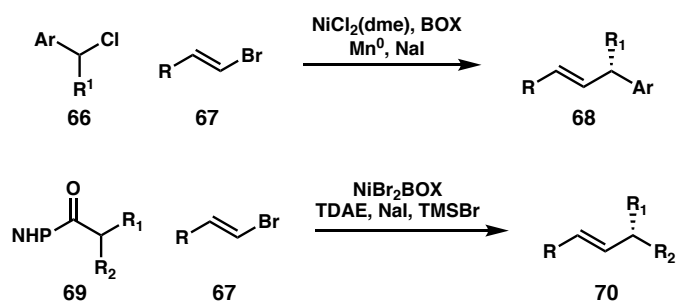


Figure 21. Selected nickel-catalyzed reductive cross-coupling methods developed by the Reisman group.

The synthesis of chiral allylic silanes by enantioselective nickel-catalyzed reductive cross-coupling proceeded in good yield only in the presence of a cobalt (II) phthalocyanine co-catalyst (Figure 22). This reagent promotes alkyl radical generation, which more than doubles the yield of the desired product in comparison to reactions run without the co-catalyst.²⁹ They hypothesize that the steric demands of the bulky silyl group disfavors oxidative addition of the silyl-substituted benzyl chloride coupling partner (71) to the nickel catalyst. The developed reaction conditions are mild and can tolerate a wide variety of functional groups, showcasing the versatility of this methodology (Figure 23). The substrate scope investigated in this method laid the foundation for the development of this

work, as chiral allylic silanes with pendant electrophiles can be synthesized using these procedures. We envisioned that these novel allylic silane products could be elaborated to more challenging heterocyclic motifs common in natural products.

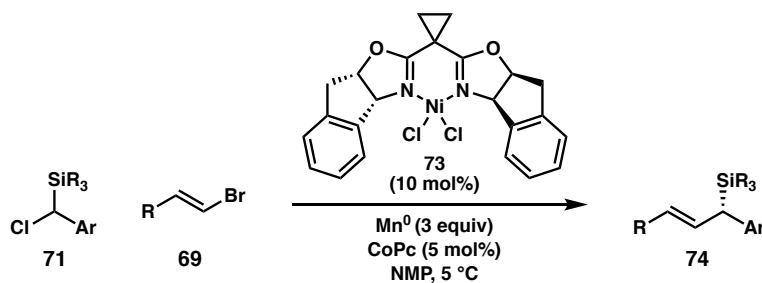


Figure 22. Reisman's asymmetric cross-coupling method to afford chiral allylic silanes under mild conditions.

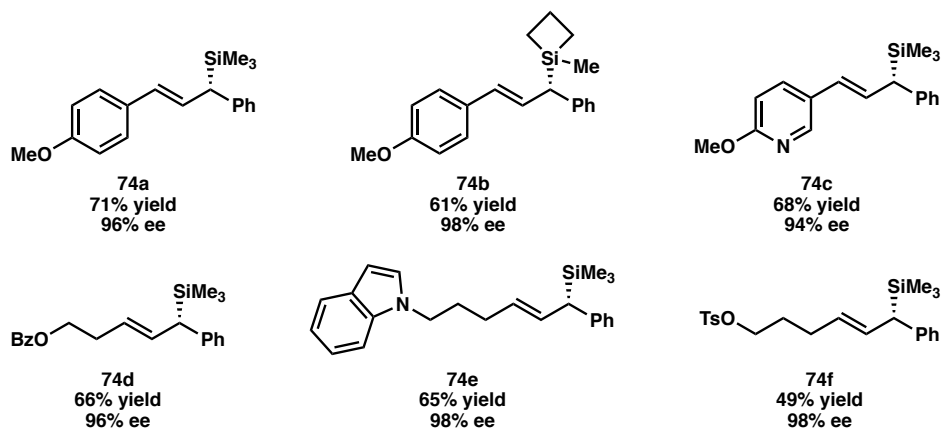


Figure 23. Selected chiral allylic silane substrates prepared using Reisman's approach.

Chapter 2

Reaction Design and Results

2.1 CONCEPTION AND BASIS FOR REACTIVITY

Recent efforts in the Reisman group have focused on new asymmetric reductive cross-coupling methods, as discussed in Chapter 1.8. Reaction conditions to synthesize chiral arylated alkenes have been modified to handle a rather sterically demanding reagent, a silyl substituted benzyl chloride (**71**). Cross-coupling between this reagent and a vinyl bromide (**69**) can produce chiral allylic silanes (**74**) with high yields and excellent enantioselectivity (Figure 24). More importantly, these cross-coupling conditions can tolerate vinyl bromides including pendant electrophiles such as alkyl chlorides, bromides, and tosylates. We envisioned these allylic silanes containing terminal electrophilicities to be useful in our endeavors to elaborate these chiral allylic silane products into a variety of heterocyclic motifs.

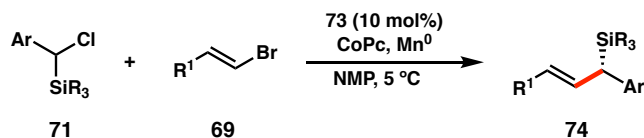


Figure 24. Asymmetric reductive cross-coupling between silyl substituted benzyl chlorides and vinyl bromides to provide access to chiral allylic silanes.

With this research, we sought to design a new cyclization reaction to aid in the construction of complex bioactive natural products, particularly those with heterocyclic motifs. Many natural products and pharmaceutical drug candidates contain five- and six-membered rings with oxygen and nitrogen incorporation (**75-79**), some of which exhibit a variety of therapeutic effects (Figure 25). These heterocyclic rings can be difficult to synthesize, so we aimed to develop a one-pot reaction to afford these chiral scaffolds.

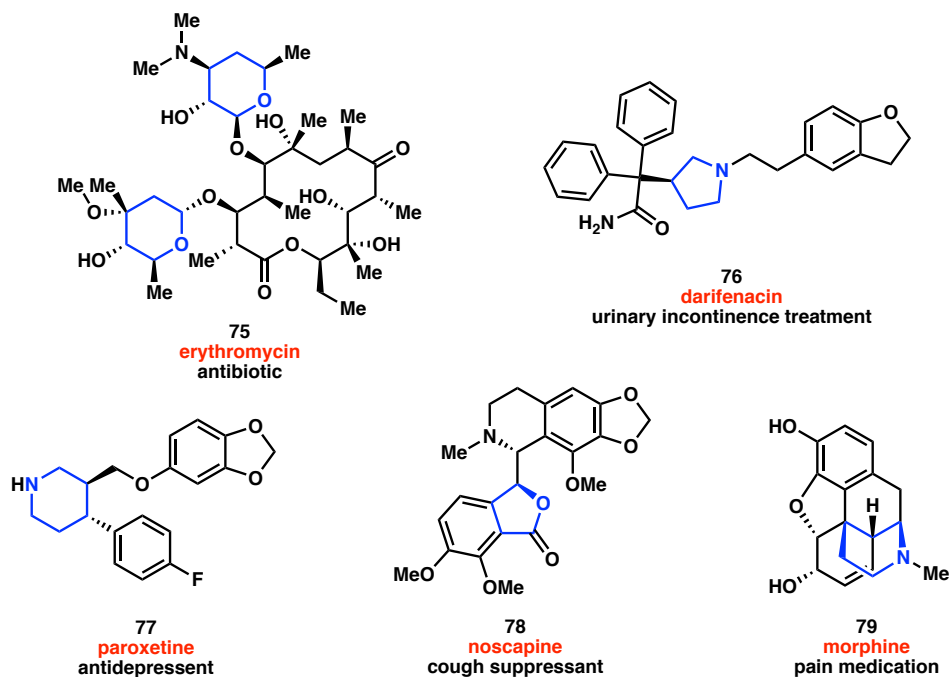
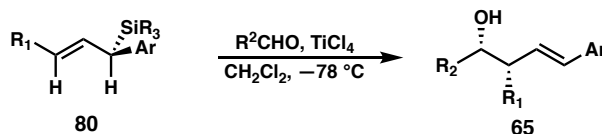


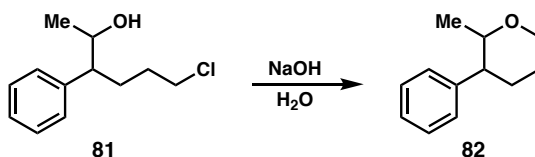
Figure 25. Heterocyclic bioactive natural products and their medicinal uses.

With the knowledge that the addition of chiral allylic silanes to carbonyl compounds can lead to the synthesis of chiral homoallylic alcohols with little to no erosion of enantioselectivity, we proposed a novel method for the synthesis of chiral heterocycles with oxygen incorporation. Allylic silanes can undergo a Sakurai allylation with a wide variety of carbon electrophiles. This allylation reaction is stereospecific and highly diastereoselective, providing two stereocenters in the product (Figure 26a).²⁸ Additionally, it is known that base-mediated S_N2 cyclization reactions can occur intramolecularly between alcohols with pendant electrophiles in order to form tetrahydropyrans (Figure 26b).³³ The aim of this research was to combine these two fundamental principles and develop a one-pot procedure to convert chiral allylic silanes into chiral heterocyclic products through a tandem allylation/cyclization approach (Figure 26c).

A) Sakurai Allylation:



B) Base Mediated Cyclization:



C) This work:

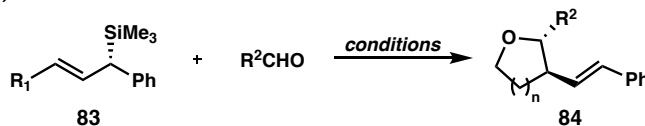


Figure 26. Literature precedent for the tandem reaction proposed in this work.

Starting from chiral allylic silanes, we propose that cyclization to heterocyclic five- and six-membered heterocyclic rings can be achieved. The cross-coupling of vinyl bromides and benzyl chlorides yields chiral allylic silanes,²⁹ which can undergo Lewis acid-catalyzed allylations with aldehydes. With these allylation products, the homoallylic alcohols are observed. We proposed that isolation of the chiral homoallylic alcohol could be avoided. Instead, intramolecular cyclization with a pendant electrophile, initially synthesized on a vinyl bromide coupling partner, could be achieved in one step during this reaction (Figure 27).

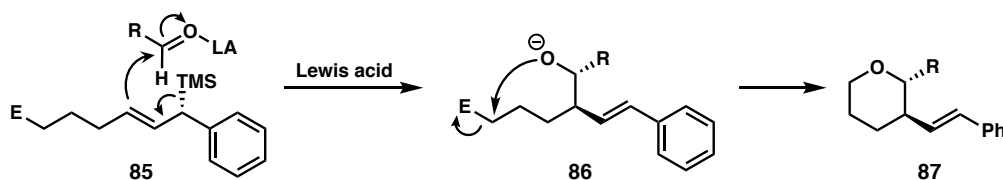


Figure 27. Proposed synthesis of tetrahydropyrans from allylic silanes.

2.2 INITIAL SCREENING OF LEWIS ACIDS

While the Sakurai allylation can be performed with either catalytic or stoichiometric amounts of Lewis acid, the majority of examples in the literature utilize stoichiometric quantities. Each molecule of Lewis acid will activate the electrophile to promote the allylation reaction via coordination to the oxygen atom of the carbonyl group. Thus, we began our investigations with stoichiometric amounts of Lewis acids in attempts to develop the aforementioned tandem reaction.

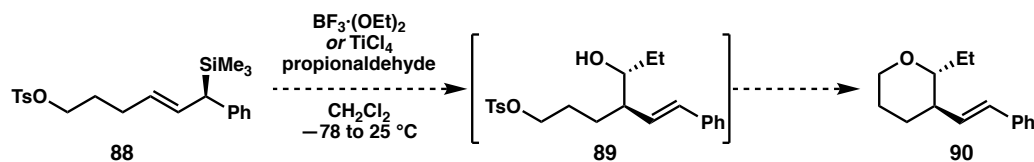


Figure 28. Preliminary screening of allylic silane with pendant electrophile with two Lewis acids commonly used in the Sakurai allylation.

Initial screening attempts investigated the use of an allylic silane with a pendant tosylate electrophile (**88**). Typical Kumada allylation conditions were employed and two different Lewis acids were tested: boron trifluoride diethyl etherate and titanium tetrachloride. Monitoring the reaction by thin layer chromatography (TLC), boron trifluoride etherate did not show significant consumption of the starting material at -78 °C, and it was not until the reaction reached room temperature that other products began to form. Four products, in addition to the starting material, were collected by preparatory TLC, however none had the predicted retention factor (R_f) for the desired cyclized product. Of these four products, proton nuclear magnetic resonance spectroscopy (^1H NMR) confirmed that the desired cyclization did not occur, as the two major products still had the tosylate group on the molecule. Liquid chromatography-mass spectrometry (LCMS) was used to analyze these two products to determine if either was the allylated alcohol intermediate, however the obtained masses (452 g/mol and 557 g/mol) did not align with this intermediate.

When the reaction was conducted with titanium tetrachloride as the Lewis acid, we observed a new major product by TLC when the reaction was cooled to -78 °C. This product had the predicted R_f for the alcohol intermediate. Similar to the reaction with boron

trifluoride diethyl etherate, warming the reaction to room temperature also resulted in four products were also collected by preparatory TLC, however LCMS confirmed that none of the products were from the desired cyclization. Furthermore, the alcohol intermediate decomposed once the reaction had warmed to room temperature, so we evaded the issue by running the reaction again and quenching with water at -78°C .

With this information in hand, we set out to quantify the amount of our alcohol intermediate. The general protocol used 1.1 equivalents of titanium chloride in dichloromethane at -45°C , the lowest temperature available in the glovebox cryocool. The model substrates we investigated included propionaldehyde and an allylic silane with a pendant chloride electrophile (this allylic silane proved more amenable to scale up to multigram scale). The reaction was quenched with water prior to warming to room temperature, which alleviated decomposition of the alcohol. Gas chromatography (GC) was used to quantify the product yields, which provided 69% yield of the alcohol intermediate and 2% yield of the desired tetrahydropyran product. With the alcohol intermediate in hand, a formal synthesis via Perrott's conditions could allow access to the heterocycle, however a reaction using a one pot procedure would be ideal. Thus, we conducted a GC assay to screen reaction conditions that would promote cyclization in good yields (Figure 29).

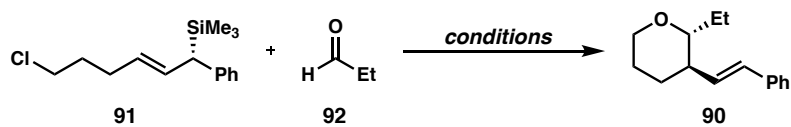


Figure 29. Method analyzed by GC assay.

2.3 SCREENING OF ADDITIVES TO PROMOTE CYCLIZATION

Given the low 2% yield of the tetrahydropyran, we proposed two hypotheses for lack of cyclization. First, we proposed that the coordination of titanium to the alkoxide prohibited intramolecular cyclization. Second, we suggested that the reaction conditions were too acidic, and rapid protonation of the alkoxide intermediate inhibited cyclization to the heterocycle.

In order to test these two hypotheses, we screened different additives and analyzed the results with our GC assay. The allylation reaction was conducted at $-78\text{ }^{\circ}\text{C}$ for two hours, and then an additive was used to promote cyclization at room temperature. Initially, a crown ether was added to see if coordination between titanium and oxygen was inhibiting cyclization to occur. We proposed that the crown ether would coordinate the titanium and displace the alkoxide. Thus would allow for the oxygen atom to attack the carbon alpha to the pendant electrophile via an $\text{S}_{\text{N}}2$ cyclization. With the addition of benzo-15-crown-5, limited cyclization (1% yield) was observed (Figure 30).

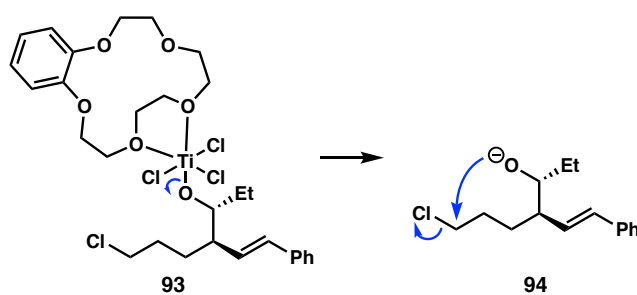


Figure 30. Proposed mechanism for crown ether additive to promote cyclization.

We then tested our second hypothesis by adding base to the reaction mixture with the intent of avoiding possible protonation to the homoallylic alcohol intermediate (Figure

31). With the addition of a mild base, 2,6-lutidine (**95**), the desired tetrahydropyran was only observed in a 2% yield. There was no improvement from the addition of either a crown ether or mild base compared to runs without any additives.

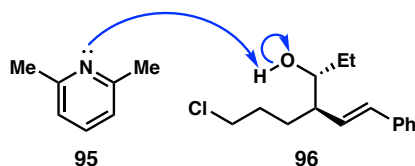


Figure 31. Proposed mechanism for mild base to promote cyclization.

Potassium *tert*-butoxide was then explored as a stronger base. When one or two equivalents were added to the reaction, minimal cyclization occurred (2% yield). However with five equivalents of potassium *tert*-butoxide, the reaction successfully produced the desired tetrahydropyran: only 1% yield of the alcohol was remaining and 69% yield of the desired product was obtained. This suggests that the issue with cyclization may be related to the displacement of the chlorides from titanium while it is coordinated to the oxygen atom (Figure 32). If the remaining three chlorides can be displaced, titanium can dissociate from the oxygen atom with a fourth equivalent of base and produce the desired cyclic product (**90**). Should this be the case, only four equivalences of potassium *tert*-butoxide are necessary to induce cyclization.

With this knowledge of the proposed mechanism, we briefly attempted to make the reaction catalytic. Instead of using titanium tetrachloride as the Lewis acid, we attempted to use titanium isopropoxide. This Lewis acid already has bulky alkoxide groups coordinated to the titanium which could render the reaction catalytic by recycling the Lewis acid in the reaction. However, with both stoichiometric (1.1 equivalents) and catalytic (0.1

equivalents) amounts of titanium isopropoxide, the reaction failed to yield any allylated product and only starting material was recovered.

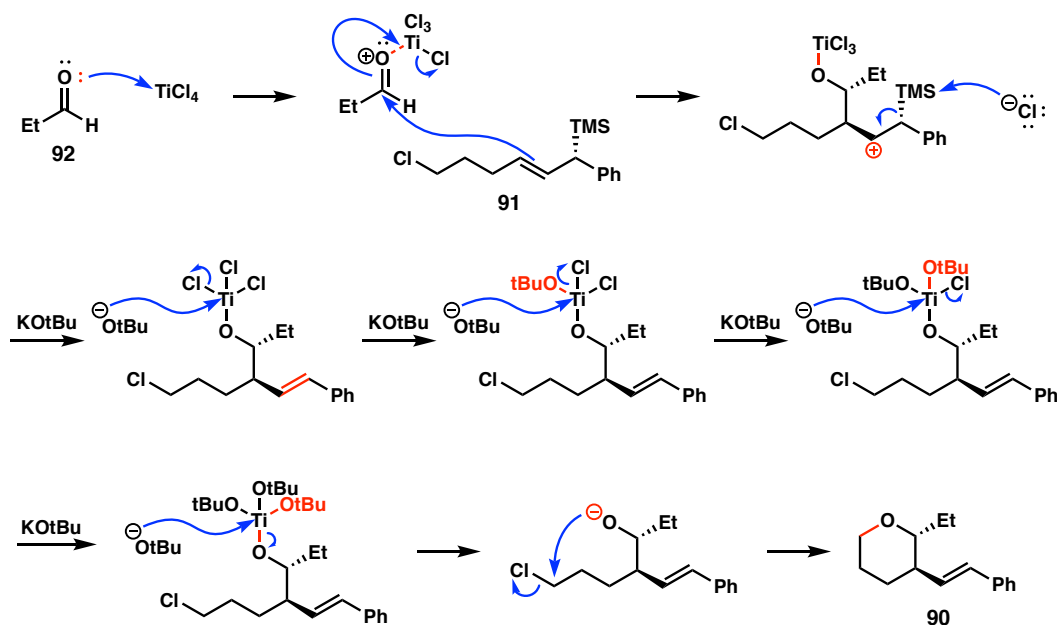


Figure 32. Proposed mechanism for cyclization with four equivalents of strong base.

2.4 APPLYING THE METHOD TO TETRAHYDROFURANS

Although our initial investigations with this new method focused primarily on the synthesis of tetrahydropyrans, we transitioned to synthesizing tetrahydrofurans for the latter half of the project. Ito and coworkers report on the use of allylic silanes in order to synthesize 2,3-disubstituted cyclic ethers through an intramolecular cyclization via an oxonium ion intermediate (Figure 33).³⁴ More specifically, they are able to construct enantioenriched tetrahydropyrans with anti-stereochemistry between the two adjacent stereocenters. With their tetrahydrofuran products, only syn stereochemistry is observed albeit with poor stereocontrol over the olefin geometry. Therefore, it became more

advantageous for us to focus our efforts in producing tetrahydrofurans with *trans* substitution as there are limited methods in the literature to synthesize these product scaffolds. Our methodology produces *trans*-substituted cyclic ethers regardless of ring size with excellent diastereoselectivity, so we focused our studies on the construction of 2,3-disubstituted tetrahydrofurans. In order to prepare the required allylic silane starting material, we performed the nickel-catalyzed cross-coupling with a vinyl bromide containing one less methylene group than in our previous methods. With the allylic silane in hand, we could begin our efforts to optimize the reaction to benchtop procedures such that it can be a practical and broadly accessible method.

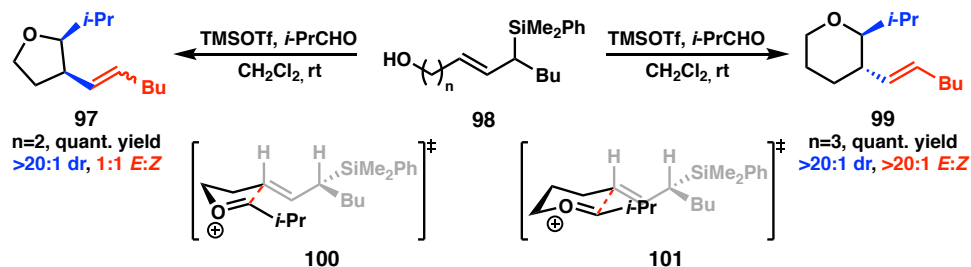


Figure 33. Ito's method involves a cyclic transition state to afford heterocycles.

2.5 A MORE EFFICIENT ROUTE TOWARD ALLYLIC SILANE

REAGENTS

The original route the allylic silane starting material provided limitations to scalability (Figure 34). In order to synthesize the desired allylic silane containing a pendent chloride electrophile, we proceed through a four-step route. The cross-coupling step at the end of the sequence was very challenging to purify. While the cross-coupling itself has

approximately a 70% yield by NMR, only a 40% yield of **91** can be isolated due to a difficult, greasy separation of numerous side products. In fact, it takes 20 liters of hexanes in one column to isolate ~1 g of clean material. In order to access large amounts of material to optimize a generalized benchtop procedure, we investigated an alternate route to allylic silane **106** with great success.

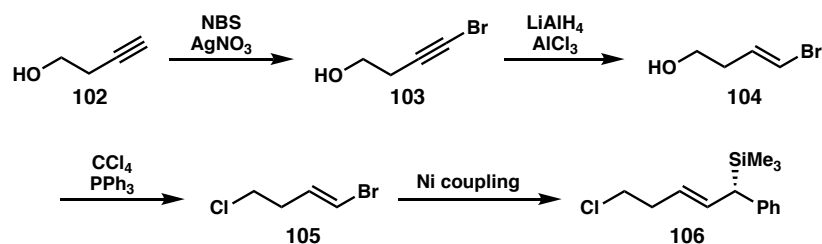


Figure 34. Original route to allylic silane starting material.

Although we targeted the lowest yielding substrate in the allylic silane cross-coupling method (pendant alcohol **107**),²⁹ the NMR yield and isolated yield were comparable at 48% and 45%, respectively. More importantly the ability to purify the allylic silane **107** was much easier than allylic silane **106**, as it only required 2.5 L of solvent in order to obtain ~3 g of material. A subsequent Appel chlorination provided 96% yield of the desired product (**106**). This route is significantly easier to perform on large scale to produce sufficient starting material for the tandem allylation/cyclization reaction. While the cross-coupling method leaves room for improvement (a low 45% yield was obtained), at the onset, we are able to isolate sizable quantities of allylic silane reagent, which speeds up the optimization and substrate screening processes.

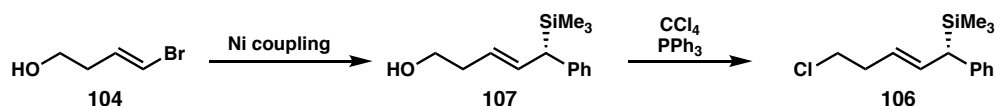


Figure 35. Improved route to allylic silane starting material.

2.6 MODIFICATIONS TO A GENERALIZED BENCHTOP

PROCEDURE

With a successful method in hand, efforts turned to adapting the protocol to a benchtop setup. The desired tetrahydropyran could be produced using the proposed tandem allylation/cyclization method, however, the conditions required the allylation step to be performed for one hour at $-45\text{ }^{\circ}\text{C}$ in a glovebox followed by cyclization at room temperature for two hours. In order to make this chemistry broadly accessible, we proceeded to optimize this methodology with common setup conditions by avoiding the need for a glovebox and a cryocool. We sought to modify the procedure such that it could be performed on a benchtop without any specialized equipment under common reaction conditions (e.g. $-78\text{ }^{\circ}\text{C}$ with a dry ice and acetone bath).

Initially, the allylation portion of the cascade reaction was allowed to proceed for a 1 hour at $-45\text{ }^{\circ}\text{C}$. Literature precedent on the Sakurai allylation described relatively short reaction times (0.5-10 minutes) at lower temperatures ($-78\text{ }^{\circ}\text{C}$) which could afford the desired homoallylic alcohol in high yields. However, our efforts to modify the tandem reaction sequence on the benchtop while using these new conditions coincided with a significant decrease in the conversion rate of the allylic silane (Figure 36). ¹H NMR was used to quantify yields using diagnostic olefin protons for the allylic silane starting material

and the allylated alcohol product. Based on these results, we believed that a problem had arisen in the reaction when conducted on the benchtop. As a result, particular emphasis was placed on optimizing the allylation step in order to regain good conversion and increase the yield of the allylated intermediate.

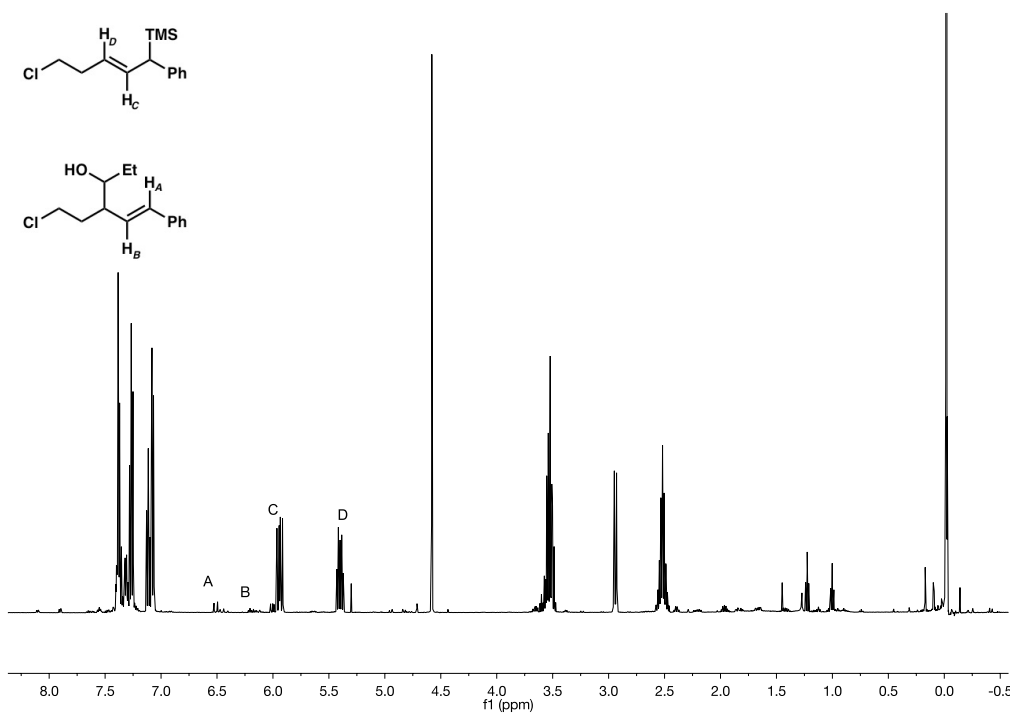


Figure 36. ^1H NMR of benchtop allylation setup shows low amounts of desired product (H_A/H_B) and low conversion of the allylic silane starting material (H_C/H_D).

We proposed that the low conversion was most likely a result of adventitious water in the reaction. Since the reaction conditions use stoichiometric titanium tetrachloride, one would predict that the starting material should be completely consumed, either to the desired product or to an undesired desilylated side product. However, since the starting

material was able to survive such harsh Lewis acidic conditions, we believed that fortuitous water was quenching the titanium tetrachloride. Once the alcohol was formed, indeed a large excess of strong base funneled the intermediate to the cyclic product. Consequently, the majority of our optimization efforts focused on remedying the allylation step.

Various parameters were investigated in order to modify our method to a generalized benchtop procedure with good conversion and high yields. To ensure purity of the reagents prior to the reaction, either newly purchased aldehyde reagents or freshly distilled reagents were used to ensure clean material. This purification became vital to the new standard setup conditions. To rid the reaction of adventitious water, the flask was purged with argon gas and 3 Å molecular sieves were added to the reaction in order to maintain dry reaction conditions. With these modifications, the allylation step could be conducted at $-78\text{ }^{\circ}\text{C}$ in only 10 minutes. Brief investigations on the cyclization portion of the cascade involved varying the equivalents of base used and altering the counterion of the base from potassium to lithium. In summary we found that this combination of these conditions restored reactivity and allowed for access to the desired heterocyclic products on the benchtop in good yields: use of argon atmosphere, addition of molecular sieves, 10 minute allylation time at $-78\text{ }^{\circ}\text{C}$, and use of 10 equivalents of potassium *tert*-butoxide for cyclization.

During these optimization studies, it also became readily apparent that the quality of the titanium tetrachloride played a large role in the success of the initial allylation step of the cascade reaction. Both argon and molecular sieves had to be utilized in the new method in order to ensure that water in the atmosphere did not quench sizable quantities of the

Lewis acid. Additionally, if sure-sealed bottles of titanium tetrachloride solution were a few weeks old and stored on the benchtop, notable decreases in yield (on the order of 10-20% less) were observed. Since buying a new reagent every month was not economical, we sought to better understand the degradation of the Lewis acid via a brief study. When comparing a new bottle, a handmade solution from neat titanium tetrachloride (stored in the glove box), and a several week old bottle that was stored in the glove box in between uses, we found that as long as the solution is stored under inert atmosphere in a glove box, the age of the titanium tetrachloride solution does not matter.

2.7 SUBSTRATE SCOPE

With a successful tandem allylation/cyclization procedure now available, we moved forward to expand the substrate scope. As mentioned previously, according to a known procedure by Ito and coworkers, allylic silanes with pendant electrophiles can be converted to the *cis* diastereomer of the tetrahydrofuran. However, with our optimized reaction conditions, we can access the *trans* diastereomer of the tetrahydrofuran. In order to fully demonstrate the utility of these allylic silane reagents, we decided to pursue the substrate scope on both the *cis* and *trans* diastereomers to investigate interesting differences between the two methods (Figure 37).

In our initial screen of various aldehydes, we were able to successfully synthesize both diastereomers of six different tetrahydrofurans. Four possible products can be obtained in this method, resulting from the *cis* and *trans* configuration of the adjacent stereocenters as well as the E and Z isomers of the olefin. The reported diastereoselectivity

is given for the *cis/trans* ratio, the E:Z olefin ratio, and the percentage of the major isomer out of the four possible products. When analyzing the substrate scope, we note several interesting observations resulting from differences in the two reaction mechanisms. The Ito

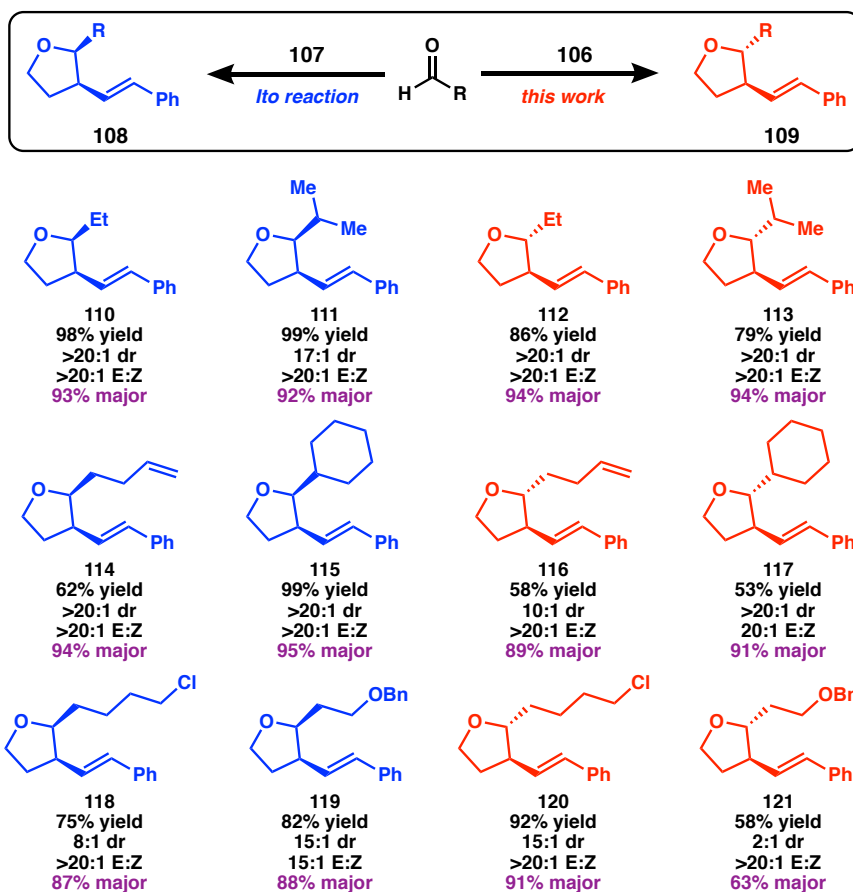


Figure 37. Substrate scope of the two diastereomers of the tetrahydrofuran products.

reaction proceeds through an intramolecular allylation and universally gives higher yields compared to the intermolecular approach. Conversely, the tandem allylation/cyclization method developed in this work proceeds through a linear transition state and is influenced heavily by the sterics of the molecule. This is evident in comparing the yields of the two methods with more substituted aldehydes. When moving from an ethyl group to an

isopropyl group, the yield does not change using the condensation/intramolecular allylation route – 98% with **110** versus 99% with **111**. However, when comparing the same aldehydes with the tandem allylation/cyclization method, the yield decreases significantly from 86% with **112** to 79% with **113**. The same steric argument contributes to the moderate yields of using cyclohexane as the R group, although further investigations on using various ring sizes suggest there is more at play in this mechanism.

Another interesting observation reveals that allylations with the aldehyde containing a pendant chloride electrophile have excellent yields with both methods. This shows that additional pendant electrophiles can be tolerated under the reaction conditions (versus eliminating to form a terminal olefin) and also provides insight into the cyclization step. With 5-chloropentanal, the alkoxide intermediate could cyclize onto the pendant electrophile of the aldehyde, rather than that of the allylic silane, providing two possible products – **120** and **123** (Figure 38). However, via our method, the proposed six-membered heterocyclic ring product is not observed. Rather, we saw great success (96% yield of **120**) using a long chain with a pendant chloride as the R group on the aldehyde. This provides interesting insight into the kinetics of the cyclization, as the five-membered heterocyclic ring was preferentially formed.

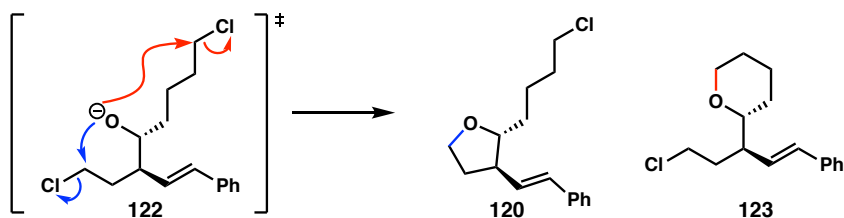


Figure 38. Mechanism showing cyclization onto two different electrophiles.

Additionally, we note that that aldehydes containing benzyl ether moieties have a drastic effect on the observed diastereomeric ratio (dr). With the tandem allylation/cyclization method, tetrahydrofuran **121** was formed with low dr of 2:1. As a result, we investigated a series of aldehydes containing benzyl ether functional groups in order to investigate coordination effects on the observed d.r. (Figure 39). In order to obtain full conversion of starting material, we modified our procedure to use 2.0 equivalents titanium tetrachloride and 15.0 equivalents base.

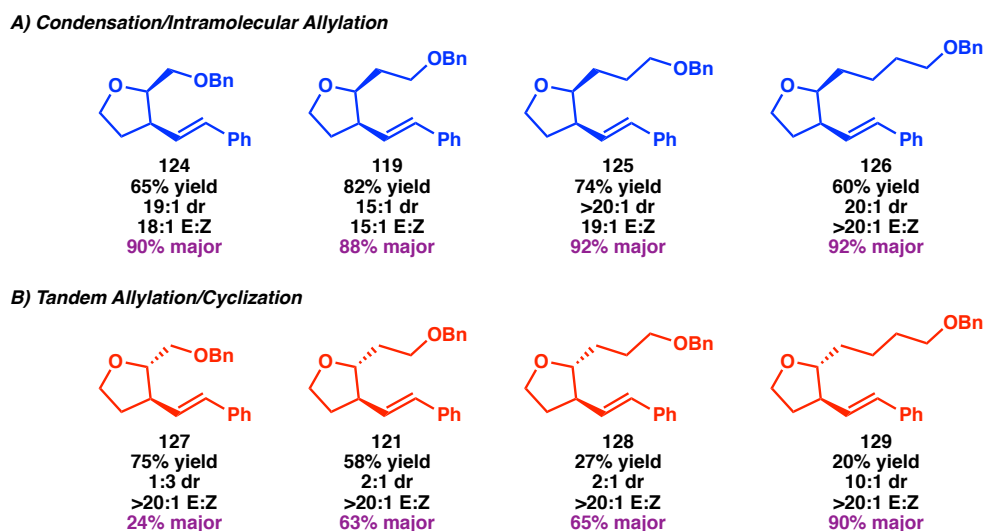


Figure 39. Substrate scope for aldehydes with various pendant benzyl ether groups.

In the case of the *trans*-2,3-tetrahydrofurans, the dr between the *trans* to *cis* diastereomers improves as the benzyl group distance from the aldehyde increases. Interestingly, as with tetrahydrofuran **127**, the benzyl group inverts the selectivity giving the *cis* product as the major diastereomer. According to Judd and coworkers, a benzyl ether group can stabilize intermediates and have effects on diastereomeric control.³⁵ In this case, the benzyl ether can coordinate to the titanium in the reaction mechanism, which alters the

transition state and leads to erosion of diastereoselectivity. The benzyl group does not become non-innocent in this transformation until four methylene units are incorporated in the aldehyde as seen in tetrahydrofuran **129**. In contrast, the diastereoselectivity of the *cis*-2,3-tetrahydrofurans (**124-126**) is not affected by the presence of the benzyl group.

2.8 CONCLUSIONS AND FUTURE DIRECTIONS

We were able to successfully develop a one-pot procedure to synthesize chiral tetrahydropyrans from chiral allylic silanes in good yields and with excellent diastereoselectivity. This procedure consists of a cascade reaction, starting with a Sakurai allylation followed by base-mediated cyclization to afford enantioenriched heterocycles – both tetrahydrofurans and tetrahydropyrans. We report on expansion of the substrate scope to use various aldehydes as well as studies on the cyclization mechanism and diastereoselectivity of the reaction with pendent benzyl ethers. Future work will involve a more detailed study into the mechanism of the reaction, as well as testing additional aldehyde and ketone substrates. Furthermore, we seek to expand the use of this method beyond the synthesis of cyclic ethers and future studies will investigate the formation of nitrogen-containing heterocycles via use of an imine in lieu of an aldehyde (Figure 40).

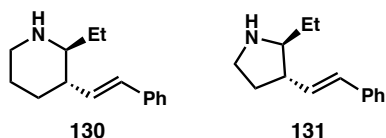
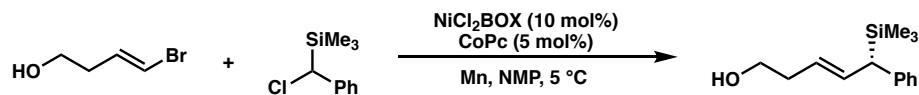


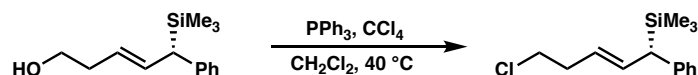
Figure 40. Proposed substrate scope for nitrogen-related heterocycles, starting from *propan-1-imine*.

Supporting Information

Unless otherwise stated, reactions were performed under a nitrogen atmosphere using freshly dried solvents. Methylene chloride (CH_2Cl_2) was dried by passing through an activated alumina column. N-methylpyrrolidinone (NMP), titanium tetrachloride (1.0 M in CH_2Cl_2), and potassium tertbutoxide (1.0 M in THF) were purchased from Sigma Aldrich and stored in the glovebox. Manganese powder (-325 mesh, 99.3%) was purchased from Alfa Aesar. Unless otherwise stated, chemicals were used as received. All reactions were monitored by thin-layer chromatography (TLC) using EMD/Merck silica gel 60 F254 pre-coated plates (0.25 mm) and were visualized by ultraviolet (UV) light or with potassium permanganate (KMnO_4) staining. Flash column chromatography was performed as described by Still et al.³⁶ using silica gel (230-400 mesh) purchased from Silicycle. Optical rotations were measured on a Jasco P-2000 polarimeter using a 100 mm path-length cell at 589 nm. ^1H and ^{13}C NMR spectra were recorded on a Bruker Avance III HD with Prodigy cyroprobe (at 400 MHz and 101 MHz, respectively). NMR data is reported relative to internal CHCl_3 (^1H , $\delta = 7.26$) and CDCl_3 (^{13}C , $\delta = 77.1$). Data for ^1H NMR spectra are reported as follows: chemical shift (δ ppm) (multiplicity, coupling constant (Hz), integration). Multiplicity and qualifier abbreviations are as follows: s = singlet, d = doublet, t = triplet, q = quartet, m = multiplet. IR spectra were recorded on a Perkin Elmer Paragon 1000 spectrometer and are reported in frequency of absorption (cm^{-1}). Analytical chiral SFC was performed with a Mettler SFC supercritical CO_2 chromatography system with Chiralcel AD-H, OD-H, AS-H, OB-H, and OJ-H columns (4.6 mm x 25 cm). HRMS were acquired from the Caltech Mass Spectral Facility using fast-atom bombardment (FAB) or electron impact (EI). X-ray diffraction and elemental analysis (EA) were performed at the Caltech X-ray Crystal Facility.

(*S,E*)-5-phenyl-5-(trimethylsilyl)pent-3-en-1-ol (107)

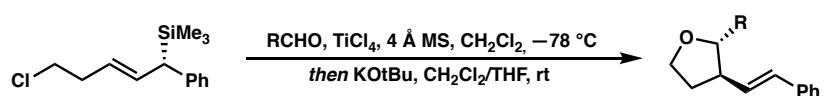
According to a procedure by Reisman and coworkers²⁹, a 250 mL round bottom flask with a stir bar was equipped with Mn⁰ powder (4.95 g, 90 mmol, 3 equiv), cobalt phthalocyanine (857 mg, 1.5 mmol, 0.05 equiv), and NiCl₂BOX complex (**73**, 1.455 g, 3 mmol, 0.1 equiv). The flask was brought into a N₂-filled glovebox, and then the NMP (60 mL, 0.5 M), (chloro(phenyl)methyl)trimethylsilane (5.96 g, 30 mmol, 1 equiv), and (*E*)-4-bromobut-3-en-1-ol (7.61 g, 45 mmol, 1.5 equiv) were added sequentially. The flask was sealed with a new rubber septum, wrapped with electrical tape, and stirred at 5 °C in a cryocool for 6 days. The crude reaction was diluted with Et₂O and H₂O, slowly quenched with 1 M HCl, and further diluted with water. The aqueous layer was extracted with Et₂O and the combined organic layers were dried with MgSO₄, filtered, and concentrated under reduced pressure. The crude material was purified by column chromatography (silica, 1:1:1 Et₂O/hexanes/PhMe) to yield 3.1 g of **107** (45% yield) in 98% ee as a blue oil. Spectral data matched those reported in literature.²⁹

(*S,E*)-(5-chloro-1-phenylpent-2-en-1-yl)trimethylsilane (106)

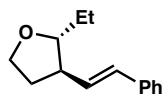
Allylic silane (**107**, 98% ee, 1.6 g, 6.83 mmol, 1 equiv), triphenylphosphine (2.685 g, 10.2 mmol, 1.5 equiv), carbon tetrachloride (1.32 mL, 13.7 mmol, 2 equiv), and DCM (7 mL, 0.98 M) were added to a 25 mL round bottom flask equipped with a stir bar. The reaction

mixture was refluxed under a N₂ atmosphere at 40 °C for 1 day. The crude reaction mixture was loaded directly onto a silica plug and flushed with 250 mL hexanes to afford 1.66 g of **106** (96% yield) in 98% ee as a colorless oil. Spectral data matched those reported in literature.²⁹

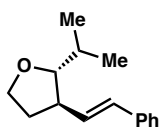
General Procedure 1: Allylation/Cyclization for *trans*-2,3-tetrahydrofurans



On a bench-top, a 10 mL round bottom flask equipped with a stir bar was sealed with a septum and electrical tape, then flame dried with a propane torch and backfilled with argon. Then 100 mg of oven-dried 3 Å molecular sieves were quickly added to the flask, which was subsequently evacuated and backfilled with argon. The allylic silane (0.22 mmol, 1.1 equiv), aldehyde (0.2 mmol, 1 equiv), and anhydrous CH₂Cl₂ (2.0 mL, 0.1 M) were added to the flask via syringe while under an Ar atmosphere. The reaction mixture was cooled to -78 °C and TiCl₄ solution (0.24 mmol, 1.2 equiv, 1 M in DCM) was added via syringe. After stirring for 10 minutes, anhydrous KOTBu solution (2 mmol, 10 equiv, 1 M in THF) was slowly added to the flask via syringe, the reaction was allowed to warm to room temperature, and continued to stir for 2 hours. The crude reaction was filtered through a plug of celite (approx. 4 cm in diameter and 1 cm thick), flushed with 50 mL of Et₂O, and concentrated under reduced pressure. The crude residue was purified by column chromatography to yield the desired product.

(2*R*,3*R*)-2-ethyl-3-((*E*)-styryl)tetrahydrofuran (112)

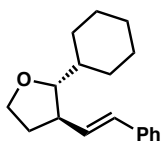
Prepared from (*S,E*)-(5-chloro-1-phenylpent-2-en-1-yl)trimethylsilane (**106**, 55.6 mg, 1.1 equiv, 0.22 mmol, 98% ee) and propionaldehyde (14.4 μ l, 1.0 equiv, 0.2 mmol) according to General Procedure 1. The crude residue was purified by column chromatography (silica, 0 to 5% Et₂O/hexanes) to yield 34.6 mg of **112** (86% yield, >20:1 dr, >20:1 *E:Z*, 94% major isomer) as a colorless oil. R_f = 0.39 (silica, 10% EtOAc/hexane, UV). $[\alpha]_D^{25}$ = +48° (c = 0.5, CHCl₃). **¹H NMR (500 MHz, CDCl₃):** δ 7.40 – 7.34 (m, 2H), 7.32 (ddd, *J* = 7.8, 6.7, 1.2 Hz, 2H), 7.25 – 7.20 (m, 1H), 6.45 (d, *J* = 15.8 Hz, 1H), 6.12 (dd, *J* = 15.8, 8.7 Hz, 1H), 3.92 (dd, *J* = 8.1, 5.9 Hz, 2H), 3.52 (td, *J* = 7.9, 4.1 Hz, 1H), 2.62 – 2.51 (m, 1H), 2.19 (ddt, *J* = 12.0, 8.1, 5.9 Hz, 1H), 1.89 (ddt, *J* = 12.4, 9.0, 8.1 Hz, 1H), 1.73 – 1.63 (m, 1H), 1.54 (dt, *J* = 13.9, 7.4 Hz, 1H), 1.01 (t, *J* = 7.4 Hz, 3H). **¹³C NMR (126 MHz, CDCl₃):** δ 137.3, 131.0, 130.9, 128.7, 127.6, 126.2, 85.3, 67.3, 48.9, 33.9, 26.9, 10.8. **FTIR (NaCl, thin film, cm⁻¹):** 2964, 2932, 2875, 1493, 1450, 1116, 1020, 965, 746, 693.

(2*R*,3*R*)-2-isopropyl-3-((*E*)-styryl)tetrahydrofuran (113)

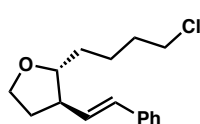
Prepared from (*S,E*)-(5-chloro-1-phenylpent-2-en-1-yl)trimethylsilane (**106**, 55.6 mg, 1.1 equiv, 0.22 mmol, 98% ee) and isobutylaldehyde (18.2 μ l, 1.0 equiv, 0.2 mmol) according to General Procedure 1. The crude residue was purified by column chromatography (silica, 0 to 5% Et₂O/hexanes) to yield 34.3 mg of **113** (79% yield, >20:1 dr, >20:1 *E:Z*, 94% major isomer) as a colorless oil. R_f = 0.46 (silica, 10% EtOAc/hexane, UV). $[\alpha]_D^{25}$ = +46° (c = 1.0, CHCl₃). **¹H NMR (400 MHz, CDCl₃):** δ 7.39

– 7.28 (m, 4H), 7.25 – 7.19 (m, 1H), 6.43 (d, $J = 15.8$ Hz, 1H), 6.14 (dd, $J = 15.8, 8.8$ Hz, 1H), 3.93 – 3.83 (m, 2H), 3.45 (dd, $J = 7.7, 5.5$ Hz, 1H), 2.74 (p, $J = 8.2$ Hz, 1H), 2.16 (dddd, $J = 12.0, 8.1, 6.6, 5.1$ Hz, 1H), 1.92 – 1.77 (m, 2H), 0.98 (dd, $J = 6.8, 1.0$ Hz, 6H). ^{13}C NMR (101 MHz, CDCl_3): δ 137.4, 132.1, 130.4, 128.7, 127.3, 126.1, 88.9, 67.5, 46.3, 34.6, 31.8, 19.7, 18.2. FTIR (NaCl, thin film, cm^{-1}): 3026, 2961, 2933, 2872, 1493, 1486, 1449, 1387, 1071, 1051, 965, 747, 693.

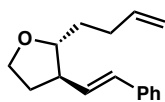
(2*R*,3*R*)-2-cyclohexyl-3-((*E*)-styryl)tetrahydrofuran (117)



Prepared from (*S,E*)-(5-chloro-1-phenylpent-2-en-1-yl)trimethylsilane (**106**, 55.6 mg, 1.1 equiv, 0.22 mmol, 98% ee) and cyclohexanecarbaldehyde (22.4 mg, 1.0 equiv, 0.2 mmol) according to General Procedure 1. The crude residue was purified by column chromatography (silica, 0 to 5% Et_2O /hexanes) to yield 27.1 mg of **117** (53% yield, >20:1 dr, 20:1 *E:Z*, 91% major isomer) as a colorless oil. $R_f = 0.42$ (silica, 10% EtOAc /hexane, UV). $[\alpha]_D^{25} = +78^\circ$ ($c = 1.0$, CHCl_3). ^1H NMR (400 MHz, CDCl_3): δ 7.40 – 7.34 (m, 2H), 7.34 – 7.28 (m, 2H), 7.25 – 7.19 (m, 1H), 6.43 (d, $J = 15.7$ Hz, 1H), 6.13 (dd, $J = 15.7, 8.8$ Hz, 1H), 3.93 – 3.79 (m, 2H), 3.44 (dd, $J = 7.6, 5.7$ Hz, 1H), 2.78 (p, $J = 8.2$ Hz, 1H), 2.19 – 2.09 (m, 1H), 1.85 (dq, $J = 12.3, 7.8$ Hz, 2H), 1.79 – 1.69 (m, 3H), 1.68 – 1.61 (m, 1H), 1.49 (tdt, $J = 11.7, 6.1, 3.3$ Hz, 1H), 1.30 – 1.04 (m, 5H). ^{13}C NMR (101 MHz, CDCl_3): δ 137.5, 132.1, 130.3, 128.7, 127.3, 126.1, 88.3, 67.4, 46.0, 41.9, 34.6, 30.1, 28.7, 26.7, 26.5, 26.3. FTIR (NaCl, thin film, cm^{-1}): 2925, 2852, 1492, 1449, 1085, 1066, 965, 887, 748, 694.

(2*R*,3*R*)-2-(4-chlorobutyl)-3-((*E*)-styryl)tetrahydrofuran (120)

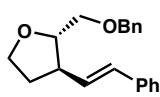
Prepared from (*S,E*)-(5-chloro-1-phenylpent-2-en-1-yl)trimethylsilane (**196**, 55.6 mg, 1.1 equiv, 0.22 mmol, 98% ee) and 5-chloropentanal (24 μ l, 1.0 equiv, 0.2 mmol) according to General Procedure 1. The crude residue was purified by column chromatography (silica, 0 to 6% Et₂O/hexanes) to yield 48.6 mg of **120** (92% yield, 15:1 dr, >20:1 *E:Z*, 91% major isomer) as a colorless oil. R_f = 0.36 (silica, 10% EtOAc/hexane, UV). $[\alpha]_D^{25}$ = +64° (c = 1.0, CHCl₃). **¹H NMR (400 MHz, CDCl₃):** δ 7.40 – 7.28 (m, 4H), 7.25 – 7.20 (m, 1H), 6.46 (d, J = 15.8 Hz, 1H), 6.10 (dd, J = 15.7, 8.8 Hz, 1H), 3.95 – 3.88 (m, 2H), 3.59 – 3.50 (m, 3H), 2.60 – 2.49 (m, 1H), 2.20 (dddd, J = 12.0, 8.1, 6.4, 5.3 Hz, 1H), 1.94 – 1.85 (m, 1H), 1.85 – 1.75 (m, 2H), 1.70 – 1.62 (m, 2H), 1.57 – 1.47 (m, 2H). **¹³C NMR (101 MHz, CDCl₃):** δ 137.2, 131.3, 130.5, 128.7, 127.4, 126.2, 83.7, 67.3, 49.4, 45.1, 33.8, 33.2, 32.8, 24.1. **FTIR (NaCl, thin film, cm⁻¹):** 2938, 2867, 1492, 1449, 1071, 1029, 1017, 966, 748, 693.

(2*R*,3*R*)-2-(but-3-en-1-yl)-3-((*E*)-styryl)tetrahydrofuran (116)

Prepared from (*S,E*)-(5-chloro-1-phenylpent-2-en-1-yl)trimethylsilane (**106**, 55.6 mg, 1.1 equiv, 0.22 mmol, 98% ee) and pent-4-enal (16.8 mg, 1.0 equiv, 0.2 mmol) according to General Procedure 1. The crude residue was purified by column chromatography (silica, 0 to 5% Et₂O/hexanes) to yield 26.5 mg of **116** (58% yield, 10:1 dr, >20:1 *E:Z*, 89% major isomer) as a colorless oil. R_f = 0.39 (silica, 10% EtOAc/hexane, UV). $[\alpha]_D^{25}$ = +69° (c = 1.0, CHCl₃). **¹H NMR (400 MHz, CDCl₃):** δ 7.40 – 7.35 (m, 2H), 7.35 – 7.28 (m, 2H), 7.26 – 7.20 (m, 1H), 6.46 (d, J = 15.7 Hz, 1H), 6.11

(dd, $J = 15.8, 8.8$ Hz, 1H), 5.84 (ddt, $J = 16.8, 10.1, 6.6$ Hz, 1H), 5.09 – 4.92 (m, 2H), 3.97 – 3.89 (m, 2H), 3.58 (td, $J = 8.3, 3.7$ Hz, 1H), 2.56 (p, $J = 8.2$ Hz, 1H), 2.35 – 2.10 (m, 3H), 1.89 (ddt, $J = 12.3, 9.0, 8.1$ Hz, 1H), 1.73 (dddd, $J = 13.7, 10.0, 6.2, 3.7$ Hz, 1H), 1.60 (dddd, $J = 13.8, 9.7, 8.1, 5.3$ Hz, 1H). ^{13}C NMR (101 MHz, CDCl_3): δ 138.6, 137.3, 131.2, 130.6, 128.7, 127.4, 126.2, 114.7, 83.4, 67.3, 49.5, 33.9, 33.4, 30.8. FTIR (NaCl, thin film, cm^{-1}): 3026, 2974, 2931, 2868, 1640, 1493, 1449, 1071, 966, 911, 747, 693.

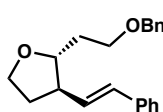
(2*S*,3*R*)-2-((benzyloxy)methyl)-3-((*E*)-styryl)tetrahydrofuran (127)



Prepared from (*S,E*)-(5-chloro-1-phenylpent-2-en-1-yl)trimethylsilane (**106**, 55.6 mg, 1.1 equiv, 0.22 mmol, 98% ee) and 2-(benzyloxy)acetaldehyde (30.0 mg, 1.0 equiv, 0.2 mmol) according to General Procedure 1 with the exception that 2.0 equivalents TiCl_4 and 15.0 equivalents KOTu were used in this procedure. The crude residue was purified by column chromatography (silica, 0 to 20% Et_2O /hexanes) to yield 44.2 mg of **127** (75% yield, 1:3 dr (*Note: trans is the minor diastereomer*), >20:1 *E:Z*, 24% major isomer) as a yellow oil. $R_f = 0.18$ (silica, 10% EtOAc /hexane, UV). $[\alpha]_D^{25} = +41^\circ$ ($c = 1.0$, CHCl_3). ^1H NMR (400 MHz, CDCl_3): *Note: mixture of diastereomers, contains additional impurity:* δ 7.39 – 7.16 (m, 10.00H), 6.50 – 6.34 (m, 0.74H), 6.25 – 6.07 (m, 0.75H), 4.68 – 4.46 (m, 1.88H), 4.18 – 4.03 (m, 1.36H), 4.01 – 3.92 (m, 0.42H), 3.92 – 3.79 (m, 0.94H), 3.66 (dd, $J = 10.5, 2.9$ Hz, 0.24H), 3.63 – 3.46 (m, 1.87H), 3.44 – 3.32 (m, 0.51H), 3.08 (dq, $J = 9.4, 6.9$ Hz, 0.57H), 2.80 (p, $J = 8.5$ Hz, 0.15H), 2.63 (dddt, $J = 7.2, 4.3, 2.9, 1.4$ Hz, 0.19H), 2.19 (dtd, $J = 12.5, 7.6, 4.9$ Hz, 0.74H), 2.03 – 1.85 (m, 0.83H). ^{13}C NMR (101 MHz, CDCl_3): *Note: mixture of diastereomers, contains additional*

impurity: δ 138.25, 137.19, 131.33, 131.07, 130.05, 128.74, 128.56, 128.51, 128.35, 128.33, 128.27, 127.73, 127.65, 127.56, 127.52, 127.37, 127.29, 126.16, 126.11, 80.81, 73.52, 70.99, 70.96, 67.93, 67.67, 45.23, 45.20, 36.24, 33.57, 32.81, 28.68, 27.59. **FTIR (NaCl, thin film, cm^{-1})**: 3027, 2973, 2930, 2866, 1495, 1452, 1364, 1197, 1092, 1028, 969, 748, 696.

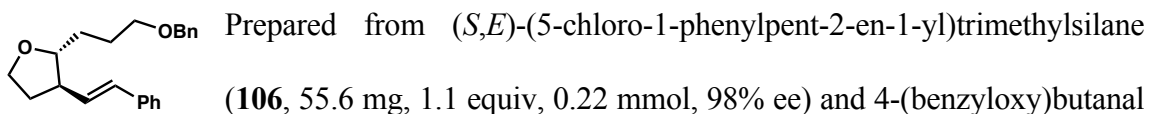
(2*R*,3*R*)-2-(2-(benzyloxy)ethyl)-3-((*E*)-styryl)tetrahydrofuran (121)



Prepared from (*S,E*)-(5-chloro-1-phenylpent-2-en-1-yl)trimethylsilane (**106**, 55.6 mg, 1.1 equiv, 0.22 mmol, 98% ee) and 3-(benzyloxy)propanal (32.8 mg, 1.0 equiv, 0.2 mmol) according to General Procedure 1 with the exception that 2.0 equivalents TiCl_4 and 15.0 equivalents KOTu were used in this procedure. The crude residue was purified by column chromatography (silica, 0 to 15% Et_2O /hexanes) to yield 35.7 mg of **121** (58% yield, 2:1 dr, >20:1 *E:Z*, 63% major isomer) as a pale yellow oil. R_f = 0.18 (silica, 10% EtOAc /hexane, UV). $[\alpha]_D^{25} = +38^\circ$ ($c = 1.0$, CHCl_3). **^1H NMR (400 MHz, CDCl_3)**: *Note: mixture of diastereomers*: δ 7.39 – 7.19 (m, 10H), 6.51 – 6.32 (m, 1H), 6.23 – 6.04 (m, 1H), 4.58 – 4.42 (m, 2H), 4.10 – 3.98 (m, 0.7H), 3.97 – 3.88 (m, 1.2H), 3.81 (td, $J = 8.4, 6.7$ Hz, 0.4H), 3.76 – 3.52 (m, 3H), 3.36 (t, $J = 6.3$ Hz, 0.3H), 3.01 – 2.90 (m, 0.3H), 2.59 (p, $J = 8.4$ Hz, 0.6H), 2.29 – 2.13 (m, 1H), 2.05 – 1.92 (m, 0.7H), 1.92 – 1.75 (m, 2.3H). **^{13}C NMR (101 MHz, CDCl_3)**: *Note: mixture of diastereomers*: δ 138.63, 137.35, 137.25, 131.35, 131.08, 130.28, 129.46, 128.67, 128.47, 128.45, 127.83, 127.79, 127.64, 127.60, 127.41, 127.35, 126.22, 81.05, 79.21, 73.21, 73.18, 68.04, 67.91, 67.36, 66.80, 49.59, 45.97, 34.28, 33.76, 32.72, 31.95, 28.79, 27.71. **FTIR (NaCl, thin**

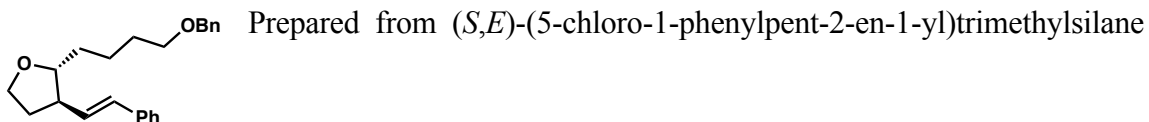
film, cm⁻¹): 3027, 2969, 2930, 2865, 1495, 1453, 1363, 1198, 1099, 1028, 967, 748, 696.

(2*R*,3*R*)-2-(3-(benzyloxy)propyl)-3-((*E*)-styryl)tetrahydrofuran (128)



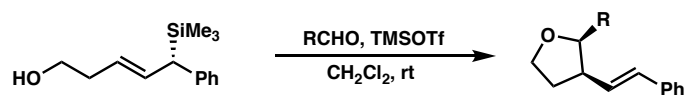
(35.6 mg, 1.0 equiv, 0.2 mmol) according to General Procedure 1 with the exception that 2.0 equivalents TiCl₄ and 15.0 equivalents K₂OtBu were used in this procedure. The crude residue was purified by column chromatography (silica, 0 to 20% Et₂O/hexanes) to yield 17.5 mg of **128** (27% yield, 2:1 dr, >20:1 *E*:*Z*, 65% major isomer) as a yellow oil. $R_f = 0.22$ (silica, 10% EtOAc/hexane, UV). $[\alpha]_D^{25} = +13^\circ$ (c = 1.0, CHCl₃). **¹H NMR (400 MHz, CDCl₃)**: Note: mixture of diastereomers: δ 7.41 – 7.19 (m, 10.0H), 6.66 – 6.36 (m, 1H), 6.26 – 5.89 (m, 1H), 4.49 (d, *J* = 8.5 Hz, 2H), 4.04 (td, *J* = 8.2, 5.7 Hz, 0.4H), 3.97 – 3.88 (m, 1.4H), 3.88 – 3.70 (m, 0.7H), 3.59 (td, *J* = 8.2, 3.3 Hz, 0.7H), 3.55 – 3.41 (m, 2H), 3.02 – 2.89 (m, 0.3H), 2.56 (p, *J* = 8.5 Hz, 0.6H), 2.28 – 2.12 (m, 1H), 1.98 – 1.66 (m, 3.6H), 1.63 – 1.50 (m, 1.4H). **¹³C NMR (101 MHz, CDCl₃)**: Note: mixture of diastereomers: δ 138.75, 138.73, 137.45, 137.28, 131.17, 130.85, 130.60, 129.61, 128.68, 128.52, 128.44, 128.43, 128.37, 127.73, 127.71, 127.56, 127.40, 127.30, 126.24, 126.21, 83.78, 82.21, 72.90, 72.84, 72.79, 70.39, 70.30, 67.27, 66.70, 49.38, 45.96, 33.88, 32.84, 30.71, 28.19, 26.91, 26.77. **FTIR (NaCl, thin film, cm⁻¹)**: 3060, 3027, 2933, 2857, 1495, 1453, 1363, 1203, 1100, 1073, 1028, 967, 747, 696.

(2*R*,3*R*)-2-(4-(benzyloxy)butyl)-3-((*E*)-styryl)tetrahydrofuran (129)



(**106**, 55.6 mg, 1.1 equiv, 0.22 mmol, 98% ee) and 5-(benzyloxy)pentanal (38.5 mg, 1.0 equiv, 0.2 mmol) according to General Procedure 1 with the exception that 2.0 equivalents TiCl_4 and 15.0 equivalents KOTBu were used in this procedure. The crude residue was purified by column chromatography (silica, 0 to 15% Et_2O /hexanes) to yield 13.7 mg of **129** (20% yield, 10:1 dr, >20:1 *E:Z*, 90% major isomer) as a colorless oil. $R_f = 0.18$ (silica, 10% EtOAc /hexane, UV). $[\alpha]_D^{25} = +48^\circ$ ($c = 1.0$, CHCl_3). $^1\text{H NMR}$ (400 MHz, CDCl_3): δ 7.39 – 7.12 (m, 10H), 6.44 (d, $J = 15.7$ Hz, 1H), 6.10 (dd, $J = 15.8, 8.8$ Hz, 1H), 4.48 (s, 2H), 3.90 (d, $J = 8.1$ Hz, 2H), 3.56 (td, $J = 7.8, 3.3$ Hz, 1H), 3.46 (td, $J = 6.5, 2.8$ Hz, 2H), 2.53 (p, $J = 8.6$ Hz, 1H), 2.19 (dddd, $J = 12.0, 8.1, 6.5, 5.3$ Hz, 1H), 1.93 – 1.82 (m, 1H), 1.69 – 1.45 (m, 6H). $^{13}\text{C NMR}$ (101 MHz, CDCl_3): δ 138.8, 137.3, 131.1, 130.7, 128.7, 128.4, 127.7, 127.6, 127.4, 126.2, 84.0, 73.0, 70.5, 67.3, 49.4, 33.9, 33.9, 30.0, 23.3. **FTIR** (NaCl, thin film, cm^{-1}): 3027, 2935, 2860, 1495, 1454, 1363, 1102, 1028, 1017, 966, 747, 696.

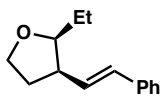
General Procedure 2: Condensation/Allylation for *cis*-2,3-tetrahydrofurans



On a bench-top open to an atmosphere of air, the allylic silane (0.22 mmol, 1.1 equiv), aldehyde (0.2 mmol, 1.0 equiv) and CH_2Cl_2 (2 mL, 0.1M) were added to a 25 mL round bottom flask equipped with a stir bar. The TMSOTf (0.06 mmol, 0.03 equiv) was added to the flask and the reaction was allowed to stir at room temperature for 5 minutes before being diluted with CH_2Cl_2 (6 mL). Celite (500 mg) was added to the crude mixture and the

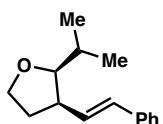
solution was concentrated under reduced pressure. The resulting powder was then loaded onto a silica column and purified via column chromatography to yield the desired product.

(2*S*,3*R*)-2-ethyl-3-((*E*)-styryl)tetrahydrofuran (110)



Prepared from (*S,E*)-5-phenyl-5-(trimethylsilyl)pent-3-en-1-ol (**107**, 51.6 mg, 1.1 equiv, 0.22 mmol, 98% ee) and propionaldehyde (11.6 mg, 1.0 equiv, 0.2 mmol) according to General Procedure 2. The crude residue was purified by column chromatography (silica, 0 to 5% Et₂O/hexanes) to yield 39.6 mg of **110** (98% yield, >20:1 dr, >20:1 *E:Z*, 93% major isomer) as a colorless oil. $R_f = 0.36$ (silica, 10% EtOAc/hexane, UV). $[\alpha]_D^{25} = +28^\circ$ (c = 1.0, CHCl₃). **¹H NMR (500 MHz, CDCl₃):** δ 7.39 – 7.34 (m, 2H), 7.34 – 7.27 (m, 2H), 7.25 – 7.19 (m, 1H), 6.41 (d, *J* = 15.8 Hz, 1H), 6.18 (dd, *J* = 15.8, 9.7 Hz, 1H), 4.05 (td, *J* = 8.3, 5.9 Hz, 1H), 3.86 – 3.73 (m, 2H), 2.95 (ddt, *J* = 12.5, 10.0, 5.2 Hz, 1H), 2.22 (dddd, *J* = 12.5, 8.4, 7.5, 5.9 Hz, 1H), 1.89 (dddd, *J* = 12.6, 8.1, 6.4, 4.7 Hz, 1H), 1.62 – 1.42 (m, 2H), 0.96 (t, *J* = 7.4 Hz, 3H). **¹³C NMR (126 MHz, CDCl₃):** δ 137.5, 130.7, 129.7, 128.7, 127.3, 126.2, 126.2, 84.0, 66.6, 45.7, 32.9, 24.5, 10.9. **FTIR (NaCl, thin film, cm⁻¹):** 3026, 2964, 2934, 2874, 1494, 1463, 1450, 1359, 1101, 1063, 1033, 970, 750, 694.

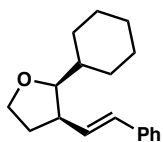
(2*S*,3*R*)-2-isopropyl-3-((*E*)-styryl)tetrahydrofuran (111)



Prepared from (*S,E*)-5-phenyl-5-(trimethylsilyl)pent-3-en-1-ol (**107**, 51.6 mg, 1.1 equiv, 0.22 mmol, 98% ee) and isobutylaldehyde (14.4 mg, 1.0 equiv, 0.2 mmol) according to General Procedure 2. The crude residue was purified by column chromatography (silica, 0 to 5% Et₂O/hexanes) to yield 44.0 mg of **111** (99% yield,

17:1 dr, >20:1 *E*:*Z*, 92% major isomer) as a colorless oil. $R_f = 0.45$ (silica, 10% EtOAc/hexane, UV). $[\alpha]_D^{25} = +58^\circ$ ($c = 1.0$, CHCl_3). $^1\text{H NMR}$ (400 MHz, CDCl_3): δ 7.40 – 7.35 (m, 2H), 7.35 – 7.29 (m, 2H), 7.25 – 7.19 (m, 1H), 6.40 (s, 1H), 6.24 (dd, $J = 15.8$, 10.0 Hz, 1H), 4.06 (q, $J = 8.0$ Hz, 1H), 3.86 (ddd, $J = 9.4$, 8.4, 4.6 Hz, 1H), 3.33 (dd, $J = 9.8$, 4.5 Hz, 1H), 2.97 – 2.89 (m, 1H), 2.27 (ddt, $J = 12.6$, 9.4, 7.5 Hz, 1H), 1.88 (dddd, $J = 12.5$, 7.9, 4.6, 2.0 Hz, 1H), 1.81 – 1.70 (m, 1H), 1.05 (d, $J = 6.5$ Hz, 3H), 0.87 (d, $J = 6.6$ Hz, 3H). $^{13}\text{C NMR}$ (101 MHz, CDCl_3): δ 137.5, 130.4, 129.6, 128.7, 127.2, 126.2, 88.8, 66.4, 45.0, 33.5, 29.5, 20.7, 18.9. FTIR (NaCl, thin film, cm^{-1}): 2958, 2872, 1494, 1450, 1388, 1066, 970, 754, 694.

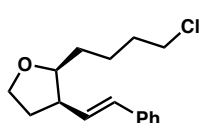
(2*S*,3*R*)-2-cyclohexyl-3-((*E*)-styryl)tetrahydrofuran (115)



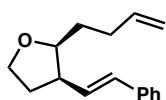
Prepared from (*S,E*)-5-phenyl-5-(trimethylsilyl)pent-3-en-1-ol (**107**, 51.6 mg, 1.1 equiv, 0.22 mmol, 98% ee) and cyclohexanecarbaldehyde (22.4 mg, 1.0 equiv, 0.2 mmol) according to General Procedure 2. The crude residue was purified by column chromatography (silica, 0 to 5% Et₂O/hexanes) to yield 50.6 mg of **115** (99% yield, >20:1 dr, >20:1 *E*:*Z*, 95% major isomer) as a colorless oil which crystallized upon standing. Crystals suitable for X-ray diffraction were grown from hexane upon standing in the freezer (-20°C). $R_f = 0.43$ (silica, 10% EtOAc/hexane, UV). $[\alpha]_D^{25} = +81^\circ$ ($c = 1.0$, CHCl_3). $^1\text{H NMR}$ (400 MHz, CDCl_3): δ 7.40 – 7.35 (m, 2H), 7.32 (dd, $J = 8.5$, 6.7 Hz, 2H), 7.26 – 7.20 (m, 1H), 6.41 (d, $J = 15.8$ Hz, 1H), 6.24 (dd, $J = 15.9$, 9.9 Hz, 1H), 4.04 (q, $J = 8.0$ Hz, 1H), 3.84 (ddd, $J = 9.5$, 8.4, 4.6 Hz, 1H), 3.39 (dd, $J = 9.7$, 4.5 Hz, 1H), 2.93 (dddd, $J = 9.6$, 6.8, 4.5, 1.9 Hz, 1H), 2.25 (ddt, $J = 12.6$, 9.4, 7.5 Hz, 1H), 2.08 – 1.99 (m,

1H), 1.87 (dddd, $J = 12.5, 7.9, 4.6, 2.0$ Hz, 1H), 1.77 – 1.68 (m, 2H), 1.68 – 1.60 (m, 2H), 1.48 (dddd, $J = 13.2, 8.1, 7.0, 3.5$ Hz, 1H), 1.32 – 1.12 (m, 3H), 1.05 (tdd, $J = 12.5, 10.9, 3.5$ Hz, 1H), 0.97 – 0.82 (m, 1H). ^{13}C NMR (101 MHz, CDCl_3): δ 137.7, 130.4, 129.7, 128.6, 127.2, 126.2, 87.3, 66.2, 44.6, 38.9, 33.4, 31.0, 28.9, 26.6, 25.9, 25.8. FTIR (NaCl, thin film, cm^{-1}): 2924, 2851, 1492, 1449, 1062, 970, 884, 753, 693.

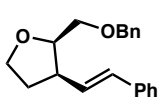
(2*S*,3*R*)-2-(4-chlorobutyl)-3-((*E*)-styryl)tetrahydrofuran (118)



Prepared from (*S,E*)-5-phenyl-5-(trimethylsilyl)pent-3-en-1-ol (**107**, 51.6 mg, 1.1 equiv, 0.22 mmol, 98% ee) and 5-chloropentanal (24.1 mg, 1.0 equiv, 0.2 mmol) according to General Procedure 2. The crude residue was purified by column chromatography (silica, 0 to 10% Et_2O /hexanes) to yield 39.9 mg of **118** (75% yield, 8:1 dr, >20:1 *E:Z*, 87% major isomer) as a colorless oil. $R_f = 0.27$ (silica, 10% EtOAc /hexane, UV). $[\alpha]_D^{25} = +29^\circ$ ($c = 0.5$, CHCl_3). ^1H NMR (400 MHz, CDCl_3): δ 7.40 – 7.35 (m, 2H), 7.35 – 7.29 (m, 2H), 7.25 – 7.20 (m, 1H), 6.42 (d, $J = 15.8$ Hz, 1H), 6.16 (dd, $J = 15.8, 9.6$ Hz, 1H), 4.05 (td, $J = 8.2, 5.8$ Hz, 1H), 3.87 – 3.77 (m, 2H), 3.51 (t, $J = 6.7$ Hz, 2H), 2.95 (ddt, $J = 10.1, 7.4, 5.3$ Hz, 1H), 2.22 (dddd, $J = 12.4, 8.4, 7.5, 5.8$ Hz, 1H), 1.89 (dddd, $J = 12.7, 8.1, 6.5, 4.8$ Hz, 1H), 1.84 – 1.72 (m, 2H), 1.66 – 1.41 (m, 4H). ^{13}C NMR (101 MHz, CDCl_3): δ 137.4, 130.9, 129.5, 128.7, 127.3, 126.2, 82.2, 66.7, 45.9, 45.1, 32.8, 32.7, 30.8, 24.1. FTIR (NaCl, thin film, cm^{-1}): 2934, 2867, 1493, 1449, 1073, 1043, 970, 752, 694.

(2*S*,3*R*)-2-(but-3-en-1-yl)-3-((*E*)-styryl)tetrahydrofuran (114)

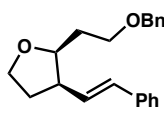
Prepared from (*S,E*)-5-phenyl-5-(trimethylsilyl)pent-3-en-1-ol (**107**, 51.6 mg, 1.1 equiv, 0.22 mmol, 98% ee) and pent-4-enal (16.8 mg, 1.0 equiv, 0.2 mmol) according to General Procedure 2. The crude residue was purified by column chromatography (silica, 0 to 5% Et₂O/hexanes) to yield 28.4 mg of **114** (62% yield, >20:1 dr, >20:1 *E:Z*, 94% major isomer) as a colorless oil. $R_f = 0.43$ (silica, 10% EtOAc/hexane, UV). $[\alpha]_D^{25} = +49^\circ$ ($c = 1.0$, CHCl₃). **¹H NMR (400 MHz, CDCl₃):** δ 7.39 – 7.34 (m, 2H), 7.34 – 7.29 (m, 2H), 7.25 – 7.20 (m, 1H), 6.42 (d, $J = 15.8$ Hz, 1H), 6.17 (dd, $J = 15.8, 9.6$ Hz, 1H), 5.82 (ddt, $J = 16.9, 10.2, 6.7$ Hz, 1H), 5.06 – 4.92 (m, 2H), 4.05 (td, $J = 8.3, 5.7$ Hz, 1H), 3.90 – 3.78 (m, 2H), 3.01 – 2.91 (m, 1H), 2.28 – 2.17 (m, 2H), 2.17 – 2.05 (m, 1H), 1.89 (dddd, $J = 12.8, 8.1, 6.6, 5.0$ Hz, 1H), 1.67 – 1.48 (m, 2H). **¹³C NMR (101 MHz, CDCl₃):** δ 138.6, 137.4, 130.7, 129.6, 128.7, 127.3, 126.2, 126.2, 114.8, 81.7, 67.0, 45.9, 32.9, 30.9, 30.8. **FTIR (NaCl, thin film, cm⁻¹):** 3026, 2974, 2937, 2871, 1640, 1449, 1066, 1051, 969, 911, 750, 694.

(2*R*,3*R*)-2-((benzyloxy)methyl)-3-((*E*)-styryl)tetrahydrofuran (124)

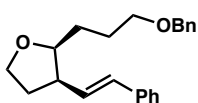
Prepared from (*S,E*)-5-phenyl-5-(trimethylsilyl)pent-3-en-1-ol (**107**, 51.6 mg, 1.1 equiv, 0.22 mmol, 98% ee) and 2-(benzyloxy)acetaldehyde (30.0 mg, 1.0 equiv, 0.2 mmol) according to General Procedure 2. The crude residue was purified by column chromatography (silica, 0 to 15% Et₂O/hexanes) to yield 38.2 mg of **124** (65% yield, 19:1 dr, 18:1 *E:Z*, 90% major isomer) as a colorless oil. $R_f = 0.17$ (silica, 10% EtOAc/hexane, UV). $[\alpha]_D^{25} = +29^\circ$ ($c = 1.0$, CHCl₃). **¹H NMR (400 MHz, CDCl₃):** δ 7.38

– 7.21 (m, 10H), 6.45 (d, $J = 15.8$ Hz, 1H), 6.20 (dd, $J = 15.8, 9.4$ Hz, 1H), 4.55 (q, $J = 12.1$ Hz, 2H), 4.18 – 4.10 (m, 2H), 3.87 (q, $J = 7.8$ Hz, 1H), 3.59 – 3.50 (m, 2H), 3.09 (dq, $J = 9.4, 6.9$ Hz, 1H), 2.20 (dtd, $J = 12.5, 7.6, 4.9$ Hz, 1H), 1.98 (dtd, $J = 12.3, 7.7, 6.4$ Hz, 1H) ^{13}C NMR (101 MHz, CDCl_3): δ 138.3, 137.3, 131.2, 128.8, 128.6, 128.4, 127.8, 127.6, 127.4, 126.2, 80.9, 73.6, 71.1, 67.8, 45.3, 32.9. FTIR (NaCl, thin film, cm^{-1}): 3027, 2919, 2861, 1495, 1451, 1361, 1076, 1027, 970, 748, 695.

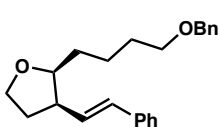
(2*S*,3*R*)-2-(2-(benzyloxy)ethyl)-3-((*E*)-styryl)tetrahydrofuran (119)



Prepared from (*S,E*)-5-phenyl-5-(trimethylsilyl)pent-3-en-1-ol (**107**, 51.6 mg, 1.1 equiv, 0.22 mmol, 98% ee) and 3-(benzyloxy)propanal (32.8 mg, 1.0 equiv, 0.2 mmol) according to General Procedure 2. The crude residue was purified by column chromatography (silica, 0 to 15% Et_2O /hexanes) to yield 50.3 mg of **119** (82% yield, 15:1 dr, 15:1 *E:Z*, 88% major isomer) as a colorless oil. $R_f = 0.20$ (silica, 10% EtOAc /hexane, UV). $[\alpha]_D^{25} = +49^\circ$ ($c = 1.0$, CHCl_3). ^1H NMR (400 MHz, CDCl_3): δ 7.39 – 7.20 (m, 10H), 6.40 (d, $J = 15.8$ Hz, 1H), 6.17 (dd, $J = 15.8, 9.5$ Hz, 1H), 4.57 – 4.48 (m, 2H), 4.10 – 4.02 (m, 2H), 3.83 (td, $J = 8.3, 6.7$ Hz, 1H), 3.62 (td, $J = 6.7, 3.6$ Hz, 2H), 2.97 (dtd, $J = 9.6, 7.3, 5.5$ Hz, 1H), 2.30 – 2.14 (m, 1H), 1.90 (dddd, $J = 12.1, 8.2, 6.7, 5.1$ Hz, 1H), 1.82 (q, $J = 6.8$ Hz, 2H). ^{13}C NMR (101 MHz, CDCl_3): δ 138.6, 137.3, 131.0, 129.4, 128.6, 128.4, 127.8, 127.6, 127.3, 126.2, 79.2, 73.2, 68.0, 66.8, 45.9, 32.7, 31.9. FTIR (NaCl, thin film, cm^{-1}): 3027, 2927, 2946, 2861, 1495, 1453, 1363, 1092, 1028, 970, 750, 737, 696.

(2*S*,3*R*)-2-(3-(benzyloxy)propyl)-3-((*E*)-styryl)tetrahydrofuran (125)

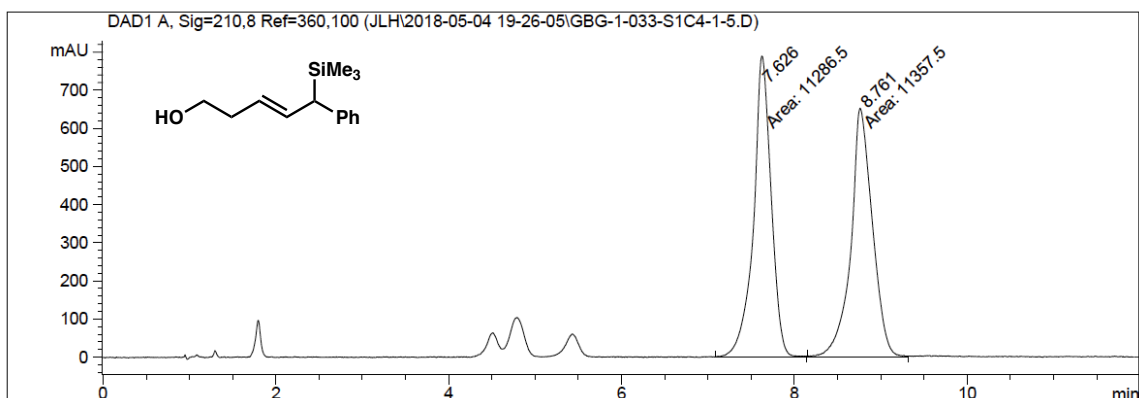
Prepared from (*S,E*)-5-phenyl-5-(trimethylsilyl)pent-3-en-1-ol (**107**, 51.6 mg, 1.1 equiv, 0.22 mmol, 98% ee) and 4-(benzyloxy)butanal (35.6 mg, 1.0 equiv, 0.2 mmol) according to General Procedure 2. The crude residue was purified by column chromatography (silica, 0 to 15% Et₂O/hexanes) to yield 47.4 mg of **125** (74% yield, >20:1 dr, 19:1 *E:Z*, 92% major isomer) as a colorless oil. $R_f = 0.17$ (silica, 10% EtOAc/hexane, UV). $[\alpha]_D^{25} = +33^\circ$ (c = 1.0, CHCl₃). **¹H NMR (400 MHz, CDCl₃):** δ 7.43 – 7.20 (m, 10H), 6.43 (d, $J = 15.8$ Hz, 1H), 6.19 (dd, $J = 15.8, 9.6$ Hz, 1H), 4.49 (s, 2H), 4.06 (td, $J = 8.3, 5.7$ Hz, 1H), 3.92 – 3.78 (m, 2H), 3.49 (qt, $J = 9.3, 6.4$ Hz, 2H), 3.02 – 2.92 (m, 1H), 2.22 (dtd, $J = 13.4, 7.9, 5.6$ Hz, 1H), 1.96 – 1.85 (m, 1H), 1.85 – 1.76 (m, 1H), 1.76 – 1.65 (m, 1H), 1.58 (q, $J = 7.1$ Hz, 2H). **¹³C NMR (101 MHz, CDCl₃):** δ 138.7, 137.4, 130.8, 129.6, 128.6, 128.4, 127.7, 127.5, 127.3, 126.2, 82.2, 72.8, 70.3, 66.7, 45.9, 32.8, 28.2, 26.9. **FTIR (NaCl, thin film, cm⁻¹):** 3027, 2934, 2855, 1495, 1452, 1362, 1100, 1073, 1028, 970, 749, 737, 696.

(2*S*,3*R*)-2-(4-(benzyloxy)butyl)-3-((*E*)-styryl)tetrahydrofuran (126)

Prepared from (*S,E*)-5-phenyl-5-(trimethylsilyl)pent-3-en-1-ol (**107**, 51.6 mg, 1.1 equiv, 0.22 mmol, 98% ee) and 5-(benzyloxy)pentanal (38.5 mg, 1.0 equiv, 0.2 mmol) according to General Procedure 2. The crude residue was purified by column chromatography (silica, 0 to 15% Et₂O/hexanes) to yield 40.1 mg of **126** (60% yield, 20:1 dr, >20:1 *E:Z*, 92% major isomer) as a colorless oil. $R_f = 0.23$ (silica, 10% EtOAc/hexane, UV). $[\alpha]_D^{25} = +38^\circ$ (c = 1.0, CHCl₃). **¹H NMR (400 MHz, CDCl₃):**

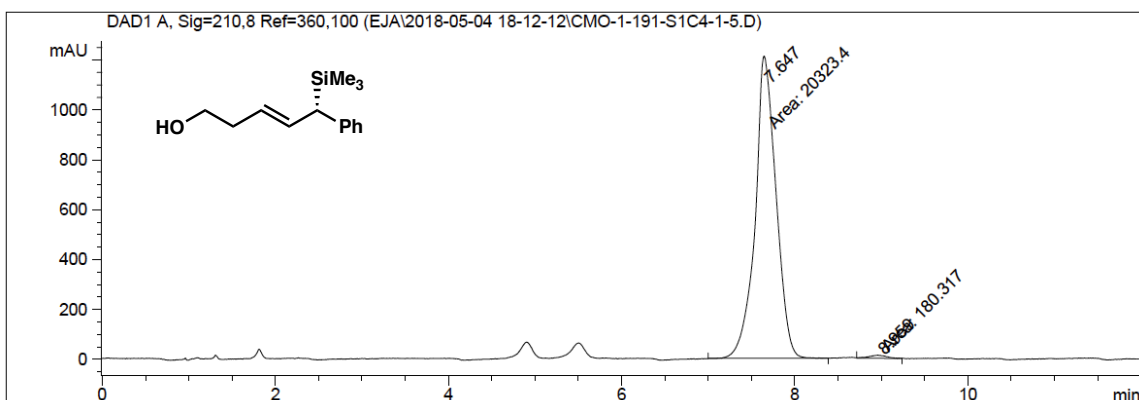
δ 7.38 – 7.21 (m, 10H), 6.41 (d, $J = 15.8$ Hz, 1H), 6.17 (dd, $J = 15.8, 9.6$ Hz, 1H), 4.47 (s, 2H), 4.05 (td, $J = 8.2, 5.8$ Hz, 1H), 3.89 – 3.78 (m, 2H), 3.46 (t, $J = 6.5$ Hz, 2H), 2.99 – 2.88 (m, 1H), 2.22 (dddd, $J = 12.5, 8.4, 7.5, 5.8$ Hz, 1H), 1.88 (dddd, $J = 12.7, 8.1, 6.4, 4.7$ Hz, 1H), 1.69 – 1.39 (m, 6H). **^{13}C NMR (101 MHz, CDCl_3):** δ 138.8, 137.5, 130.7, 129.7, 128.7, 128.4, 127.7, 127.5, 127.3, 126.2, 82.4, 72.9, 70.4, 66.6, 45.9, 32.9, 31.3, 29.9, 23.3. **FTIR (NaCl, thin film, cm^{-1}):** 3027, 2936, 2860, 1495, 1452, 1361, 1102, 1073, 970, 750, 736, 696.

107: racemic



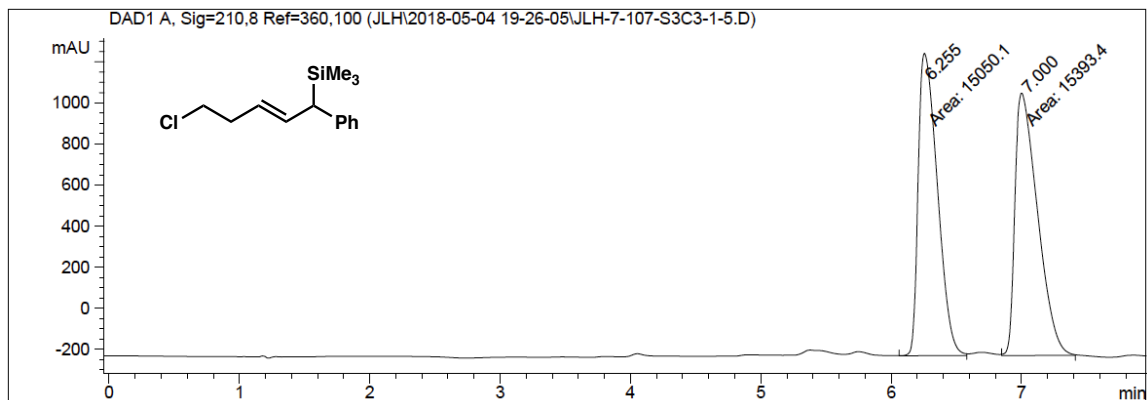
Peak #	RetTime [min]	Type	Width [min]	Area [mAU*s]	Height [mAU]	Area %
1	7.626	MM	0.2380	1.12865e4	790.36163	49.8431
2	8.761	MM	0.2899	1.13575e4	652.97833	50.1569

107: enantioenriched, 98% ee



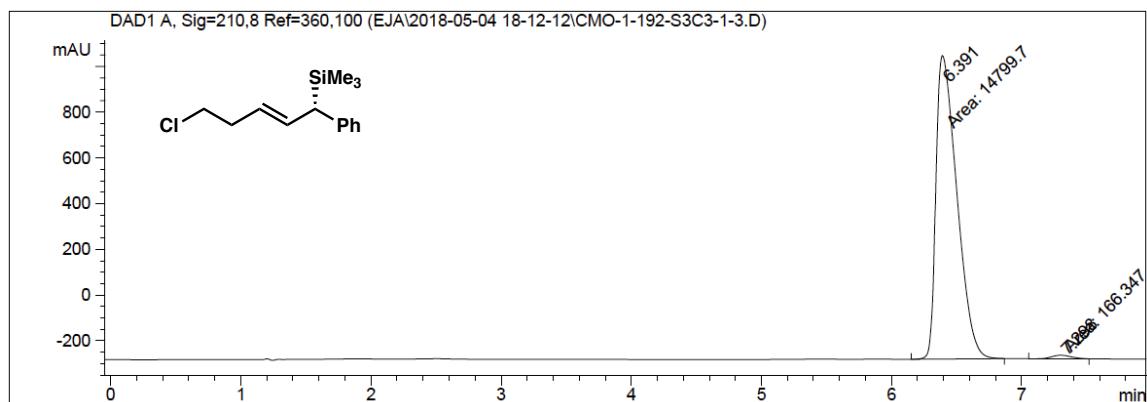
Peak #	RetTime [min]	Type	Width [min]	Area [mAU*s]	Height [mAU]	Area %
1	7.647	MM	0.2796	2.03234e4	1211.60693	99.1206
2	8.959	MM	0.2368	180.31700	12.69365	0.8794

106: racemic



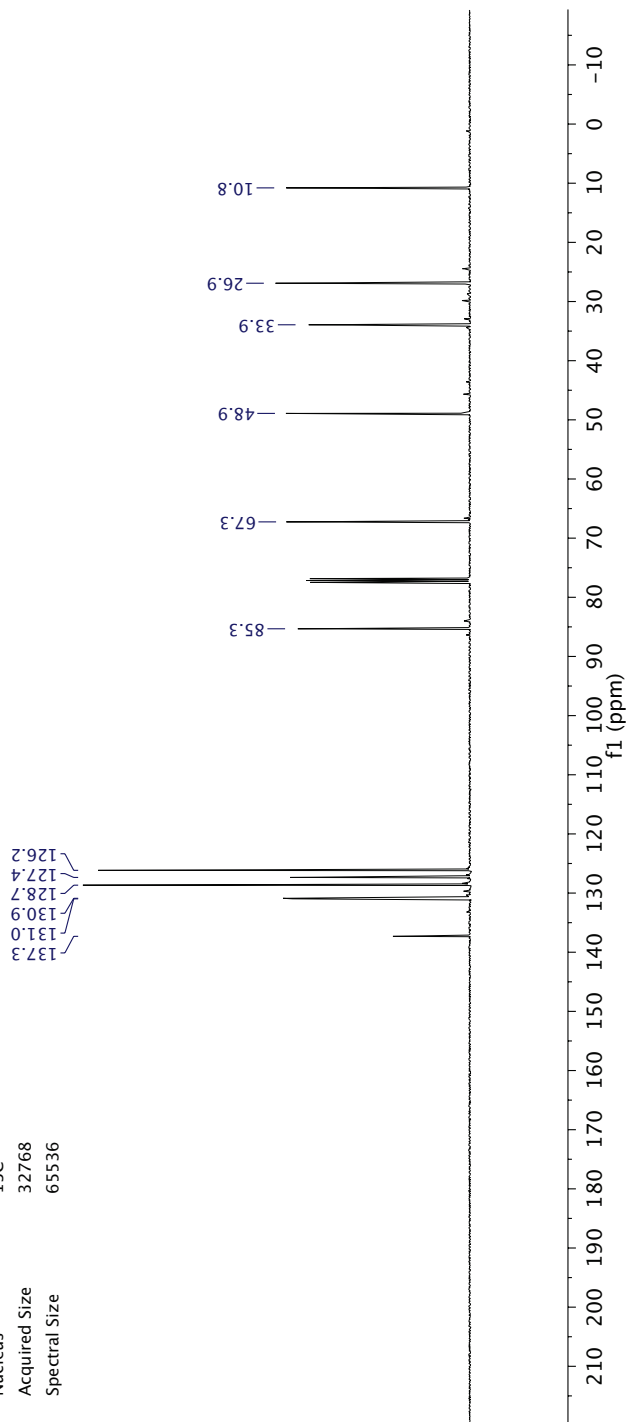
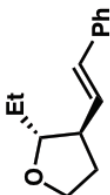
Peak #	RetTime [min]	Type	Width [min]	Area [mAU*s]	Height [mAU]	Area %
1	6.255	MM	0.1702	1.50501e4	1473.66772	49.4362
2	7.000	MM	0.2005	1.53934e4	1279.81885	50.5638

106: enantioenriched, 98% ee

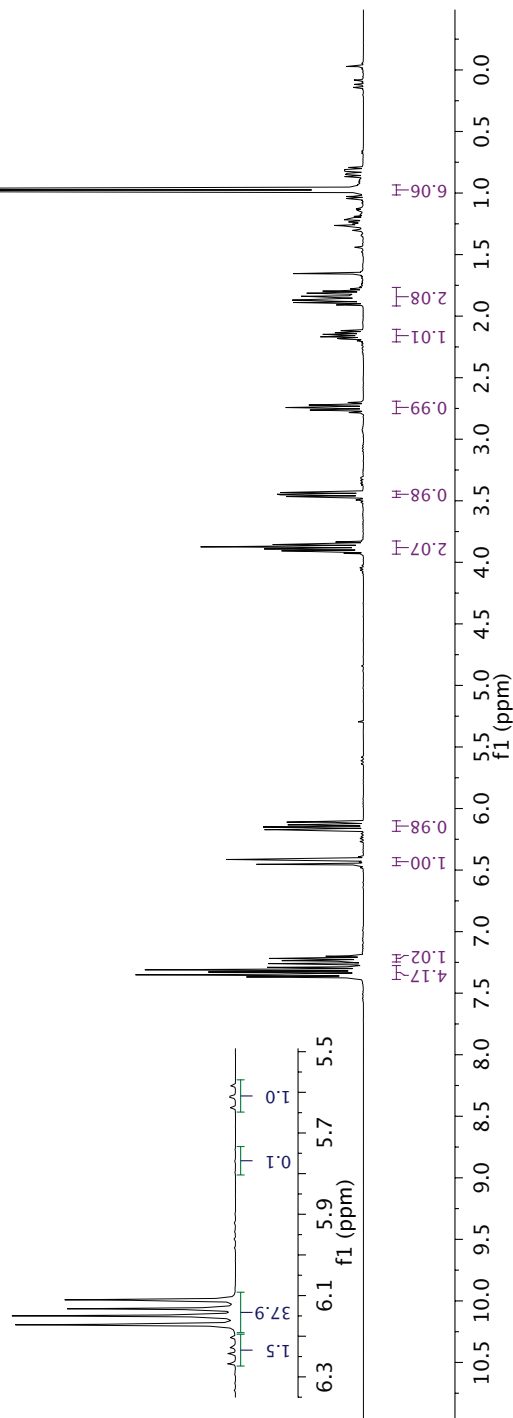
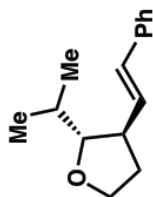


Peak #	RetTime [min]	Type	Width [min]	Area [mAU*s]	Height [mAU]	Area %
1	6.391	MM	0.1857	1.47997e4	1328.39636	98.8885
2	7.298	MM	0.1762	166.34677	15.73906	1.1115

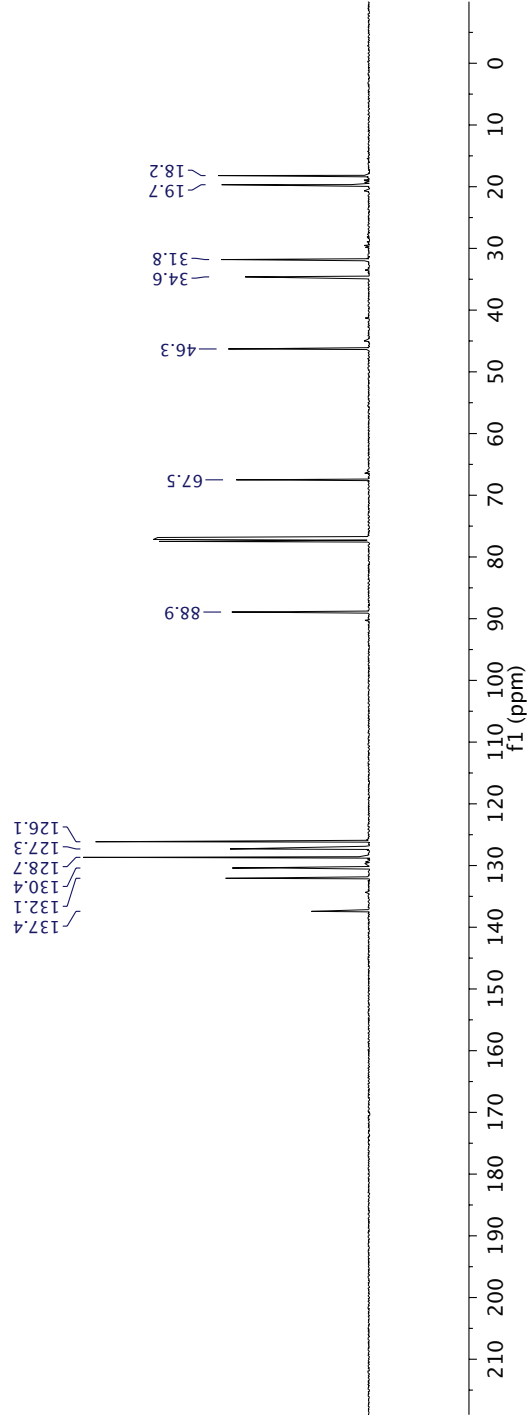
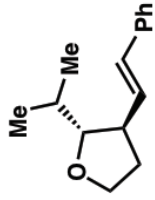
Parameter	Value
Title	CMO-1-170-pure.2.fid
Origin	Bruker BioSpin GmbH
Solvent	CDCl3
Temperature	295.0
Pulse Sequence	zgpg30
Number of Scans	256
Receiver Gain	64.2
Relaxation Delay	1.0000
Pulse Width	10.0000
Acquisition Time	1.3631
Acquisition Date	2017-08-30T21:00:47
Spectrometer Frequency	100.62
Spectral Width	24038.5
Lowest Frequency	-1949.8
Nucleus	13C
Acquired Size	32768
Spectral Size	65536



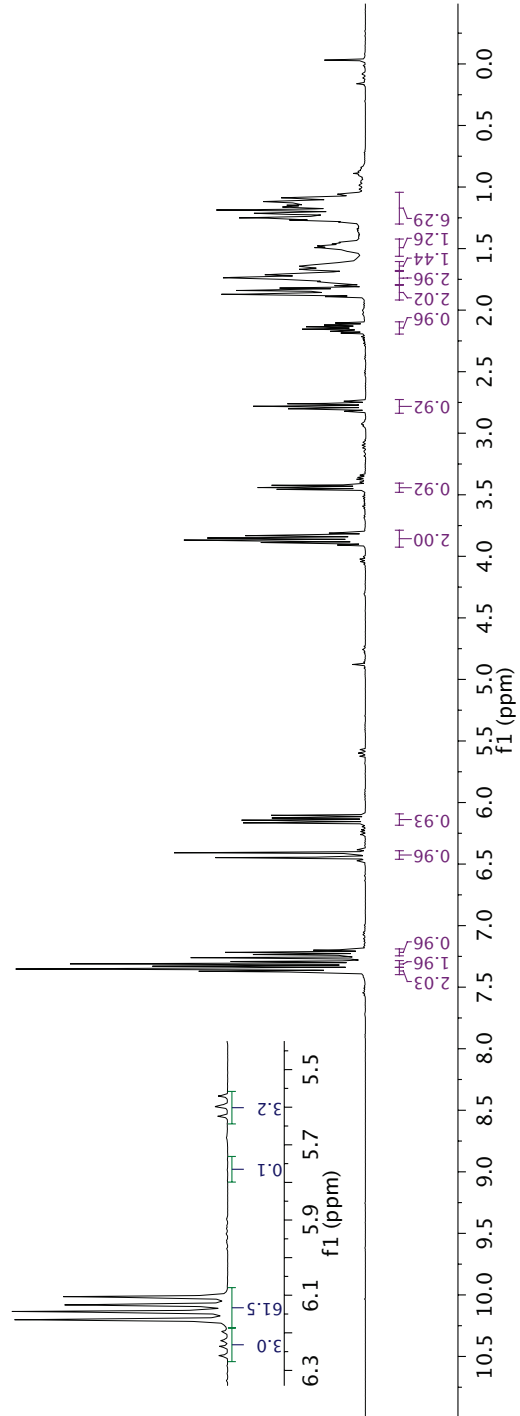
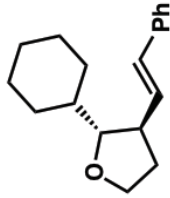
Parameter	Value
Title	CMO-1-173-pure.1.fid
Origin	Bruker BioSpin GmbH
Solvent	CDCl3
Temperature	295.0
Pulse Sequence	zg30
Number of Scans	16
Receiver Gain	30.3
Relaxation Delay	1.0000
Pulse Width	11.7000
Acquisition Time	4.0894
Acquisition Date	2017-09-04T18:44:17
Spectrometer Frequency	400.13
Spectral Width	8012.8
Lowest Frequency	-1534.3
Nucleus	¹ H
Acquired Size	32768
Spectral Size	65536



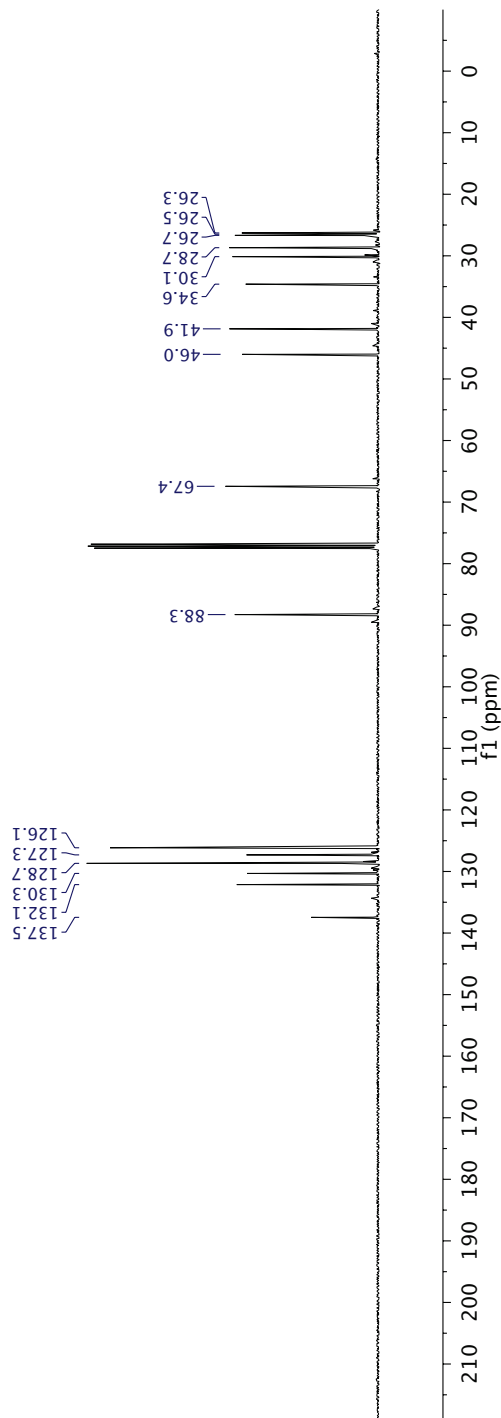
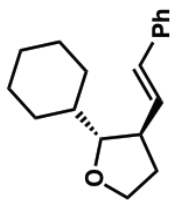
Parameter	Value
Title	CMO-1-173-pure.4.fid
Origin	Bruker BioSpin GmbH
Solvent	CDCl3
Temperature	295.0
Pulse Sequence	zgpg30
Number of Scans	512
Receiver Gain	64.2
Relaxation Delay	1.0000
Pulse Width	10.0000
Acquisition Time	1.3631
Acquisition Date	2017-09-04T19:13:16
Spectrometer Frequency	100.62
Spectral Width	24038.5
Lowest Frequency	-1958.4
Nucleus	¹³ C
Acquired Size	32768
Spectral Size	65536



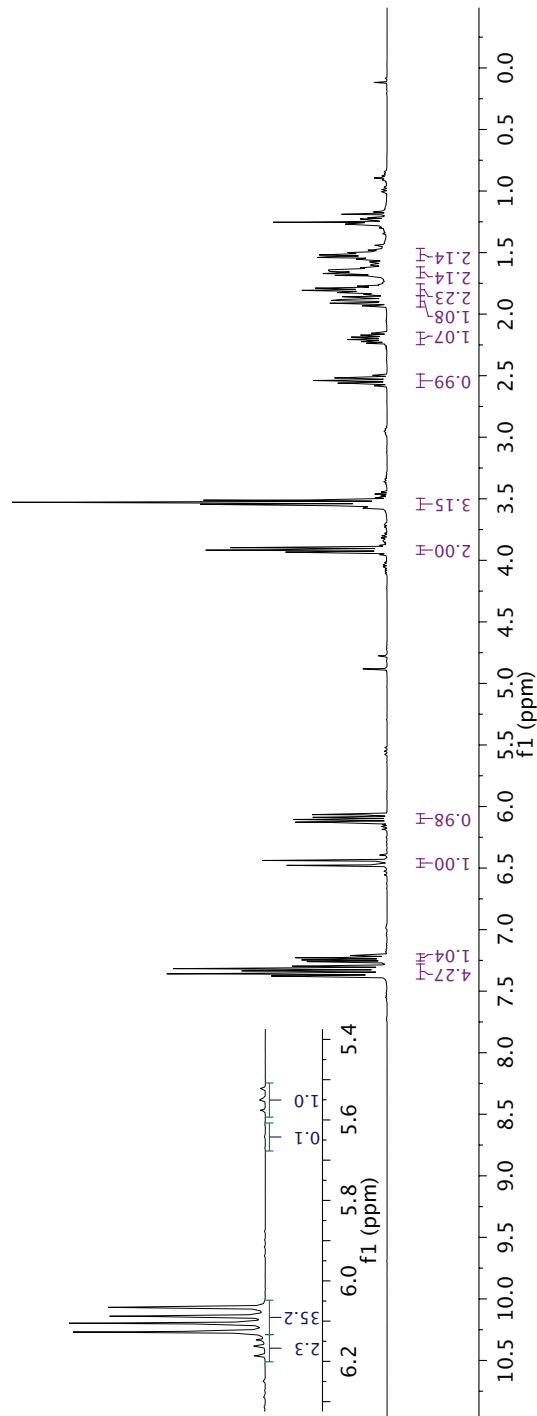
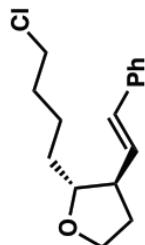
Parameter	Value
Title	GBG-1-022.2.fid
Origin	Bruker BioSpin GmbH
Solvent	CDCl3
Temperature	295.1
Pulse Sequence	zg30
Number of Scans	16
Receiver Gain	55.5
Relaxation Delay	1.0000
Pulse Width	11.7000
Acquisition Time	4.0894
Acquisition Date	2018-01-11T21:32:00
Spectrometer Frequency	400.13
Spectral Width	8012.8
Lowest Frequency	-1545.3
Nucleus	¹ H
Acquired Size	32768
Spectral Size	65536



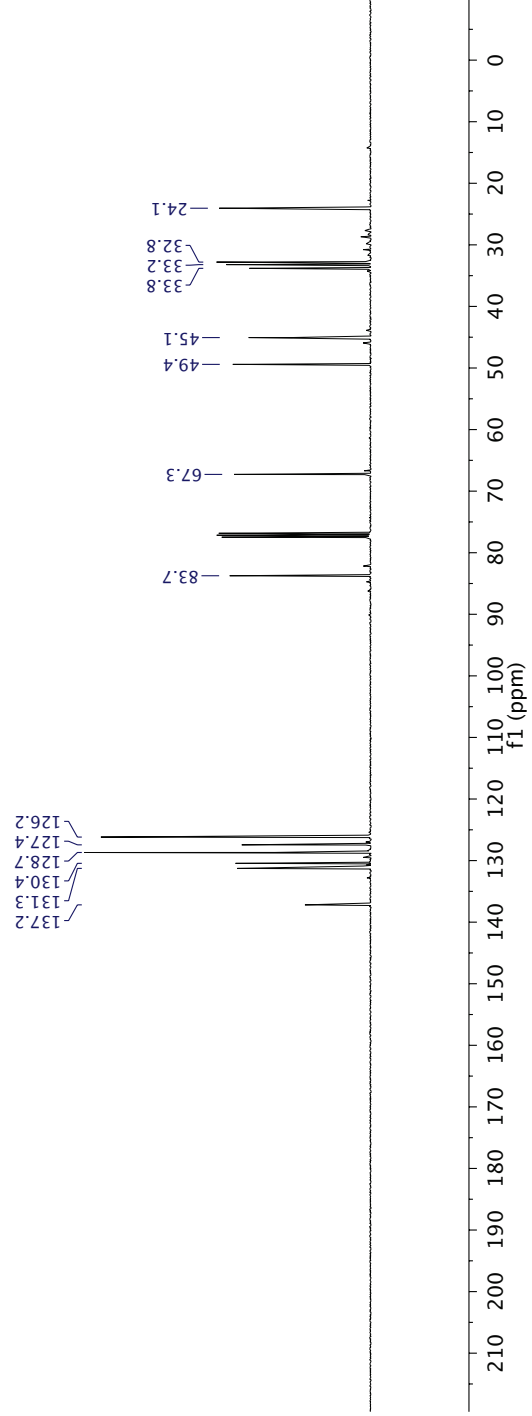
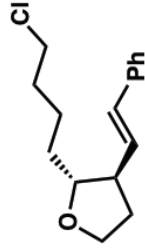
Parameter	Value
Title	GBG-1-022.1.fid
Origin	Bruker BioSpin GmbH
Solvent	CDCl3
Temperature	295.1
Pulse Sequence	zgpg30
Number of Scans	512
Receiver Gain	72.0
Relaxation Delay	1.0000
Pulse Width	10.0000
Acquisition Time	1.3631
Acquisition Date	2018-01-11T21:53:14
Spectrometer Frequency	100.62
Spectral Width	24038.5
Lowest Frequency	-1947.1
Nucleus	¹³ C
Acquired Size	32768
Spectral Size	65536



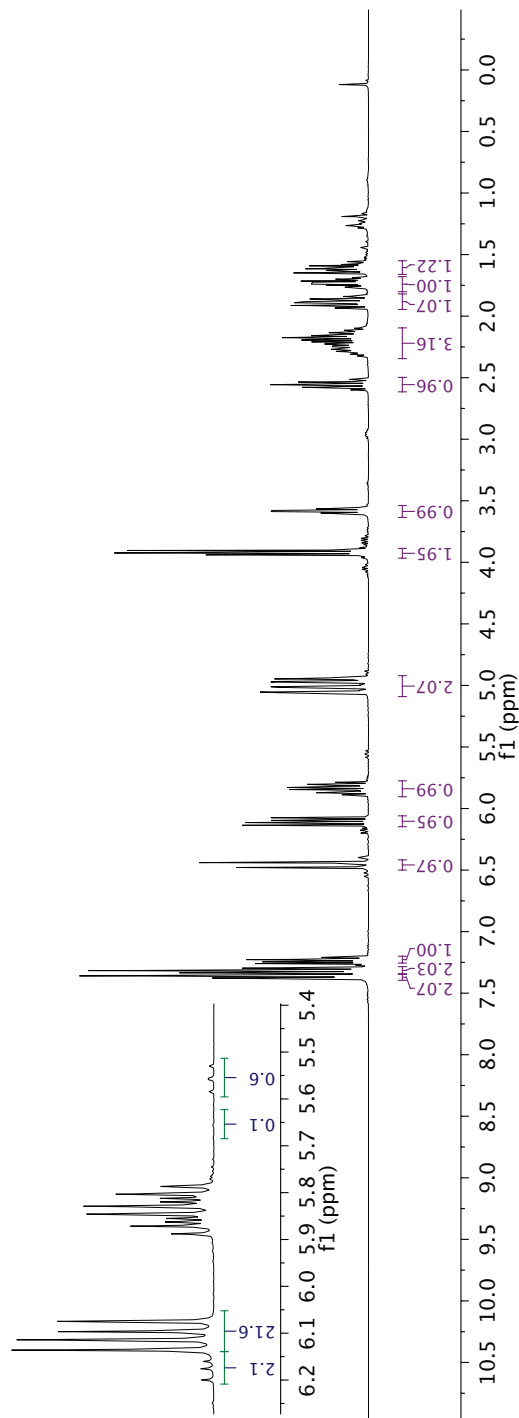
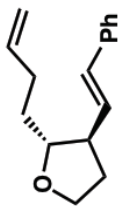
Parameter	Value
Title	CMO-1-175-pure.1.fid
Origin	Bruker BioSpin GmbH
Solvent	CDCl3
Temperature	295.0
Pulse Sequence	zg30
Number of Scans	16
Receiver Gain	30.3
Relaxation Delay	1.0000
Pulse Width	11.7000
Acquisition Time	4.0894
Acquisition Date	2017-09-05T18:42:05
Spectrometer Frequency	400.13
Spectral Width	8012.8
Lowest Frequency	-1592.5
Nucleus	¹ H
Acquired Size	32768
Spectral Size	65536



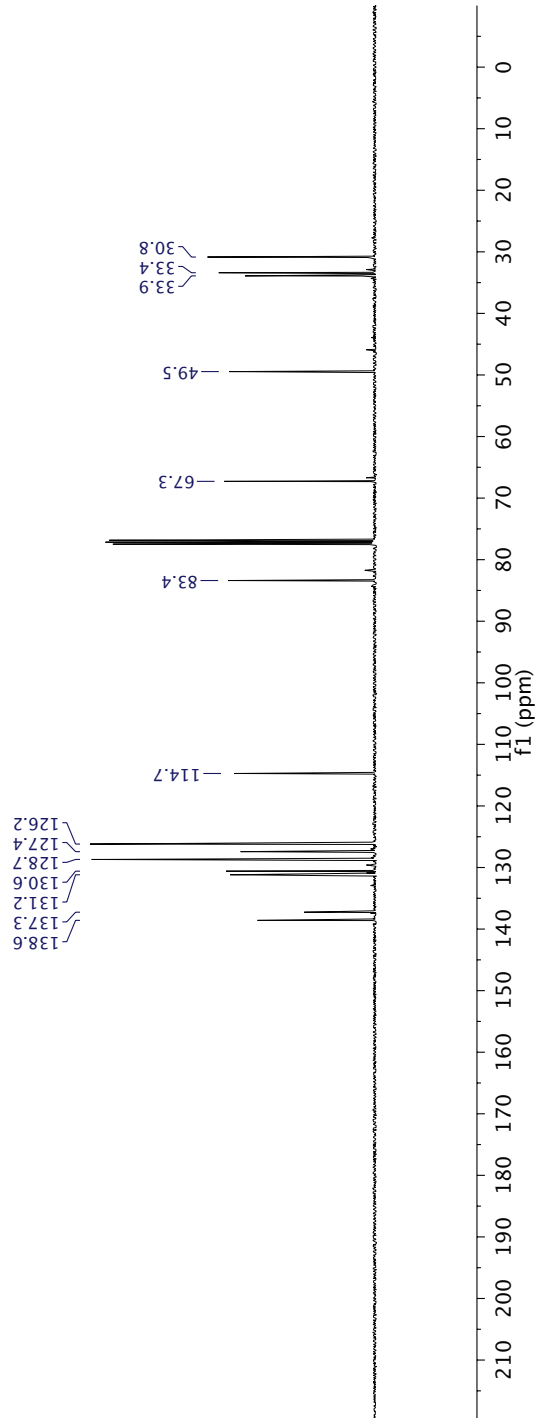
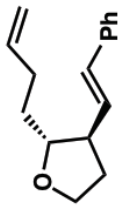
Parameter	Value
Title	CMO-1-175-pure.2.fid
Origin	Bruker BioSpin GmbH
Solvent	CDCl3
Temperature	295.0
Pulse Sequence	zgpg30
Number of Scans	512
Receiver Gain	78.7
Relaxation Delay	1.0000
Pulse Width	10.0000
Acquisition Time	1.3631
Acquisition Date	2017-09-05T19:03:52
Spectrometer Frequency	100.62
Spectral Width	24038.5
Lowest Frequency	-1958.4
Nucleus	¹³ C
Acquired Size	32768
Spectral Size	65536



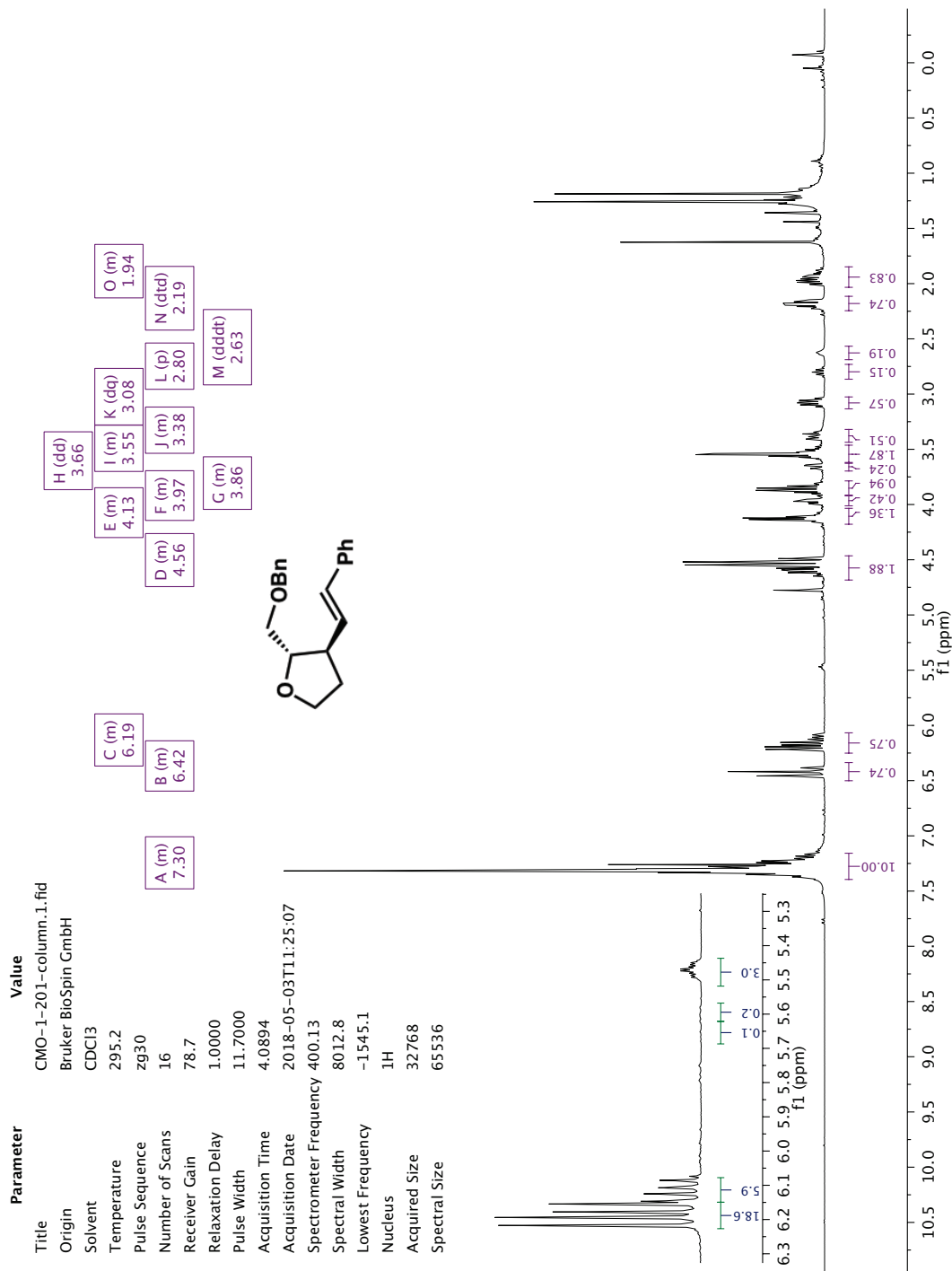
Parameter	Value
Title	JLH-7-127-column-2.11
Origin	Bruker BioSpin GmbH
Solvent	CDCl3
Temperature	295.2
Pulse Sequence	zg30
Number of Scans	16
Receiver Gain	30.3
Relaxation Delay	1.0000
Pulse Width	11.7000
Acquisition Time	4.0894
Acquisition Date	2018-02-03T23:35:57
Spectrometer Frequency	400.13
Spectral Width	8012.8
Lowest Frequency	-1593.2
Nucleus	¹ H
Acquired Size	32768
Spectral Size	65536



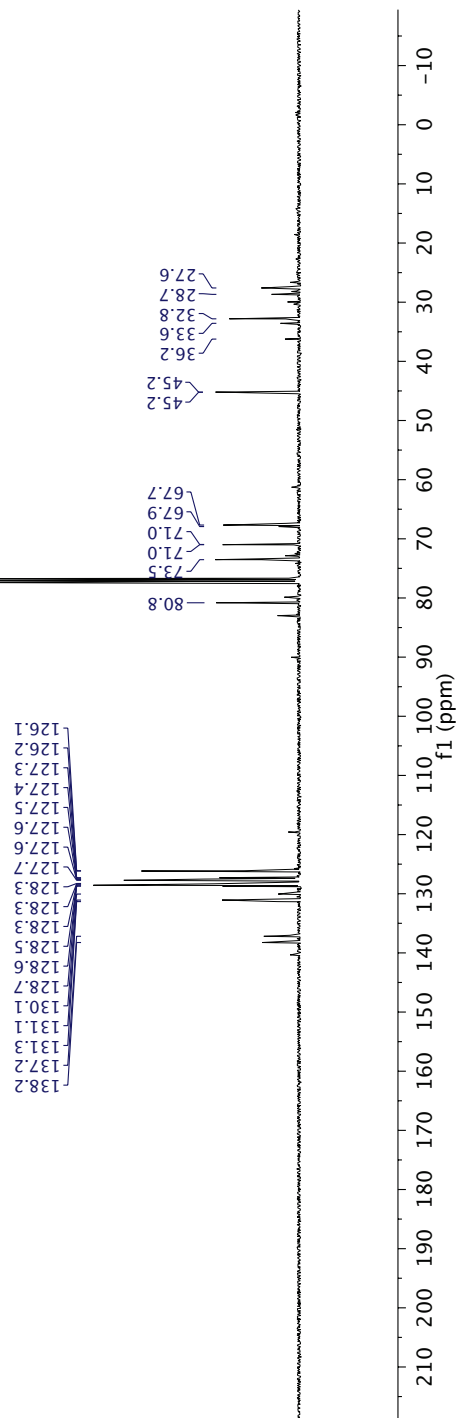
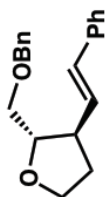
Parameter	Value
Title	JLH-7-127-column-2.2.fid
Origin	Bruker BioSpin GmbH
Solvent	CDCl3
Temperature	295.2
Pulse Sequence	zgpg30
Number of Scans	128
Receiver Gain	64.2
Relaxation Delay	2.0000
Pulse Width	10.0000
Acquisition Time	1.3631
Acquisition Date	2018-02-03T23:43:47
Spectrometer Frequency	100.62
Spectral Width	24038.5
Lowest Frequency	-1958.0
Nucleus	¹³ C
Acquired Size	32768
Spectral Size	65536

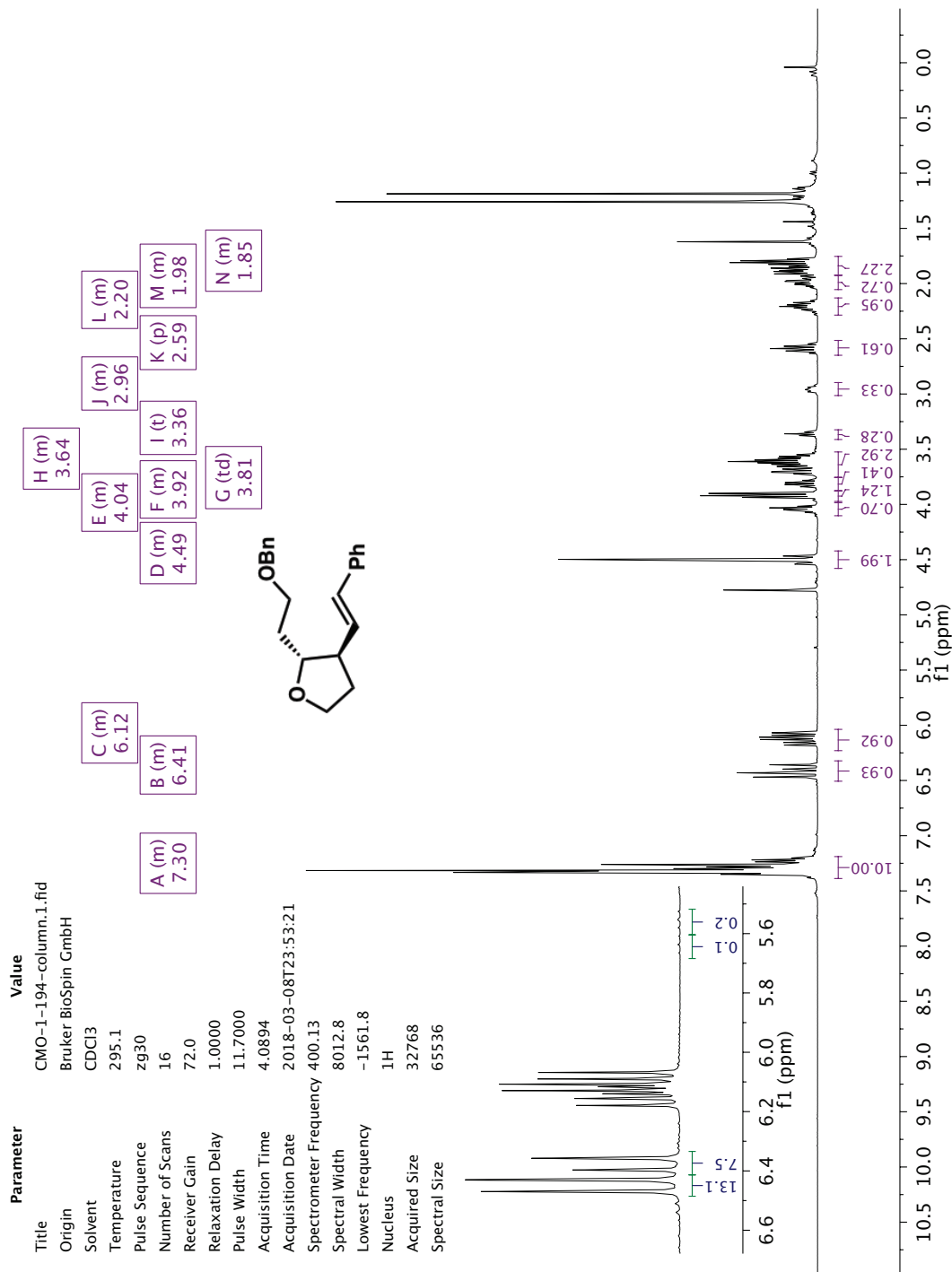


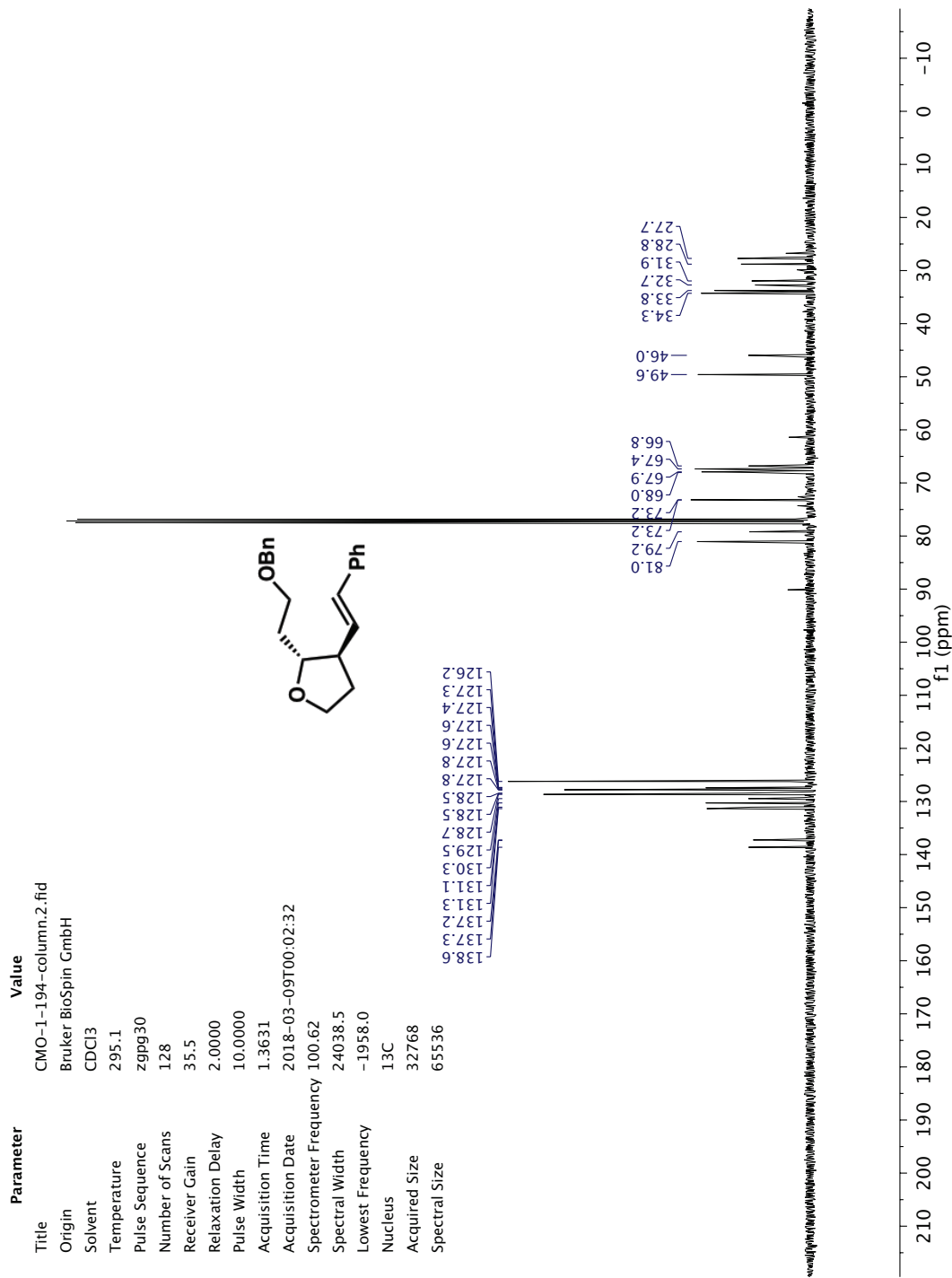
Parameter	Value
Title	CMO-1-201-column.1.fid
Origin	Bruker BioSpin GmbH
Solvent	CDCl3
Temperature	295.2
Pulse Sequence	zg30
Number of Scans	16
Receiver Gain	78.7
Relaxation Delay	1.0000
Pulse Width	11.7000
Acquisition Time	4.0894
Acquisition Date	2018-05-03T11:25:07
Spectrometer Frequency	400.13
Spectral Width	8012.8
Lowest Frequency	-1545.1
Nucleus	¹ H
Acquired Size	32768
Spectral Size	65536



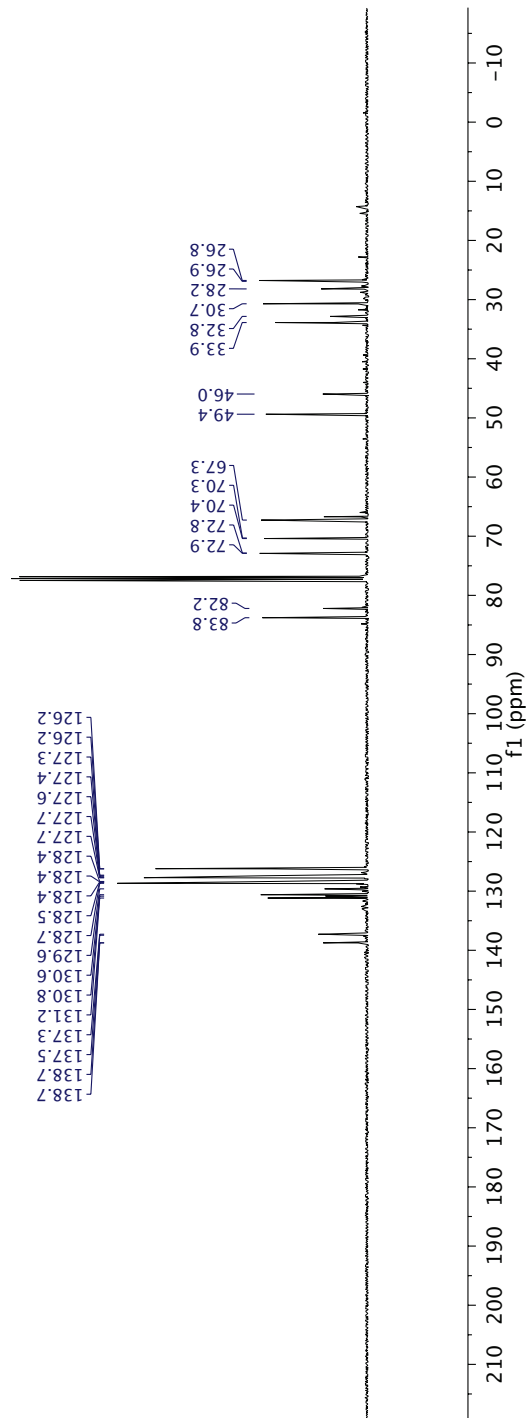
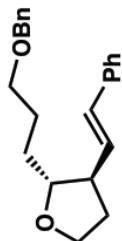
Parameter	Value
Title	CMO-1-201-column.2.fid
Origin	Bruker BioSpin GmbH
Solvent	CDCl3
Temperature	295.2
Pulse Sequence	zgpg30
Number of Scans	512
Receiver Gain	64.2
Relaxation Delay	1.0000
Pulse Width	10.0000
Acquisition Time	1.3631
Acquisition Date	2018-05-03T11:46:20
Spectrometer Frequency	100.62
Spectral Width	24038.5
Lowest Frequency	-1958.4
Nucleus	¹³ C
Acquired Size	32768
Spectral Size	65536

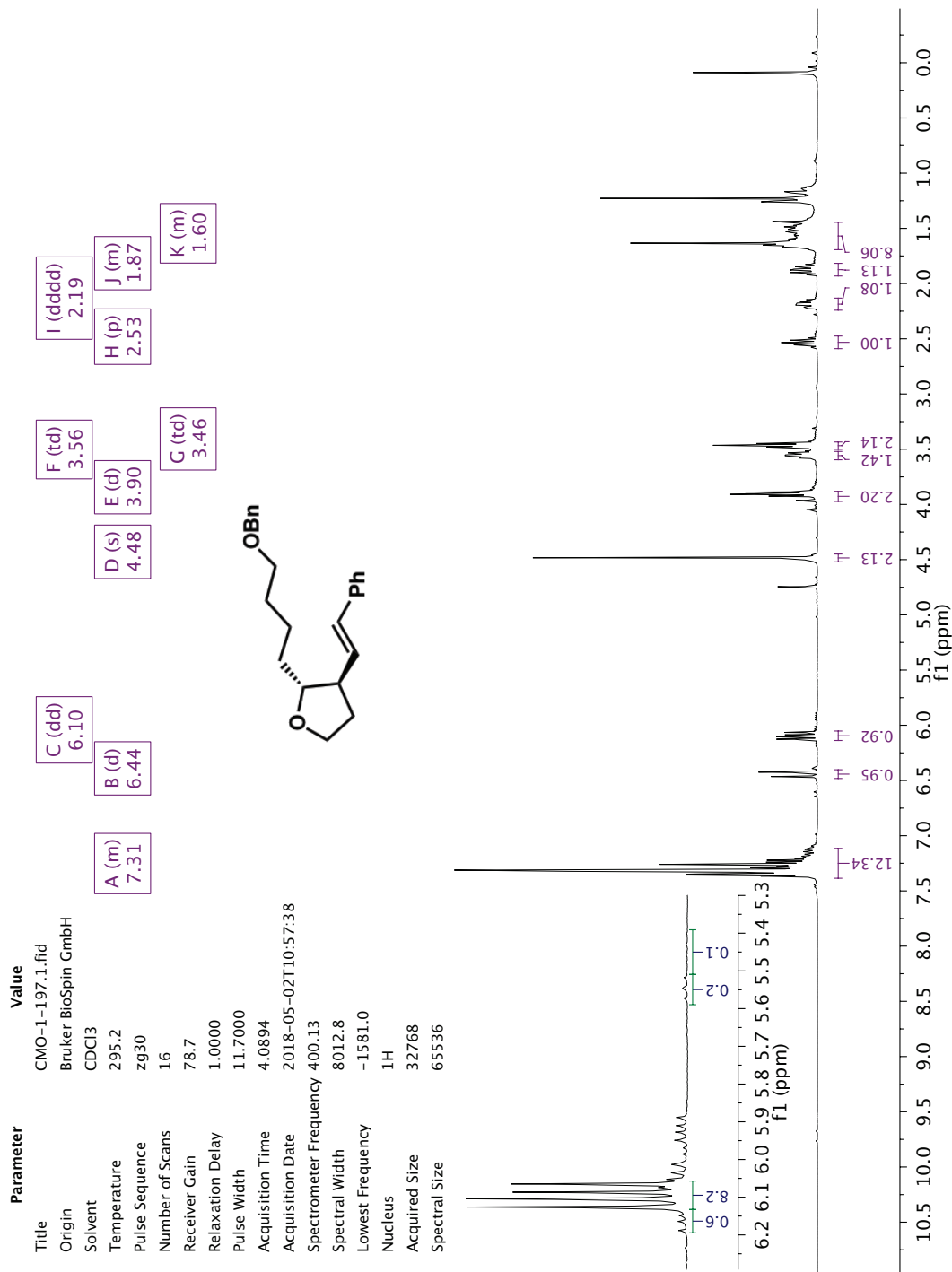




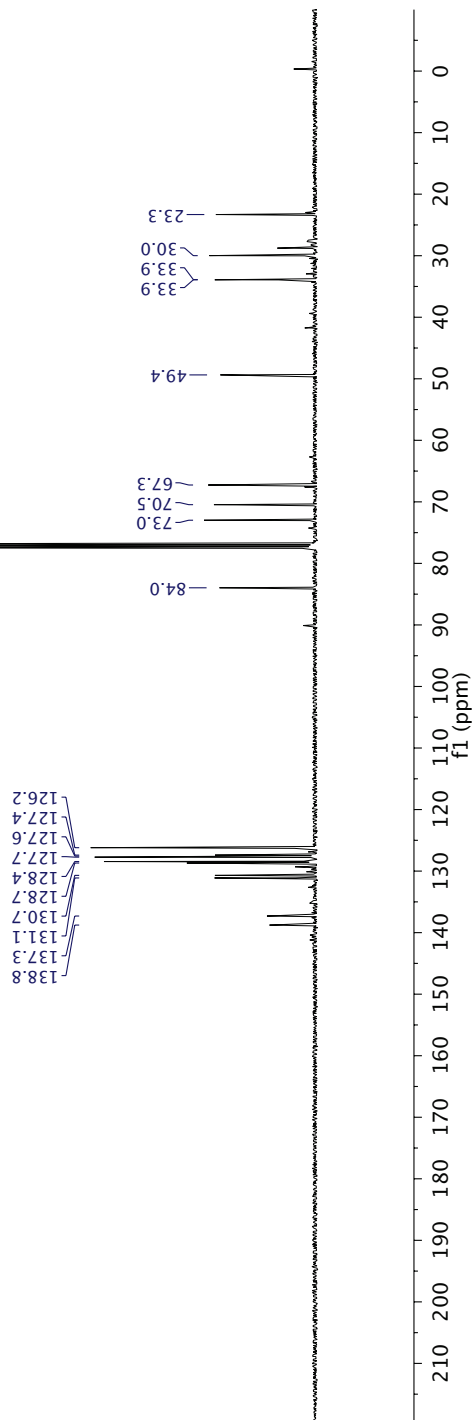


Parameter	Value
Title	CMO-1-202.2.fid
Origin	Bruker BioSpin GmbH
Solvent	CDCl3
Temperature	295.1
Pulse Sequence	zgpg30
Number of Scans	512
Receiver Gain	72.0
Relaxation Delay	1.0000
Pulse Width	10.0000
Acquisition Time	1.3631
Acquisition Date	2018-05-03T13:39:14
Spectrometer Frequency	100.62
Spectral Width	24038.5
Lowest Frequency	-1948.3
Nucleus	¹³ C
Acquired Size	32768
Spectral Size	65536

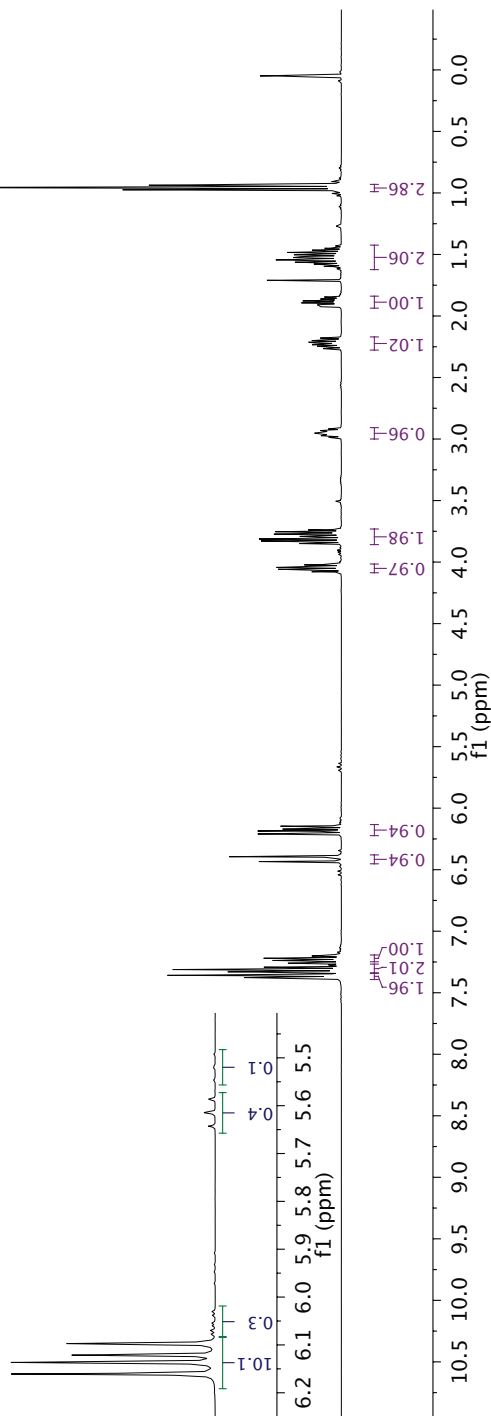
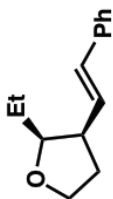




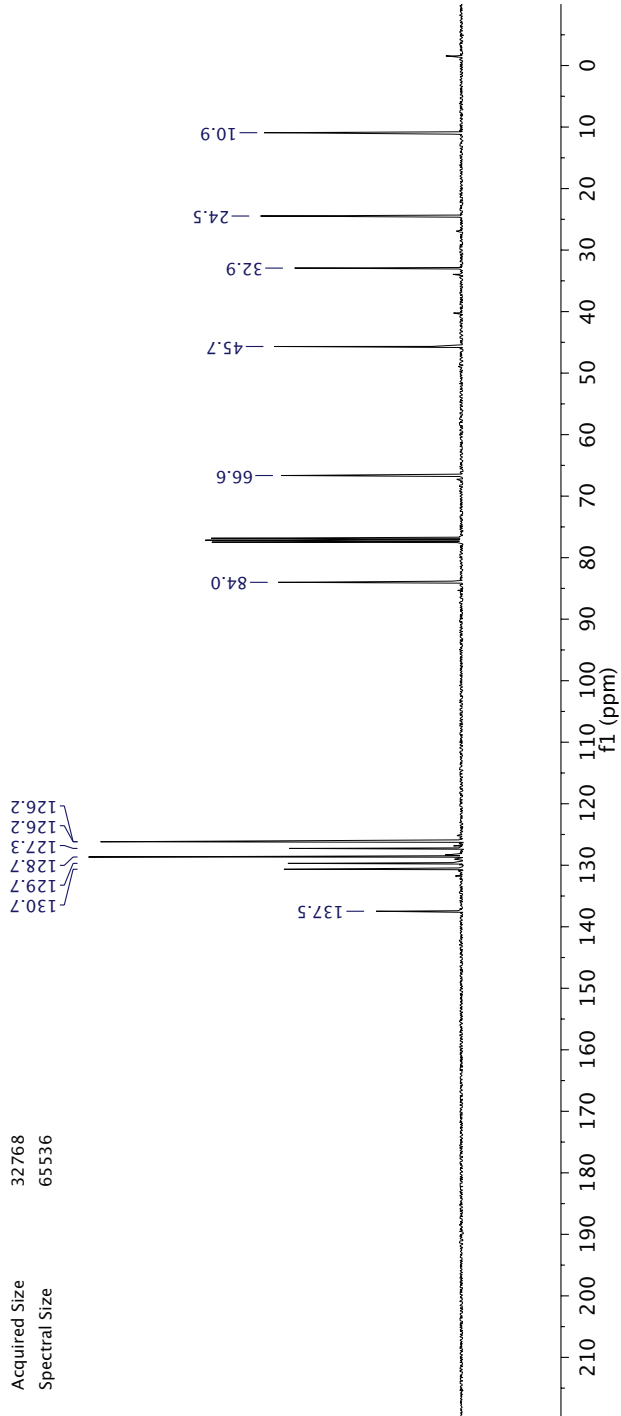
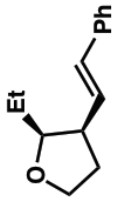
Parameter	Value
Title	CMO-1-197.2.fid
Origin	Bruker BioSpin GmbH
Solvent	CDCl3
Temperature	295.2
Pulse Sequence	zgpg30
Number of Scans	512
Receiver Gain	72.0
Relaxation Delay	1.0000
Pulse Width	10.0000
Acquisition Time	1.3631
Acquisition Date	2018-05-02T11:18:52
Spectrometer Frequency	100.62
Spectral Width	24038.5
Lowest Frequency	-1947.1
Nucleus	¹³ C
Acquired Size	32768
Spectral Size	65536



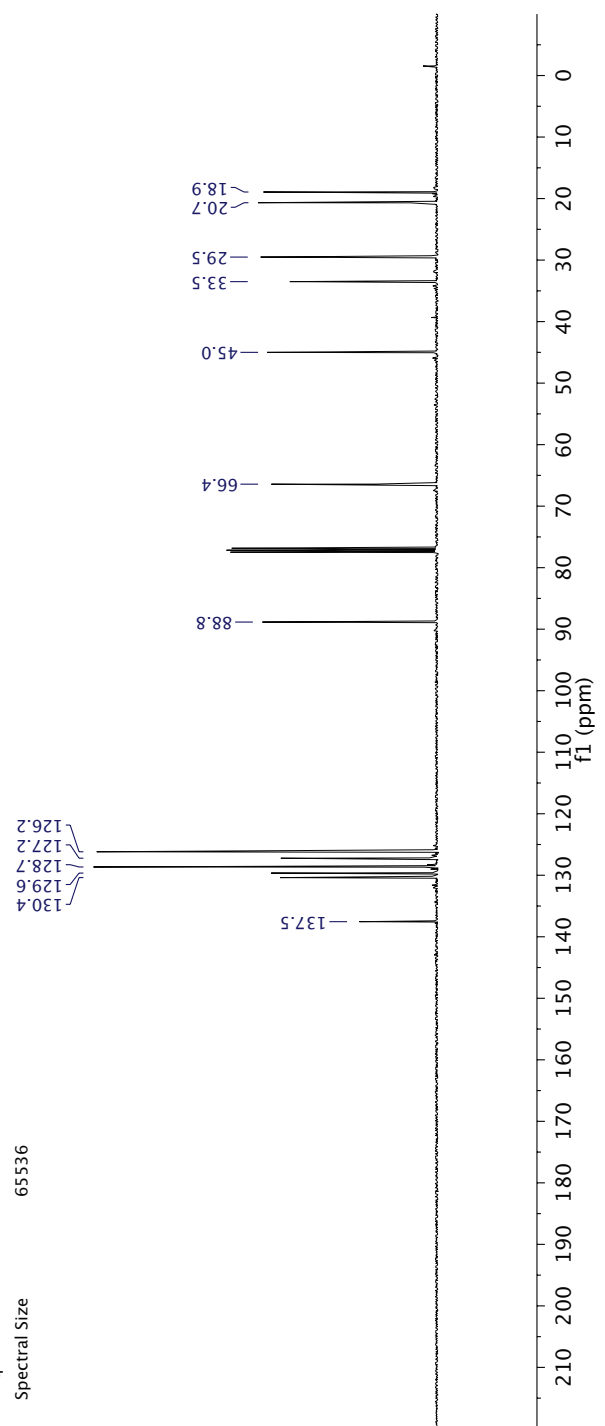
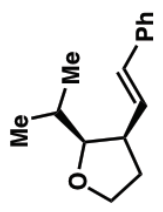
Parameter	Value
Title	JLH-7-172-column.1.fid
Origin	Bruker BioSpin GmbH
Solvent	CDCl3
Temperature	295.2
Pulse Sequence	zg30
Number of Scans	16
Receiver Gain	30.3
Relaxation Delay	1.0000
Pulse Width	11.7000
Acquisition Time	4.0894
Acquisition Date	2018-03-17T08:57:05
Spectrometer Frequency	400.13
Spectral Width	8012.8
Lowest Frequency	-1564.9
Nucleus	¹ H
Acquired Size	32768
Spectral Size	65536



Parameter	Value
Title	JLH-7-172-column.2.fid
Origin	Bruker BioSpin GmbH
Solvent	CDCl3
Temperature	295.2
Pulse Sequence	zgpg30
Number of Scans	128
Receiver Gain	55.5
Relaxation Delay	2.0000
Pulse Width	10.0000
Acquisition Time	1.3631
Acquisition Date	2018-03-17T09:04:55
Spectrometer Frequency	100.62
Spectral Width	24038.5
Lowest Frequency	-1791.7
Nucleus	13C
Acquired Size	32768
Spectral Size	65536

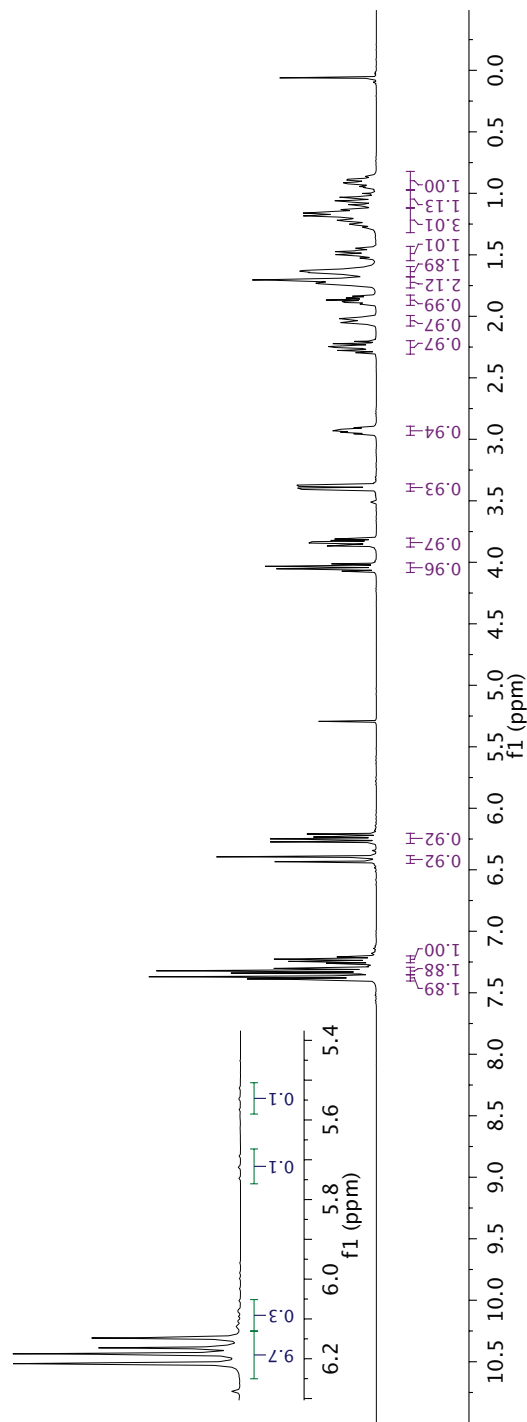
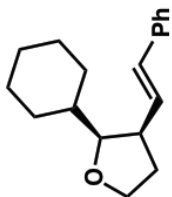


Parameter	Value
Title	JLH-7-174-column.2.fid
Origin	Bruker BioSpin GmbH
Solvent	CDCl3
Temperature	295.1
Pulse Sequence	zgpg30
Number of Scans	128
Receiver Gain	87.8
Relaxation Delay	2.0000
Pulse Width	10.0000
Acquisition Time	1.3631
Acquisition Date	2018-03-17T11:09:32
Spectrometer Frequency	100.62
Spectral Width	24038.5
Lowest Frequency	-1793.0
Nucleus	13C
Acquired Size	32768
Spectral Size	65536

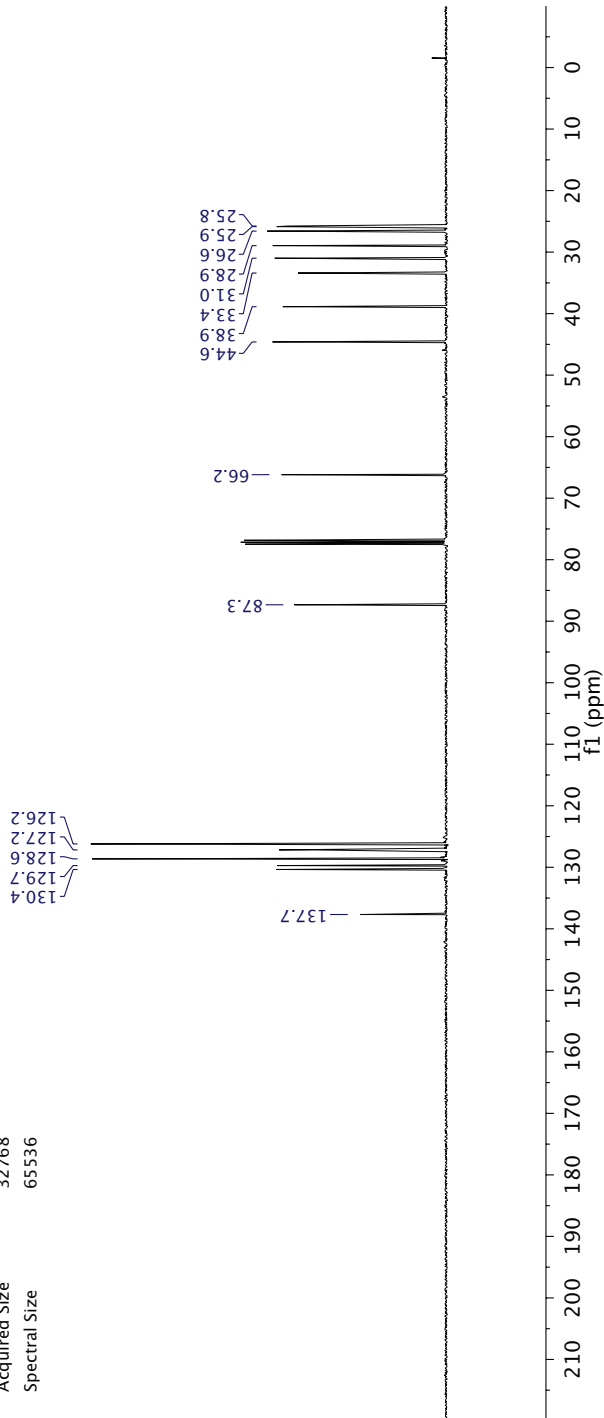
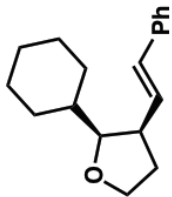


Parameter	Value
Title	JLH-7-173-column.1.fid
Origin	Bruker BioSpin GmbH
Solvent	CDCl3
Temperature	295.2
Pulse Sequence	zg30
Number of Scans	16
Receiver Gain	30.3
Relaxation Delay	1.0000
Pulse Width	11.7000
Acquisition Time	4.0894
Acquisition Date	2018-03-17T10:34:53
Spectrometer Frequency	400.13
Spectral Width	8012.8
Lowest Frequency	-1569.5
Nucleus	¹ H
Acquired Size	32768
Spectral Size	65536

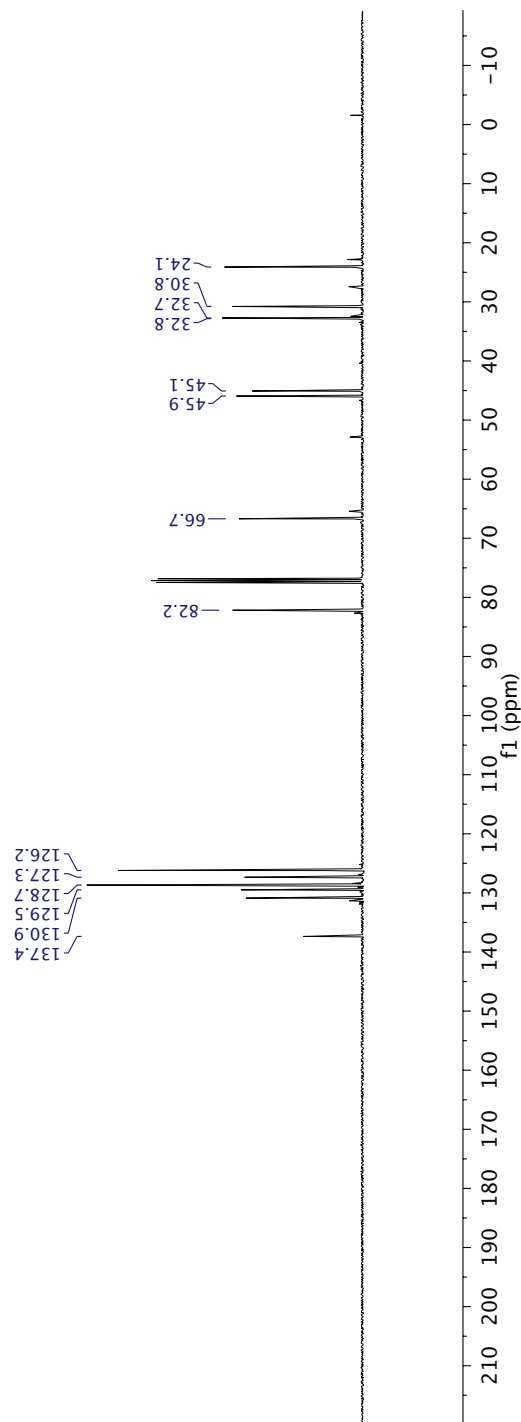
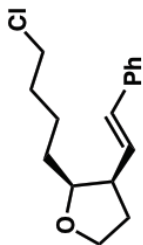
M (m)	1.72
K (m)	2.03
P (m)	1.19
J (ddt)	2.25
N (m)	1.64
R (m)	0.91
L (dddd)	1.87
Q (tdd)	1.05
O (dddd)	1.48
I (dddd)	2.93
G (ddd)	3.84
H (dd)	3.39
F (q)	4.04
E (dd)	6.24
D (d)	6.41
B (dd)	7.32
A (m)	7.38
C (m)	7.23



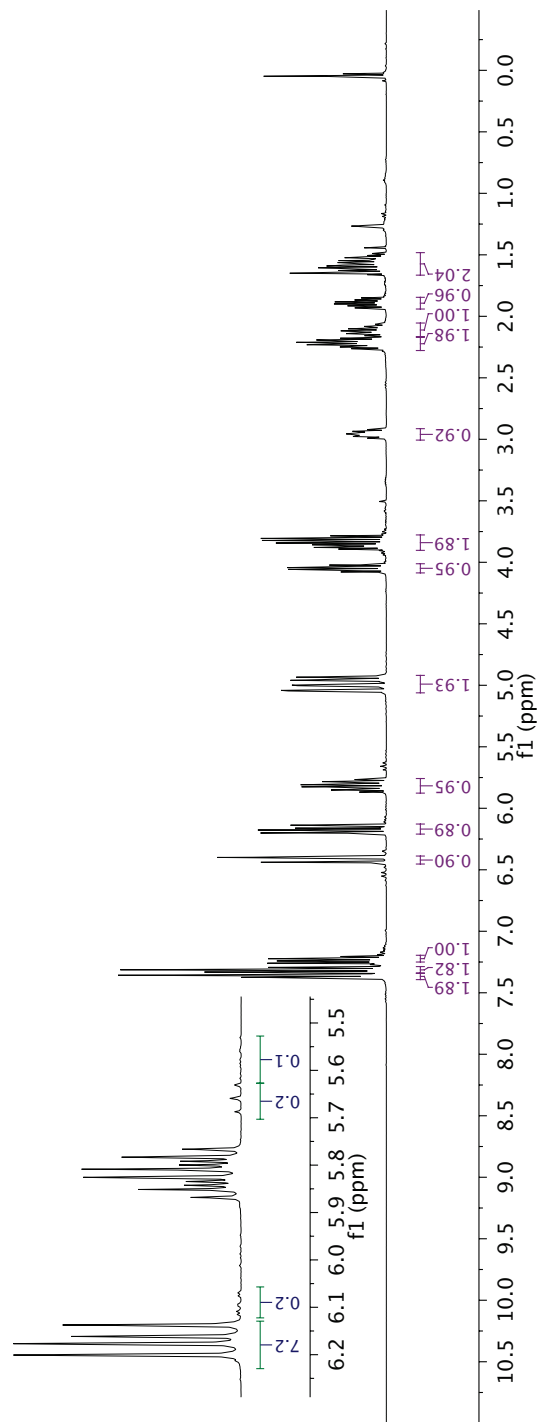
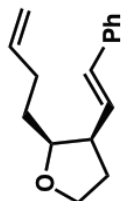
Parameter	Value
Title	JLH-7-173-column.2.fid
Origin	Bruker BioSpin GmbH
Solvent	CDCl3
Temperature	295.2
Pulse Sequence	zgpg30
Number of Scans	128
Receiver Gain	78.7
Relaxation Delay	2.0000
Pulse Width	10.0000
Acquisition Time	1.3631
Acquisition Date	2018-03-17T10:42:43
Spectrometer Frequency	100.62
Spectral Width	24038.5
Lowest Frequency	-1793.6
Nucleus	13C
Acquired Size	32768
Spectral Size	65536



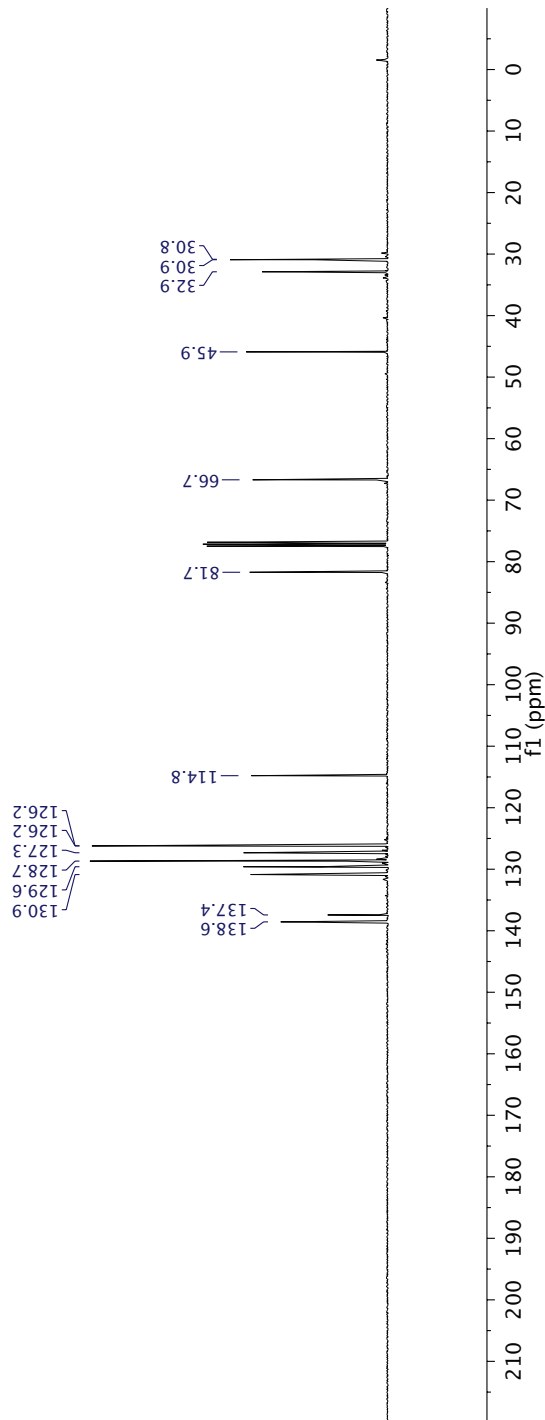
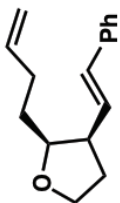
Parameter	Value
Title	JLH-7-176-column.4.fid
Origin	Bruker BioSpin GmbH
Solvent	CDCl3
Temperature	295.1
Pulse Sequence	zgpg30
Number of Scans	128
Receiver Gain	72.0
Relaxation Delay	2.0000
Pulse Width	10.0000
Acquisition Time	1.3631
Acquisition Date	2018-03-17T23:31:19
Spectrometer Frequency	100.62
Spectral Width	24038.5
Lowest Frequency	-1949.4
Nucleus	13C
Acquired Size	32768
Spectral Size	65536



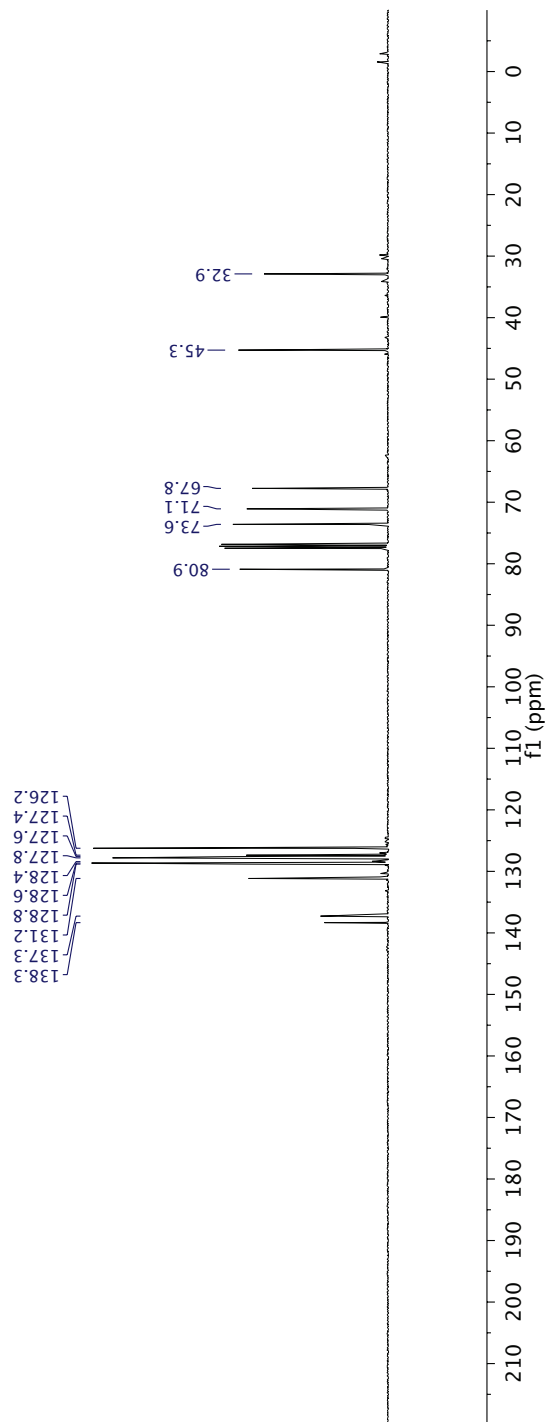
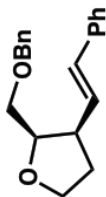
Parameter	Value
Title	JLH-7-228.1.fid
Origin	Bruker BioSpin GmbH
Solvent	CDCl ₃
Temperature	295.1
Pulse Sequence	zg30
Number of Scans	16
Receiver Gain	30.3
Relaxation Delay	1.0000
Pulse Width	11.7000
Acquisition Time	4.0894
Acquisition Date	2018-05-04T11:59:39
Spectrometer Frequency	400.13
Spectral Width	8012.8
Lowest Frequency	-1545.5
Nucleus	¹ H
Acquired Size	32768
Spectral Size	65536



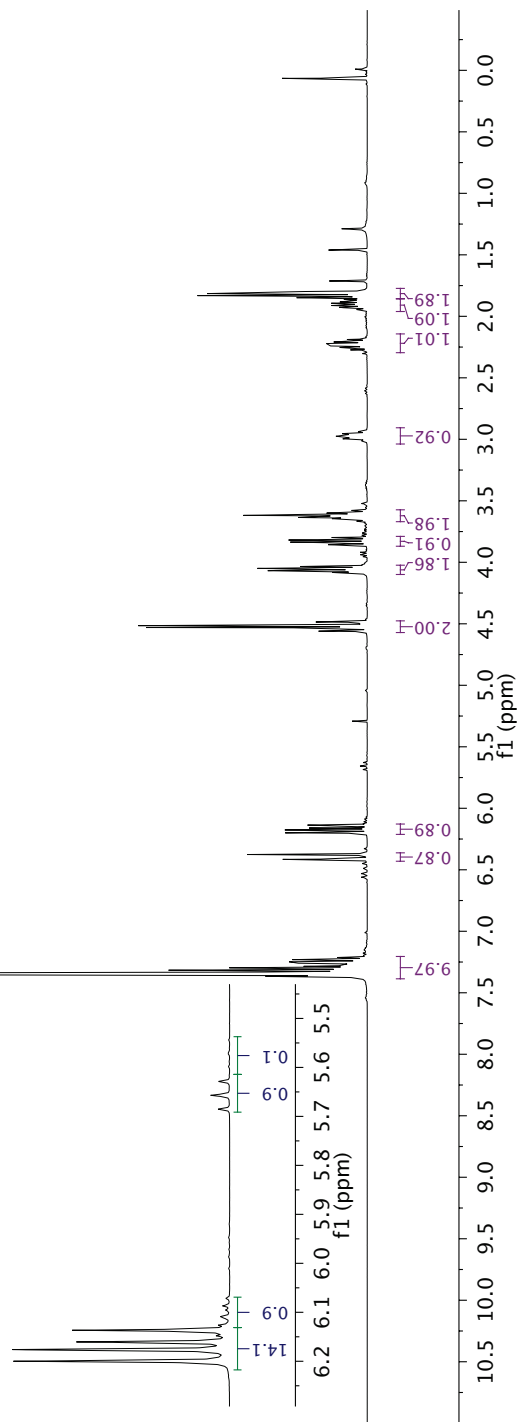
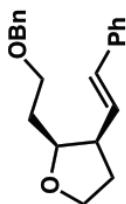
Parameter	Value
Title	JLH-7-228.2.fid
Origin	Bruker BioSpin GmbH
Solvent	CDCl3
Temperature	295.1
Pulse Sequence	zgpg30
Number of Scans	512
Receiver Gain	55.5
Relaxation Delay	1.0000
Pulse Width	10.0000
Acquisition Time	1.3631
Acquisition Date	2018-05-04T12:20:53
Spectrometer Frequency	100.62
Spectral Width	24038.5
Lowest Frequency	-1948.3
Nucleus	13C
Acquired Size	32768
Spectral Size	65536



Parameter	Value
Title	CBG-1-039.2.fid
Origin	Bruker BioSpin GmbH
Solvent	CDCl ₃
Temperature	295.2
Pulse Sequence	zgpg30
Number of Scans	512
Receiver Gain	55.5
Relaxation Delay	1.0000
Pulse Width	10.0000
Acquisition Time	1.3631
Acquisition Date	2018-05-04T13:38:06
Spectrometer Frequency	100.62
Spectral Width	24038.5
Lowest Frequency	-1794.4
Nucleus	¹³ C
Acquired Size	32768
Spectral Size	65536

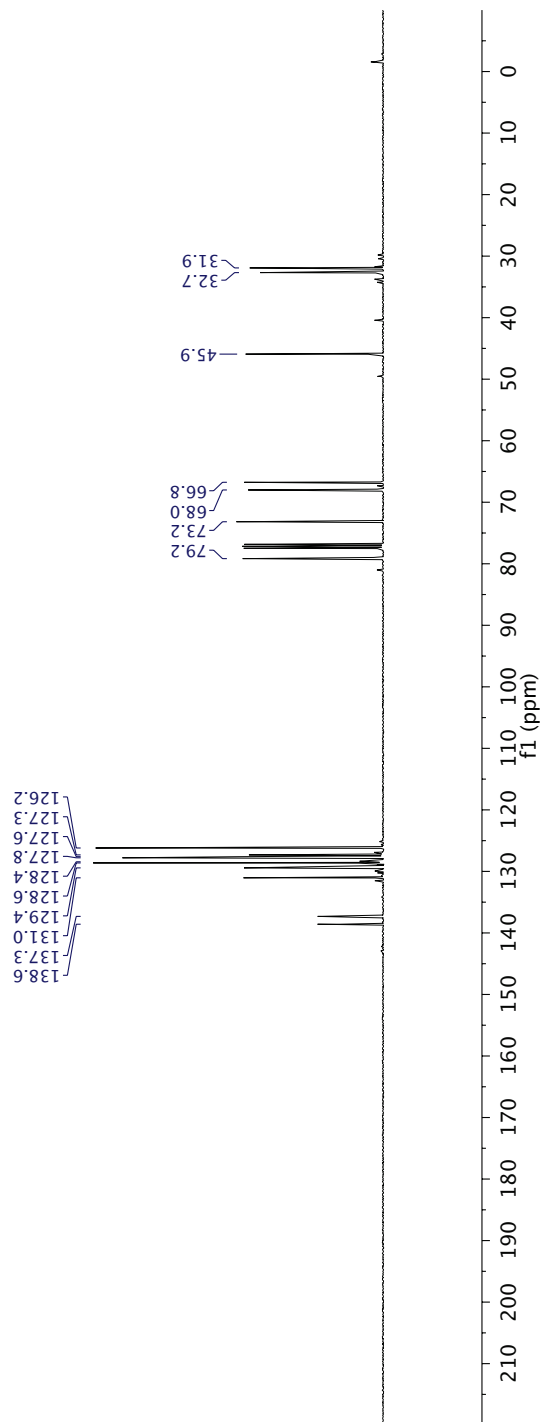
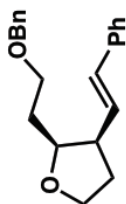


Parameter	Value
Title	JLH-7-226.1.fid
Origin	Bruker BioSpin GmbH
Solvent	CDCl3
Temperature	295.2
Pulse Sequence	zg30
Number of Scans	16
Receiver Gain	30.3
Relaxation Delay	1.0000
Pulse Width	11.7000
Acquisition Time	4.0894
Acquisition Date	2018-05-04T12:25:11
Spectrometer Frequency	400.13
Spectral Width	8012.8
Lowest Frequency	-1545.4
Nucleus	¹ H
Acquired Size	32768
Spectral Size	65536

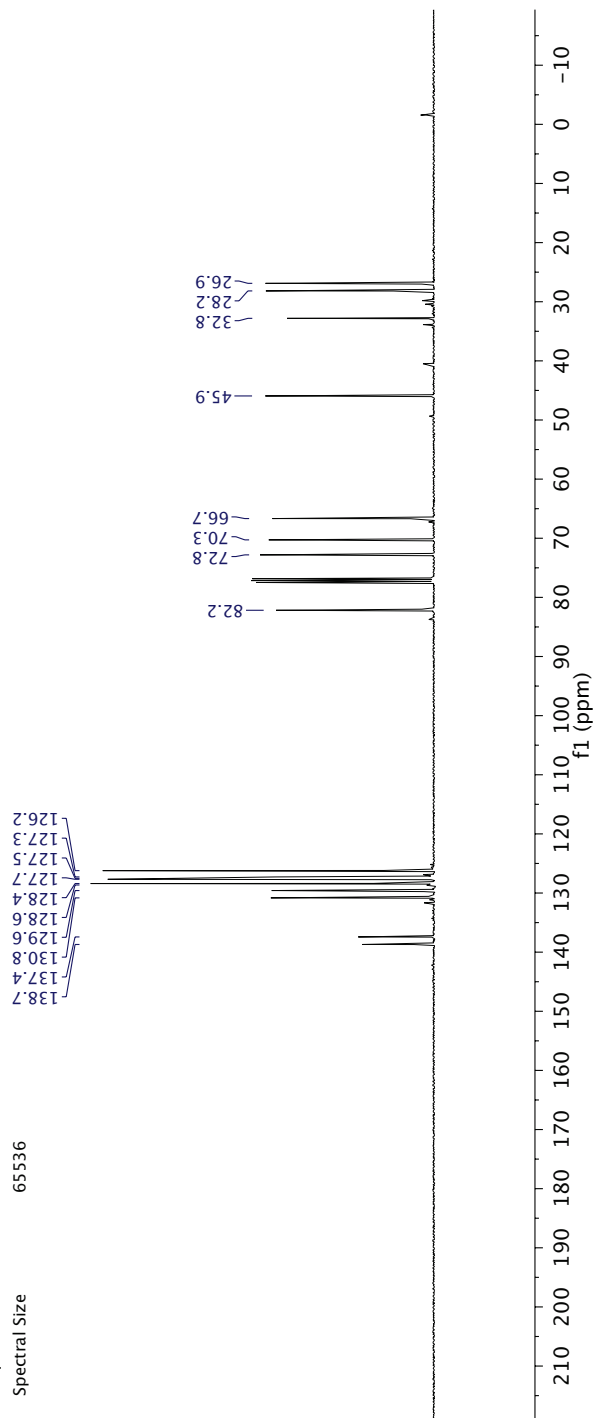
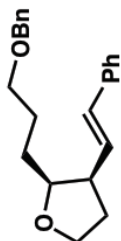


A (m)	7.33
B (d)	6.40
C (dd)	6.17
D (m)	4.51
E (m)	4.06
F (td)	3.83
G (td)	3.62
H (ddt)	2.97
I (m)	2.23
J (dddd)	1.90
K (q)	1.82

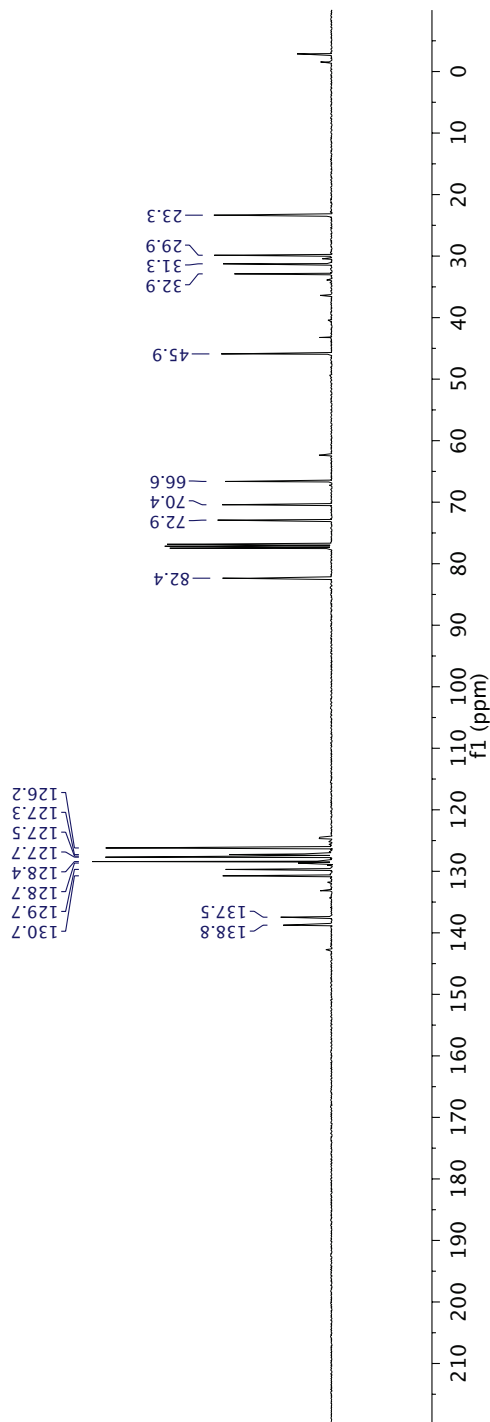
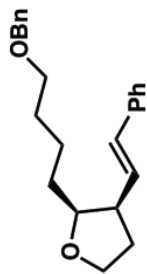
Parameter	Value
Title	JLH-7-2262.fid
Origin	Bruker BioSpin GmbH
Solvent	CDCl3
Temperature	295.2
Pulse Sequence	zgpg30
Number of Scans	512
Receiver Gain	35.5
Relaxation Delay	1.0000
Pulse Width	10.0000
Acquisition Time	1.3631
Acquisition Date	2018-05-04T12:46:23
Spectrometer Frequency	100.62
Spectral Width	24038.5
Lowest Frequency	-1953.0
Nucleus	13C
Acquired Size	32768
Spectral Size	65536



Parameter	Value
Title	GBG-1-038.2.fid
Origin	Bruker BioSpin GmbH
Solvent	CDCl ₃
Temperature	295.1
Pulse Sequence	zgpg30
Number of Scans	512
Receiver Gain	78.7
Relaxation Delay	1.0000
Pulse Width	10.0000
Acquisition Time	1.3631
Acquisition Date	2018-05-04T13:12:20
Spectrometer Frequency	100.62
Spectral Width	24038.5
Lowest Frequency	-1953.0
Nucleus	¹³ C
Acquired Size	32768
Spectral Size	65536



Parameter	Value
Title	JLH-7-2272.fid
Origin	Bruker BioSpin GmbH
Solvent	CDCl3
Temperature	295.1
Pulse Sequence	zgpg30
Number of Scans	512
Receiver Gain	78.7
Relaxation Delay	1.0000
Pulse Width	10.0000
Acquisition Time	1.3631
Acquisition Date	2018-05-04T11:54:42
Spectrometer Frequency	100.62
Spectral Width	24038.5
Lowest Frequency	-1793.9
Nucleus	13C
Acquired Size	32768
Spectral Size	65536



BIBLIOGRAPHY

- (1) Franz, A. K.; Wilson, S. O. *J. Med. Chem.* **2013**, *56* (2), 388–405.
- (2) Showell, G. A.; Mills, J. S. *Drug Discov. Today* **2003**, *8* (12), 551–556.
- (3) Chan, T. H.; Fleming, I. *Synthesis* **1979**, *1979* (10), 761–786.
- (4) Sarkar, T. K. *Synthesis* **1990**, *1990* (12), 1101–1111.
- (5) Chabaud, L.; James, P.; Landais, Y. *Eur. J. Org. Chem.* **2004**, *2004* (15), 3173–3199.
- (6) Denmark, S. E.; Fu, J. *Chem. Rev.* **2003**, *103* (8), 2763–2794.
- (7) Hosomi, A.; Sakurai, H. *Tet. Lett.* **1976**, *17* (16), 1295–1298.
- (8) Slutsky, J.; Kwart, H. *J. Am. Chem. Soc.* **1973**, *95* (26), 8678–8685.
- (9) Calas, R.; Dunogues, J.; Deleris, G.; Pisciotti, F. *J. Organomet. Chem.* **1974**, *69* (2), C15–C17.
- (10) Deleris, G.; Dunogues, J.; Calas, R. *J. Organomet. Chem.* **1975**, *93* (1), 43–50.
- (11) Hosomi, A.; Endo, M.; Sakurai, H. *Chem. Lett.* **1976**, *5* (9), 941–942.
- (12) Ishihara, K.; Mouri, M.; Gao, Q.; Maruyama, T.; Furuta, K.; Yamamoto, H. *J. Am. Chem. Soc.* **1993**, *115* (24), 11490–11495.
- (13) Wadamoto, M.; Yamamoto, H. *J. Am. Chem. Soc.* **2005**, *127* (42), 14556–14557.
- (14) Williams, D. R.; Myers, B. J.; Mi, L. *Org. Lett.* **2000**, *2* (7), 945–948.
- (15) Trost, B. M.; Thiel, O. R.; Tsui, H.-C. *J. Am. Chem. Soc.* **2003**, *125* (43), 13155–13164.
- (16) de Fays, L.; Adam, J.-M.; Ghosez, L. *Tet. Lett.* **2003**, *44* (38), 7197–7199.

- (17) Heo, J.-N.; Micalizio, G. C.; Roush, W. R. *Org. Lett.* **2003**, *5* (10), 1693–1696.
- (18) Heo, J.-N.; Holson, E.B.; Roush, W. R. *Org. Lett.* **2003**, *5* (10), 1697–1700.
- (19) Sparks, M. A.; Panek, J. S. *J. Org. Chem.* **1991**, *56* (10), 3431–3438.
- (20) Panek, J. S.; Clark, T. D. *J. Org. Chem.* **1992**, *57* (15), 4323–4326.
- (21) Suginome, M.; Matsumoto, A.; Ito, Y. *J. Am. Chem. Soc.* **1996**, *118* (12), 3061–3062.
- (22) Bourque, L. E.; Cleary, P. A.; Woerpel, K. A. *J. Am. Chem. Soc.* **2007**, *129* (42), 12602–12603.
- (23) Landais, Y.; Planchenault, D.; Weber, V. *Tet. Lett.* **1994**, *35* (51), 9549–9552.
- (24) Davies, H. M. L.; Hansen, T.; Rutberg, J.; Bruzinski, P. R. *Tet. Lett.* **1997**, *38* (10), 1741–1744.
- (25) Wu, J.; Chen, Y.; Panek, J.S. *Org. Lett.* **2010**, *12* (9), 2112–2115.
- (26) Kacprzynski, M.A.; May, T.L.; Kazane, S. A.; Hoveyda, A.H. *Angew. Chem. Int. Ed.* **2007**, *46*(24), 4554–4558.
- (27) Hayashi, T.; Konishi, M.; Ito, H.; Kumada, M. *J. Am. Chem. Soc.* **1982**, *104* (18), 4962–4963.
- (28) Hayashi, T.; Konishi, M.; Kumada, M. *J. Am. Chem. Soc.* **1982**, *104* (18), 4963–4965.
- (29) Hofstra, J. L.; Cherney, A. H.; Ordner, C. M.; Reisman, S. E. *J. Am. Chem. Soc.* **2018**, *140* (1), 139–142.
- (30) Cherney, A. H.; Reisman, S. E. Nickel-Catalyzed Asymmetric Reductive Cross-Coupling Between Vinyl and Benzyl Electrophiles. *J. Am. Chem. Soc.* **2014**, *136* (41), 14365–14368.

- (31) Suzuki, N.; Hofstra, J. L.; Poremba, K. E.; Reisman, S. E. *Org. Lett.* **2017**, *19* (8), 2150–2153.
- (32) Tasker, S. Z.; Standley, E. A.; Jamison, T. F. *Nature* **2014**, *509* (7500), 299–309.
- (33) Perrott, A.L.; De Lijser, H.J.P.; Arnold, D.R. *Can. J. Chem.* **1997**, *75*(4), 384-397.
- (34) Suginome, M.; Iwanami, T.; Ito, Y. *J. Org. Chem.* **1998**, *63* (18), 6096–6097.
- (35) Judd, W. R.; Ban, S.; Aubé, J. *J. Am. Chem. Soc.* **2006**, *128* (42), 13736–13741.
- (36) Still, W. C.; Kahn, M.; Mitra, A. *J. Org. Chem.* **1978**, *43* (14), 2923–2925.